To the Graduate Council

I am submitting herewith a thesis written by Sorin Homescu entitled "Design and Testing of a Feedback Position Control System Using Extremely Low Pressure Air". I have examined the final copy of this thesis for form and content and recommend that it be accepted in partial fulfillment of the requirements for the degree of Master of Science, with a major in Mechanical Engineering.

Frank H. Speckhart, Major Professor

We have read this thesis

and recommend its acceptance:

William R. Hamel

Joe Iannelli

Accepted for the Council:

Interim Vice Provost and

Dean of the Graduate School

DESIGN AND TESTING OF A FEEDBACK POSITION CONTROL SYSTEM USING EXTREMELY LOW PRESSURE AIR

A Thesis

Presented for the

Master of Science

Degree

The University of Tennessee, Knoxville

Sorin Homescu

May 2001

DEDICATION

This thesis is dedicated to my loving parents who will not be able to share with me this important accomplishment of my career in mechanical engineering. They always showed me the right path in life, supporting and encouraging me through every step of my education. I will always thank God for the blessing of having such helping and understanding parents. They will always be in my heart!!!

ACKNOWLEDGMENTS

I would like to thank my major professor, Dr. Frank Speckhart, for his support in preparing this thesis. It was a great honor for me to work and learn from such an experienced engineer.

I would also like to thank my other committee members, Dr. William Hamel and Dr. Joe Iannelli for their assistance with this thesis and throughout my time in graduate school.

There are a number of other people whose assistance should be recognized. I would like to thank Dennis Higdon from the Electronic Shop for his help and also would like to thank the Mechanical Shop for helping me with the prototype model involved in this project. I have also received generous financial support from the Department of Mechanical and Aerospace Engineering and Engineering Science and Dr. Frank Speckhart.

Lastly, the greatest debt is owed to my family. My wife Diana offered me help and encouragement all these years and my young daughter Alyssa gifted me with joyful days in hard times.

ABSTRACT

This thesis involved the development of a low pressure pneumatic feedback position control system for reducing the gap between the printing head of an inkjet printer and the paper. Because of variation of paper thickness (i.e. envelopes) and deformations of structural members the print head is positioned further from the paper than desired (approximately 0.8 mm). Evaluation of this feedback position control system was accomplished in two ways: a computer analytical model was developed, and the airflow equations were solved numerically; and a prototype model of the control system was designed, constructed and tested. The results of the computer simulation showed the feedback position control system to significantly reduce the gap between the printing head and the paper. Steady-state analysis also revealed the best combination of the geometrical parameters of the prototype model.

The measurements conducted on the prototype model led to the conclusion that the computer adequately described the feedback position control system. Suggestions and recommendations were given for improvements in the existing design.

TABLE OF CONTENTS

LIST OF FIGURES

FIGURE PAGE

LIST OF SYMBOLS

Greek

Symbol	*Explanation / Definition*
α	adiabatic constant (for air $\alpha = 1.4$)

Standard

Symbol	
A_1	flow area of the regulating pressure nozzle
A_2	flow area between the measuring pressure nozzle and paper
d_1	inside diameter of the regulating pressure nozzle
d_2	inside diameter of the measuring pressure nozzle
g	gravitational acceleration ($g = 32.16$ ft/sec^2)
m_{12}	mass flow into measuring chamber
m_{20}	mass flow out of measuring chamber
m_2	mass flow difference in measuring chamber at transient analysis
p_0	atmospheric pressure
p_1	pressure inside the regulating chamber
p_2	pressure inside the measuring chamber
R	gas constant (for air $R = 53.3$ ft·lb/lbm·°R)
T	ambient temperature
V_2	measuring chamber volume
V_s	specific volume

CHAPTER 1

INTRODUCTION

Proposed Design Solution and Prototype Model

Improved printing quality for an inkjet printer can be achieved if the printing head is positioned closer to the paper and the gap between the printing head and paper is held constant. Because the paper thickness varies as quality, manufacturer and type (i.e. envelopes) changes and because of the deflection and inaccurateness of sustaining structural members during printing, the printing head is positioned further from the paper than desired (approximately 0.8 mm).

The challenge was to design a system that can provide dynamic control of the gap for a minimum cost eventually using components that an inkjet printer already includes. The feedback position control system that is proposed uses the extremely low pressure air of approximately 0.1 inches of H_2O supplied by a standard cooling fan.

Air is directed through a flexible tube to a pneumatic transducer. The pneumatic transducer is used to measure the gap during the printing process. As shown by Figure 1 the entire feedback position control device is attached to the printing head. As the measuring nozzle and pneumatic transducer are moved closer to

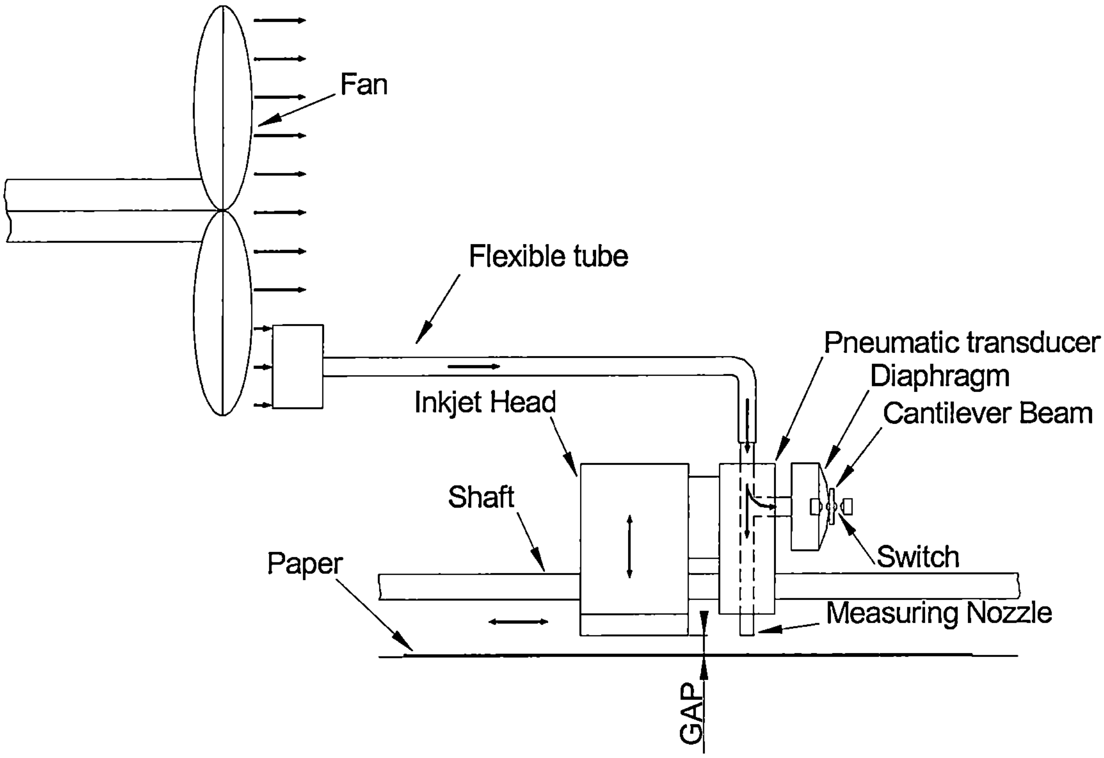

Figure 1 Design Solution of the Feedback Position Control System

the paper, flow opening becomes smaller and the pressure acting on the diaphragm surface increases. A detailed drawing and description of the pneumatic transducer is shown by Figure 4, on page 4.

When the pressure increases the very flexible diaphragm will apply a force to the cantilever beam, which closes the limit switch. An electrical device can then be used to change the paper - printing head gap to the desired value. The axial position of the diaphragm can be detected and/or measured by several different means including the following: contact points (as presented above), capacitance means, optical (electro-optical), etc.

The proposed design solution of the feedback position control system was tested using a prototype model as shown by Figure 2. An eccentric wheel powered by a variable speed gear motor was used to simulate the time varying gap. The eccentric sleeve will permit the variation of the gap in a very wide range by adjusting the eccentricity of both wheel and sleeve. The pressure transducer is equipped with an inductive probe that moves simultaneously with the measuring nozzle. The voltage generated by the inductive probe is a measurement of the gap change and is read by an A/D computer card at given sampling frequency.

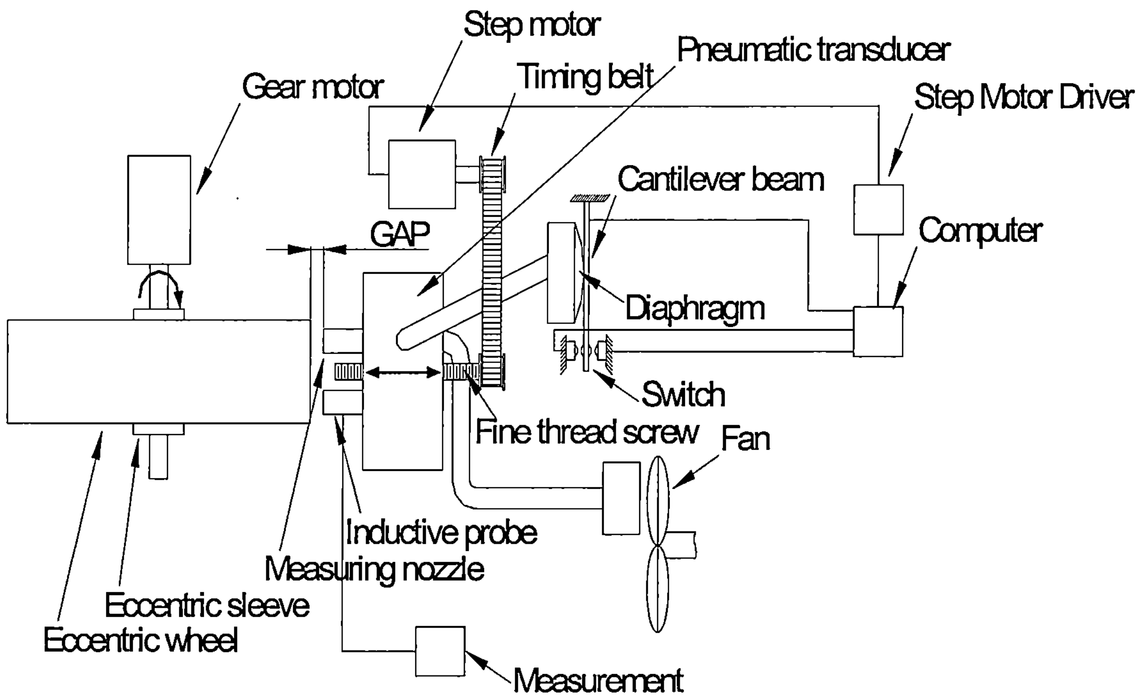

Figure 2 Feedback Position Control System Prototype Model

The feedback system is designed to regulate the gap between the eccentric disk and measuring nozzle. When the gap is not at the desired value, the back pressure of the pneumatic transducer will deflect the diaphragm. The diaphragm axial deflection will force a brass cantilever beam to move and close the limit switch. The contacts of the limit switch are connected to the parallel port of a PC. The PC through a program written in BASIC controls the stepping motor rotation in a manner to hold the gap constant. The complete functioning principle can be seen in the block diagram presented in Figure 3. The inductive probe is used to measure the magnitude of the gap. Tests will be conducted for a wide range of conditions.

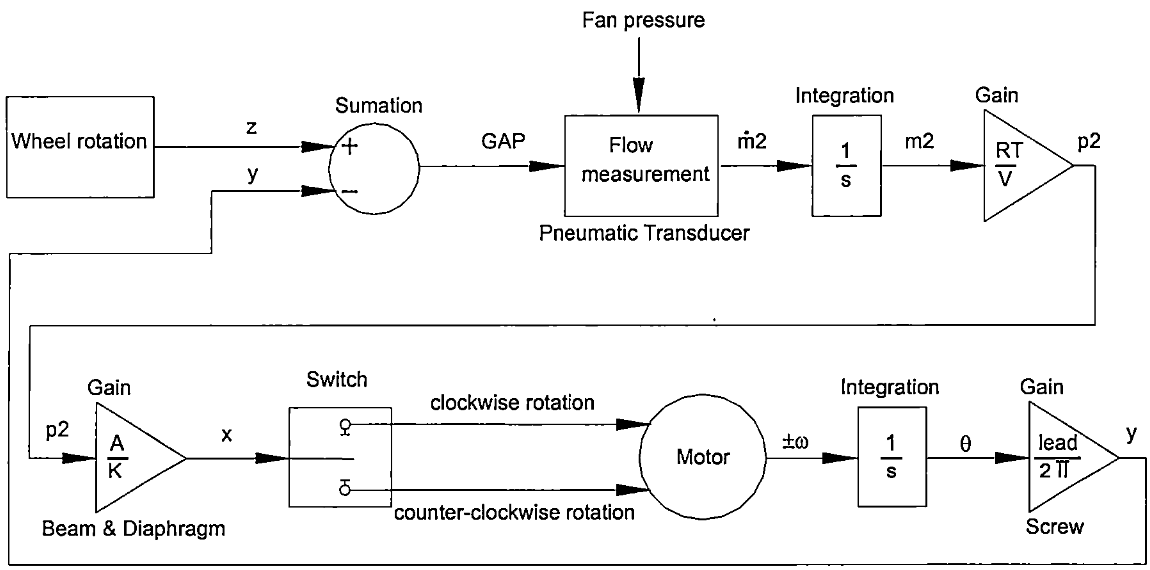

Figure 3 Feedback Position Control System Block Diagram

Pneumatic Transducer

The gap measurement is performed with a pneumatic transducer. Figure 4 shows a schematic of the pneumatic transducer used to measure the gap between the printing head and the paper. A standard cooling fan supplies low pressure (< 0.1 inch H_2O) to the device. The fan and the tube from fan are capable of supplying sufficient mass flow rate of air to keep pressure p1 approximately constant. The pressure in chamber 2 is p_2 and varies depending on mass flow rate of air into and out of the chamber. The mass flow rate into chamber 2 depends on p_1, p_2 and d_1 and the mass flow rate out depends on p_1, d_2 and the magnitude of gap. For fixed values of d_1 and d_2 and a constant supply pressure (p_1), the pressure p_2 can be shown to be a function of the gap. A detailed description of the pneumatic transducer and analysis is contained in Chapter 2.

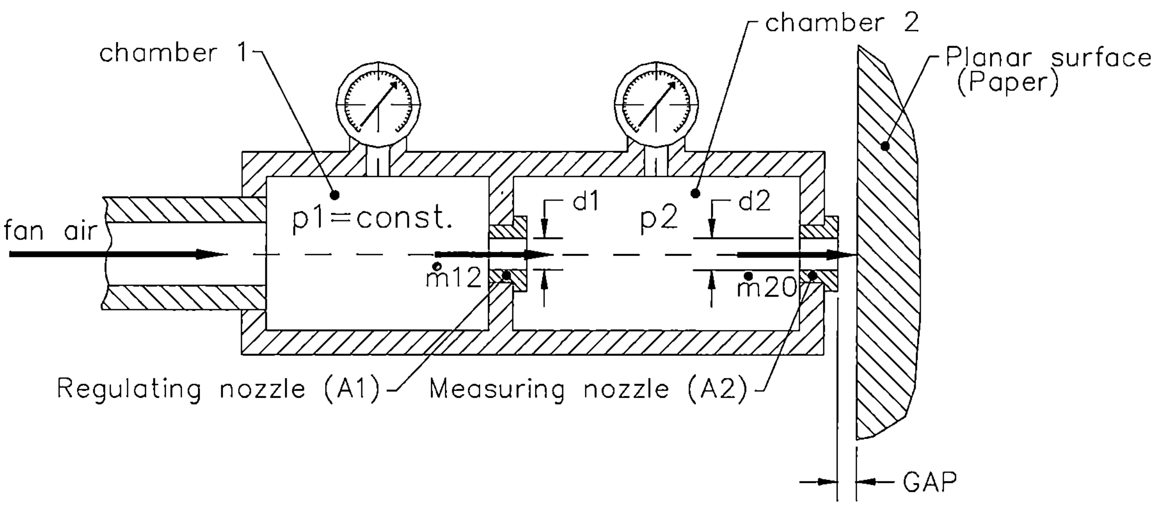

Figure 4 Pneumatic Transducer Principle

Outline of Objectives

The topic of this thesis was the analysis, design and testing of a feedback position control system using the extremely low pressure of a small fan. The objective of this feedback position control system is to help improve the printing quality of the inkjet printers by reducing the actual gap of approximately 0.8 mm between the printing head and paper. The biggest challenge of this project was to cope with the very low pressure supplied by a small cooling fan.

The task was to derive the equations which govern the functioning of the feedback position control system, to simulate its performance by the numerical solution of the equation of motion and to compare that to the experimental tests and results given by the designed prototype model. Thus, the thesis was intended to describe the theory of operation, demonstrate the effectiveness in reducing the gap between the printing head and paper, and suggest improvements in the system.

Method of Attack

A computer program was used to simulate the motion of the feedback position control system, namely computational fluid mechanic analysis was performed. The equation of the airflow was nonlinear and necessitated the use of a numerical solver. A fourth-order, Runge-Kutta-Fehlberg was used for the numerical integration. The pertinent geometrical proportions and material properties were included in the programming. Thus, a computer model for the system was established, engaging in numerical simulation of fluid dynamics, using the computer while changing at will various parameters of interest built into the program.

Next, the model was used to assess the effectiveness of the feedback position control system in reducing the gap between the printing head and the paper. This was determined by comparing the results from the output of the program for different values of wheel amplitude and rotation frequency. In addition a prototype model was designed so that the actual performance in reducing the gap could be measured.

Finally, improvements to the original prototype model design were suggested. Also the computer model was used to demonstrate the improved sensitivity and performance of the feedback position control system obtained by minimizing the volume of the chamber 2. Further improvements and study were formulated as warranted by the results of the computer simulation and the prototype model testing.

CHAPTER 2

ANALYTICAL ANALYSIS OF THE FEEDBACK POSITION CONTROL SYSTEM

Steady-State Analysis of Pneumatic Transducer

The first part of the analysis is to describe the performance of the pneumatic transducer. The device is shown by Figure 4,on page 5. As noted in Chapter 1 a standard cooling fan supplies low-pressure air (on the order of 0.1 inches H_2O).

Since the flow rate of air through the pressure transducer is small, the fan and delivery system can provide a constant pressure (p_1) to the pneumatic transducer. The flow through the pneumatic transducer will depend upon the pressure in chamber 2 (p_2) and the area of outflow that is controlled by the distance (gap) between the measuring nozzle and the paper.

The flow area of the measuring nozzle depends upon the smaller of the area of the nozzle or the area of flow between the paper and nozzle. The flow area of the measuring nozzle is:

$$\pi \cdot \frac{d_2^2}{4}$$

The flow area between the measuring nozzle and paper is:

$$\pi \cdot d_2 \cdot gap$$

By equaling the two flow areas, the maximum value of the gap can be shown to be the following:

$$gap_{\max} = \frac{d_2}{4}$$

When the gap is greater than d_2 / 4, the flow area of the nozzle will limit the flow. For gap values smaller than d_2 / 4, the flow area is controlled by the gap.

For a given value of measuring nozzle diameter d_2, it is necessary to find the value of regulating nozzle diameter d_1 that will provide the best performance of the pneumatic transducer. For subsonic, adiabatic compressible flow without losses, the mass steady-state flow into chamber 2 is given by the following expression:

$$\dot{m}_{12} = A_1 \cdot p_1 \cdot \sqrt{\frac{2 \cdot g \cdot \alpha}{(\alpha - 1) \cdot R \cdot T}\left[\left(\frac{p_2}{p_1}\right)^{2/\alpha} - \left(\frac{p_2}{p_1}\right)^{\frac{\alpha+1}{\alpha}}\right]} \qquad \textbf{(1)}$$

The derivation of the mass flow equations is shown in Appendix A.

The mass steady-state flow out of chamber 2 is the following:

$$\dot{m}_{20} = \pi \cdot d_2 \cdot gap \cdot p_2 \cdot \sqrt{\frac{2 \cdot g \cdot \alpha}{(\alpha - 1) \cdot R \cdot T}\left[\left(\frac{p_0}{p_2}\right)^{2/\alpha} - \left(\frac{p_0}{p_2}\right)^{\frac{\alpha+1}{\alpha}}\right]} \qquad \textbf{(2)}$$

For steady-state conditions, the mass flow rates shown above are equal:

$$\dot{m}_{12} = \dot{m}_{20} \tag{3}$$

For a value of d_2 = 4 mm, equation (3) was solved using the Newton's method presented in Appendix B and a MatLab program presented in Appendix D. Figure 5 shows the results obtained at the steady-state analysis.

As can be seen, a value of d_1 = 3 mm gives the greatest slope at the mid point of the gap (0.5 mm) with the measuring pressure (p_2) variation approximately linear within the gap range. Consequently, this is the value of d_1 that was used. The feedback position control system prototype model was designed using the nozzle diameters established above, the drawings being presented in Appendix C.

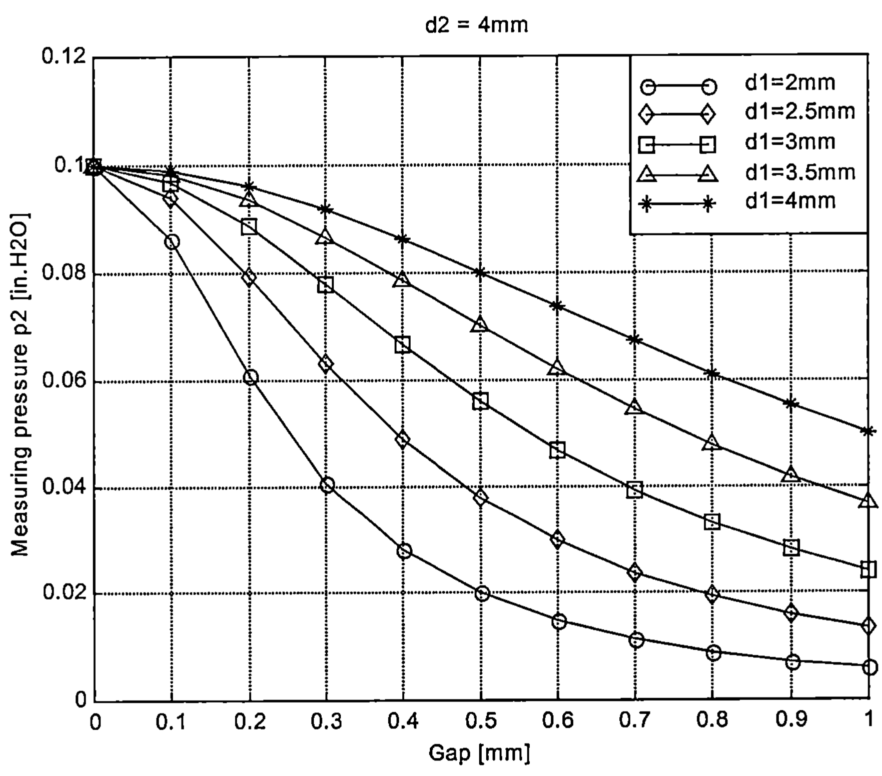

Figure 5 Steady-State Analysis of the Measuring Pressure p_2

Transient Analysis

The transient analysis was performed on the model to determine the time response for different gap ranges and wheel rotation frequencies. We now consider the unsteady flow when the gas is subject to a time-varying difference of mass flows between the entrance and the exit of the chamber.

The mass flow rate expressions derived at the steady-state analysis and shown in Appendix A were used, but they are not equal for the transient analysis. Their difference is the time-varying difference of mass flows as shown by equation (4):

$$\dot{m}_{12} - \dot{m}_{20} = \frac{dm_2}{dt} = \dot{m}_2 \tag{4}$$

The further development of equation (4) is shown in Appendix E. This equation is nonlinear so that necessitates the use of a numerical solver. A fourth-order Runge-Kutta-Fehlberg method was used for the numerical integration. The initial mass $m_2(0)$ used for this numerical integration can be deducted from the perfect gas law:

$$p_0 \cdot V_2 = m_2(0) \cdot R \cdot T \Rightarrow m_2(0) = \frac{p_0 \cdot V_2}{R \cdot T} \tag{5}$$

A MatLab program (see Appendix F) was written to solve equation (4) and also simulate the feedback position control system.

The object of the control system is to minimize the variation in the gap as the paper thickness changes. The mass airflow in and out of chamber 2 (Equation

(4)) is a function of the gap. Equation (4) is integrated with respect to time to calculate the mass in chamber 2. Using the perfect gas low, the pressure in chamber 2 is calculated. This pressure then acts on the cantilever beam via the diaphragm, which controls the motor that regulates the gap.

A sinusoidal variation of paper thickness having the single amplitudes of 0.2, 0.4 and 0.6 was simulated. The eccentric wheel in the prototype model provides the sinusoidal variation. The parameters of the system are given in Appendix G.

Figure 6 shows the gap variation obtained using the chamber volume of the prototype model. Figure 7 shows the results obtained by reducing this volume by one-half.

As can be seen from both figures the gap reduction obtained is directly proportional to the wheel amplitude and frequency of rotation. Also we can conclude that there is no gap reduction change for lower chamber volumes. For higher volumes of the chamber the results will be different showing a significant change in gap reduction. We have to note that for the wheel single amplitude of 0.2 mm the gap reduction is the same for all frequencies.

The higher the pressure change the higher the sensitivity of the pneumatic transducer and implicitly the higher the gap reduction. Even thought the system is nonlinear, the gap variation over time resembles a sine curve.

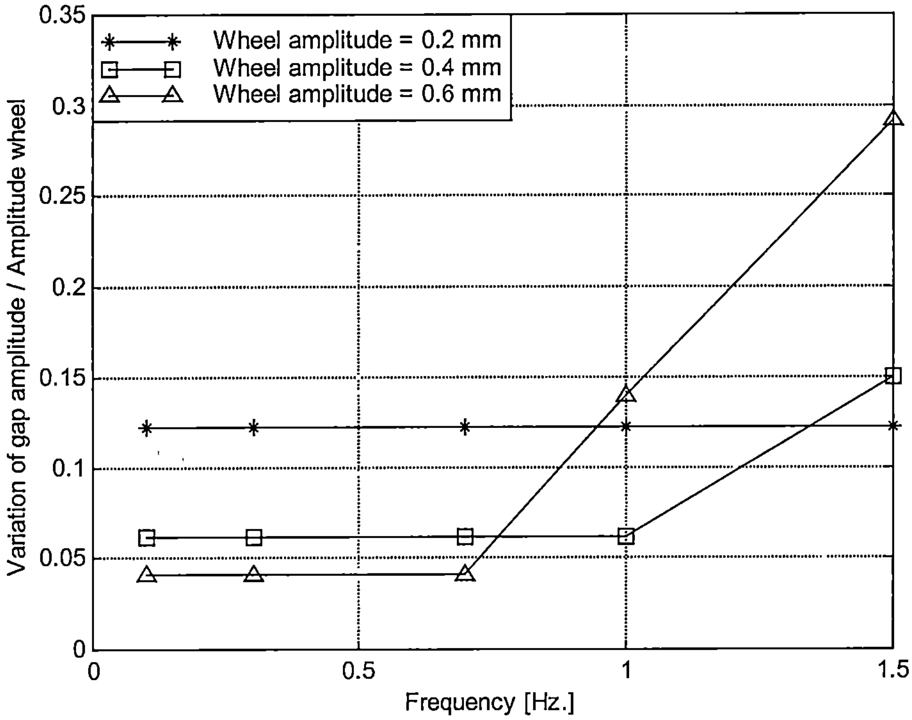

Figure 6 Gap Variation Using the Prototype Model Chamber Volume

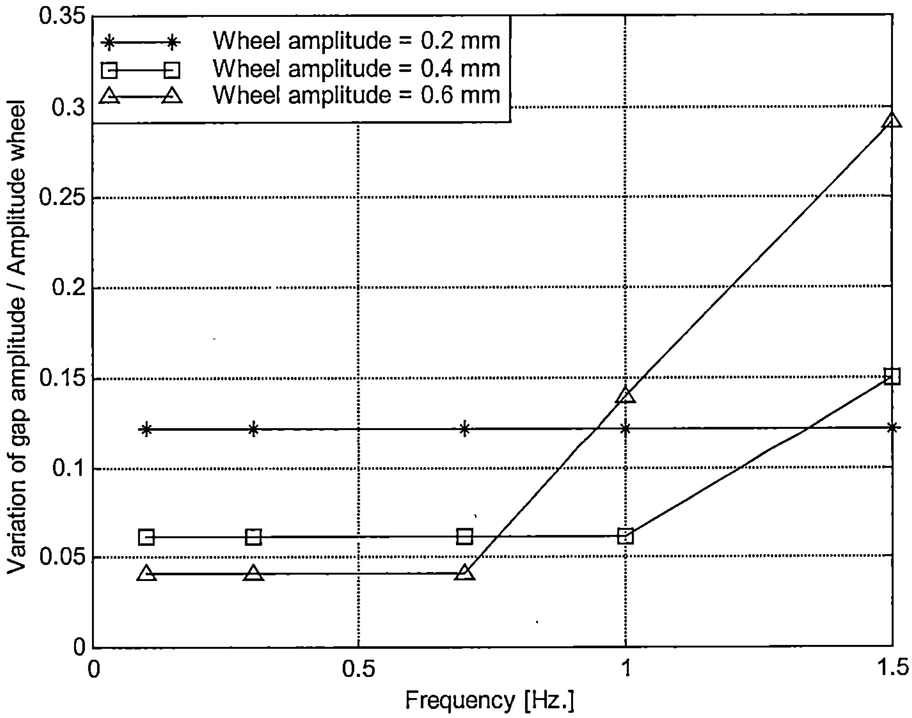

Figure 7 Gap Variation Using One-Half of the Prototype Model Chamber Volume

Using this sine curve and the sine curve generated by the wheel motion it was possible to calculate the phase angle between the eccentric wheel motion (paper variation) and the gap using the same MatLab program. The results are presented in Figure 8.

The phase angle is defined to be:

$$\Phi_{wheel} - \Phi_{gap}$$

Looking at the plot it was concluded that the phase angle significantly increases at higher rotation frequencies and amplitudes.

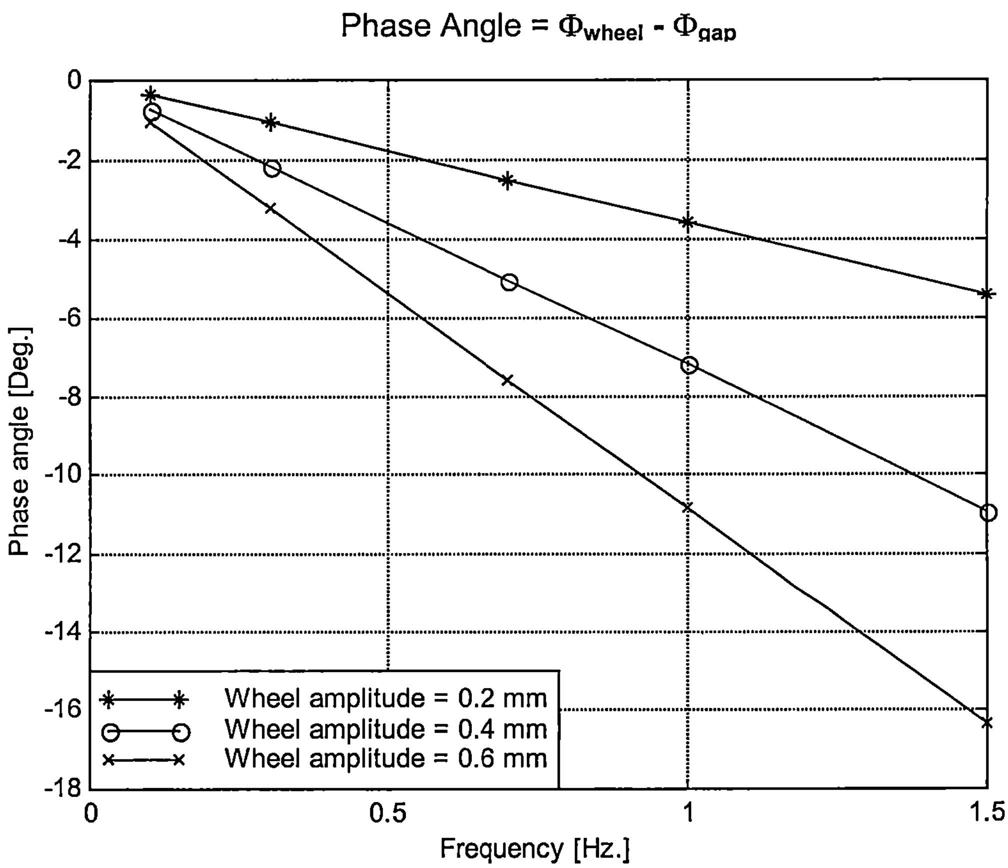

Figure 8 Analytical Phase Angle Variation

For low rotation frequencies and amplitudes the phase angle is very small showing an almost in-phase motion of both wheel and pneumatic transducer.

CHAPTER 3

PROTOTYPE MODEL TESTING

Prototype Model Detailed Description

For testing purposes a prototype model of the feedback position control system was designed and constructed. The assembly and detailed drawings can be consulted in Appendix C. A top view of the model is presented in Figure 9.

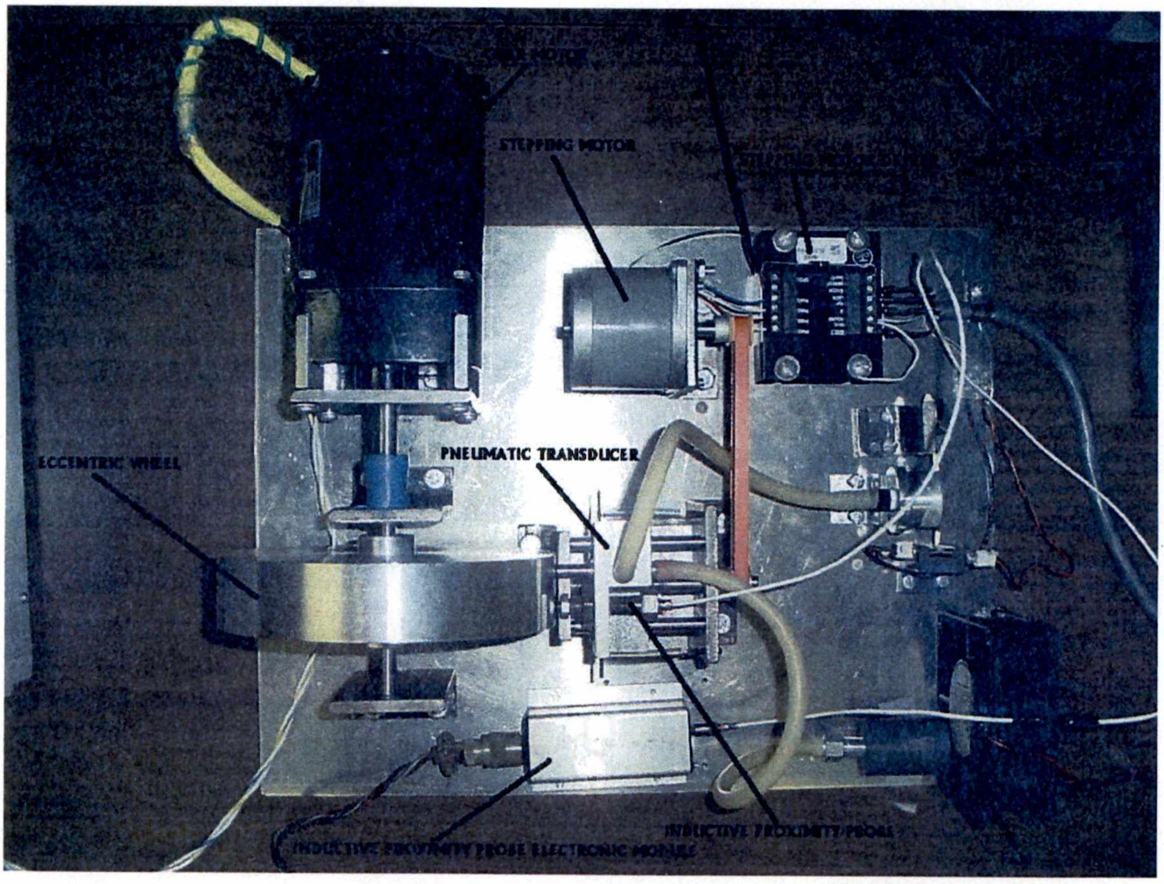

Figure 9 Prototype Model Top View

The time-varying gap was obtained by using an adjustable eccentric wheel powered by a variable speed DC gear motor. The wheel is made from aluminum and has an outside diameter of 5.9 in. An eccentric sleeve placed inside the wheel will permit the variation of the gap over a very wide range by adjusting the eccentricity of both wheel and sleeve. The variable rotation speed of the gear motor is obtained by varying its input voltage.

The side view of the pneumatic transducer is shown in Figure 10. This pneumatic transducer consists of an aluminum block sustained and guided by two steel shafts. The back and forth linear movement of the pneumatic transducer is obtained using a 5/16 – 24 UNF screw and a brass nut mounted inside the

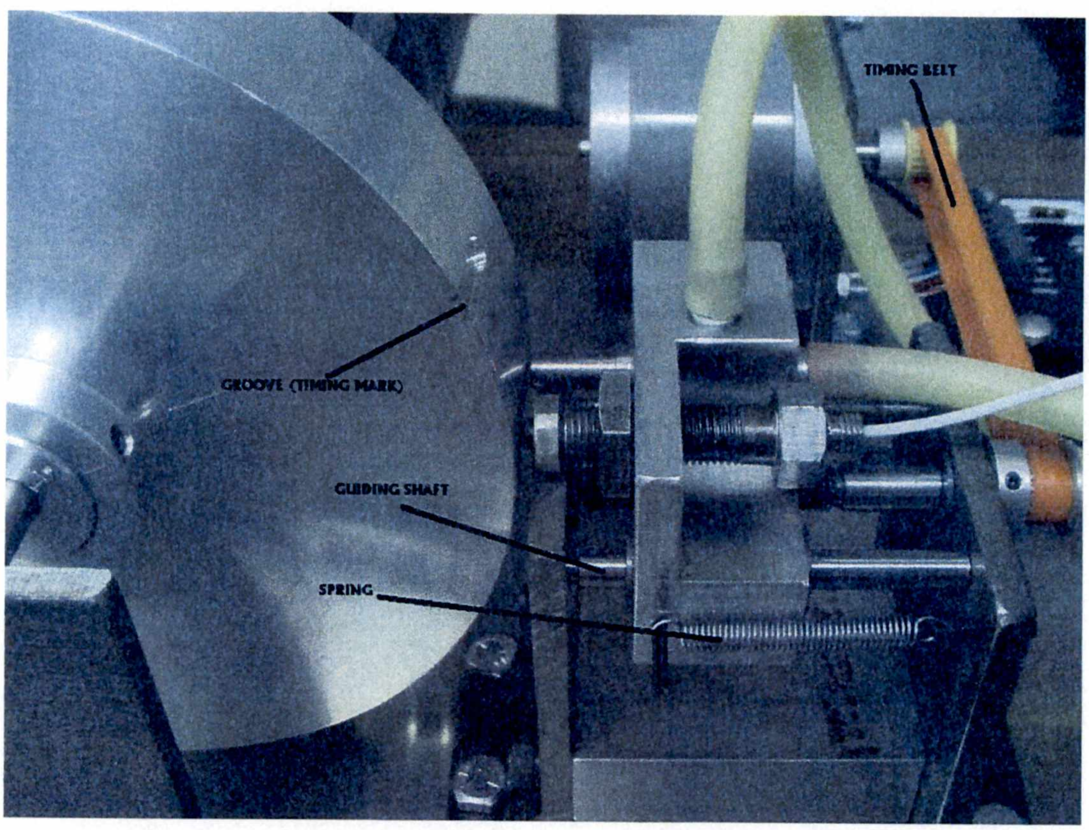

Figure 10 Pneumatic Transducer Side View

aluminum block. The design is made to permit only linear movement and the precision and smoothness is obtained using plastic bearings along with the guiding shafts. The axial free play of the fine-thread screw is reduced by using two springs that provide an axial force on the screw. A top view of the pneumatic transducer showing also the tensioning springs is presented in Figure 11. The free axial movement (play) after tensioning was measured to be approximately ± 0.001 inches. This corresponded to be approximately ± 8 degrees of screw rotation.

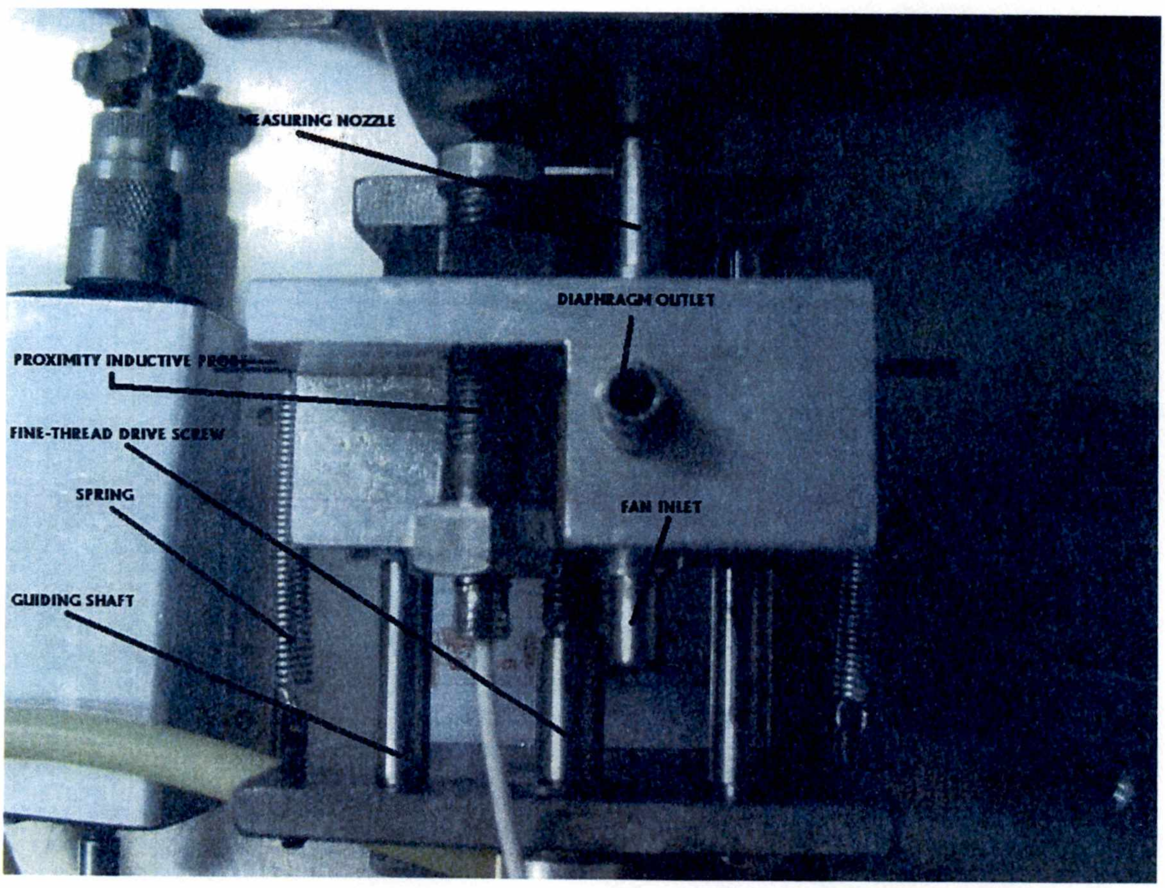

Figure 11 Pneumatic Transducer Top View

A proximity inductive probe is attached to the pneumatic transducer as can be seen in both figures. Since the inkjet head will be attached to the pneumatic transducer, the inductive probe will measure the variation in paper / inkjet distance. The output from the proximity inductive probe is read and stored by an A/D card of a laptop computer. The aluminum wheel is provided with a groove on the inductive probe side. When the inductive probe aligns with the groove the voltage generated by the inductive probe increases significantly signaling that particular position of the wheel. The voltage peaks were used to observe and measure the phase angle that occurs between the wheel and head movements. The groove is at the highest radius of the wheel but because the amplitude is obtained adjusting both wheel and sleeve, the peak will not occur at the highest radius. The phase angle was measured by comparing the two sinusoids generated: wheel and pneumatic transducer.

The back pressure of the pneumatic transducer deflects the diaphragm. The diaphragm and limit switch assembly is shown in Figure 12. The diaphragm is made from liquid latex using a special aluminum mold. The liquid latex is coated on the mold surface twice at approximately 3 hours difference between the layers and with a total drying time of 24 hours. The diaphragm cavity is made from an aluminum cylinder with the inside diameter of 1 inch and length 0.5 in. The cantilever beam is made from brass and its thickness is 0.004 in. It has a circular shape at contact area with the diaphragm and rectangular shape outside the contact area. Detail specifications are given in Appendix G. The limit switch is

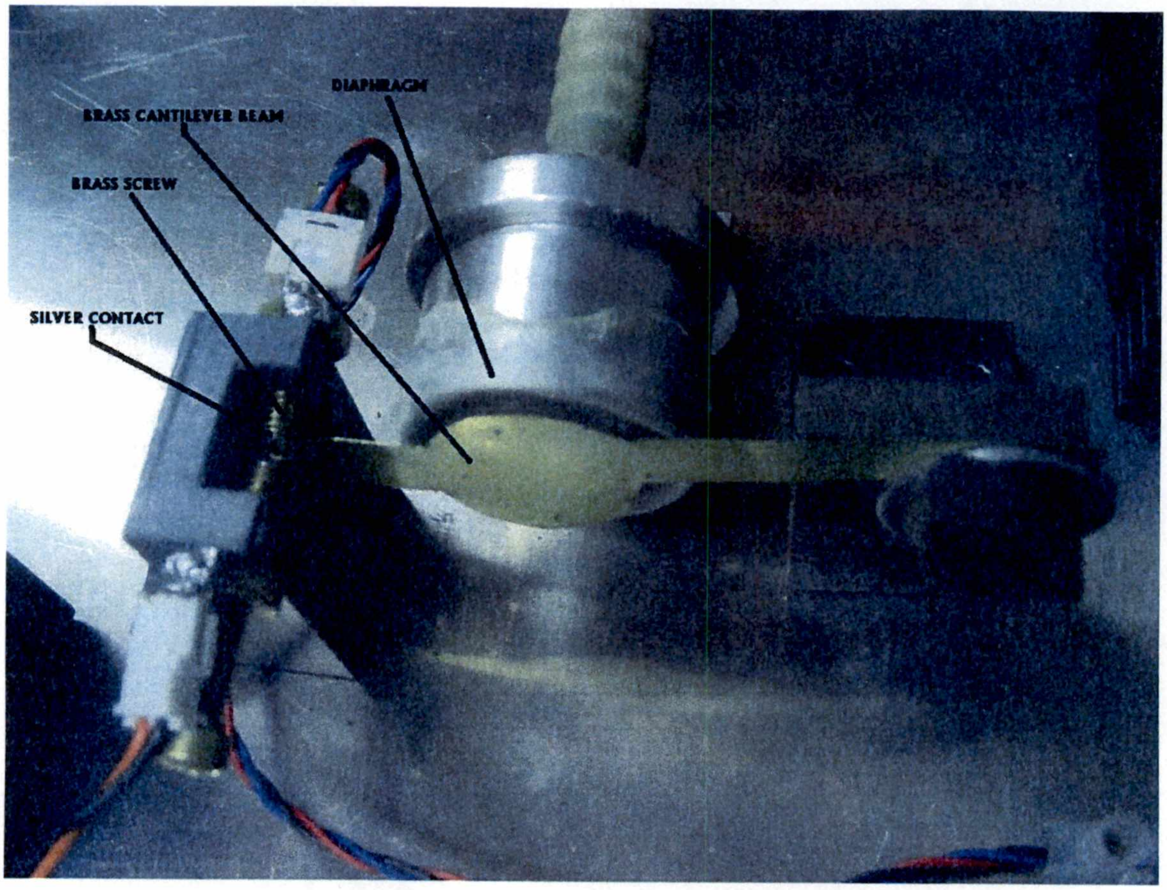

Figure 12 Diaphragm and Switch Assembly

made from two brass screws mounted on a plastic block, each having at the end a silver contact for a better electrical conduction with the cantilever beam. The brass screws of the limit switch are connected to the parallel port of a PC.

A stepping motor is used to move the pressure transducer via a 5/16 – 24 UNF thread screw and to obtain the gap reduction. The stepping motor and the screw are connected each other using a 1:1 ratio timing belt and pulleys. The PC through a program written in BASIC (see Appendix H) controls the stepping motor rotation angle and direction accordingly to the gap distance. The stepping motor rotational motion is executed in half steps (400 steps/rotation) as commanded by the BASIC program. The resolution of the movement of the pressure transducer is 0.0027 mm (~0.001 inches).

Prototype Model Testing

The aluminum wheel was adjusted to obtain single amplitudes of 0.2 mm, 0.4 mm and 0.6 mm. The amplitude was measured using a feeler gauge. For each wheel amplitude the gear motor speed was measured and adjusted to obtained rotation frequencies of 0.1 Hz, 0.3 Hz, 0.7 Hz, 1.0 Hz and 1.5 Hz. For each single combination – wheel amplitude and rotation frequency – measurements were made using the computer A/D card. The voltages generated at each measurement were converted into gap distance lengths. Figure 13 shows a typical gap variation for 0.2 mm single amplitude and 0.1 Hz rotation frequency. The complete results of the measurements are presented in Appendix I.

The gap variations for all the corresponding amplitudes and rotation frequencies were gathered on a single graph presented in Figure 14. Figure 14 clearly shows that the feedback position control system constructed is capable of significantly reducing the gap variation, especially for lower values of wheel amplitude and rotation frequency. For example, the reduction factor for the mid amplitude value of 0.4 mm and a rotation frequency of 1.0 Hz is approximately ¼. This means (due to paper and structural variations) by a factor of 4.

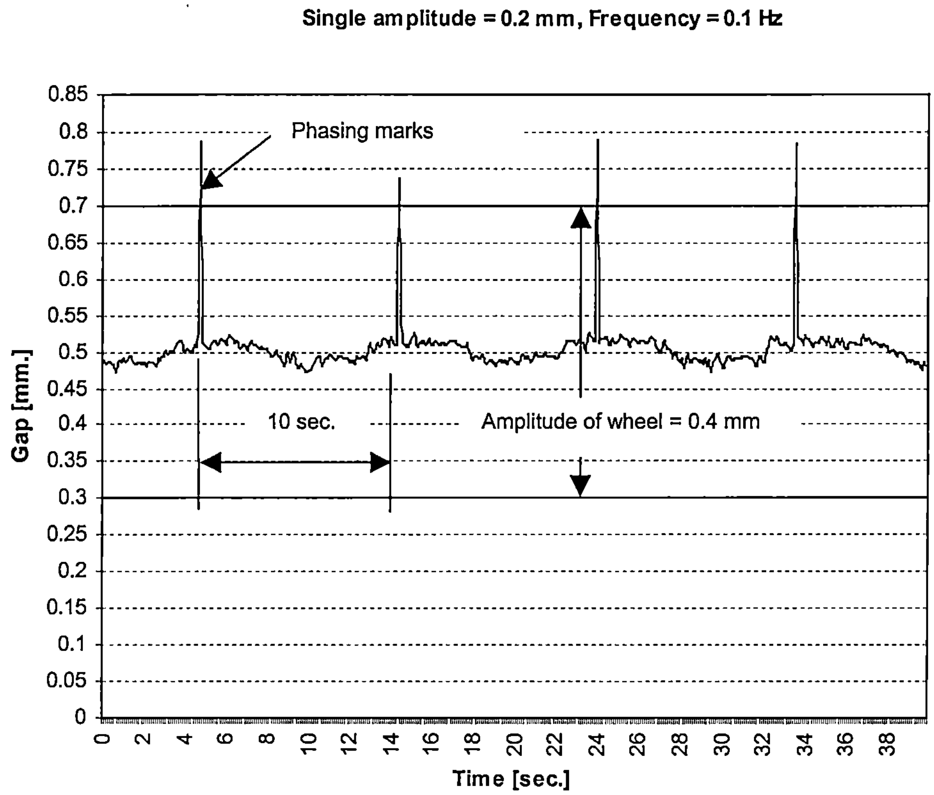

Figure 13 Typical Gap Variation Measurement Result

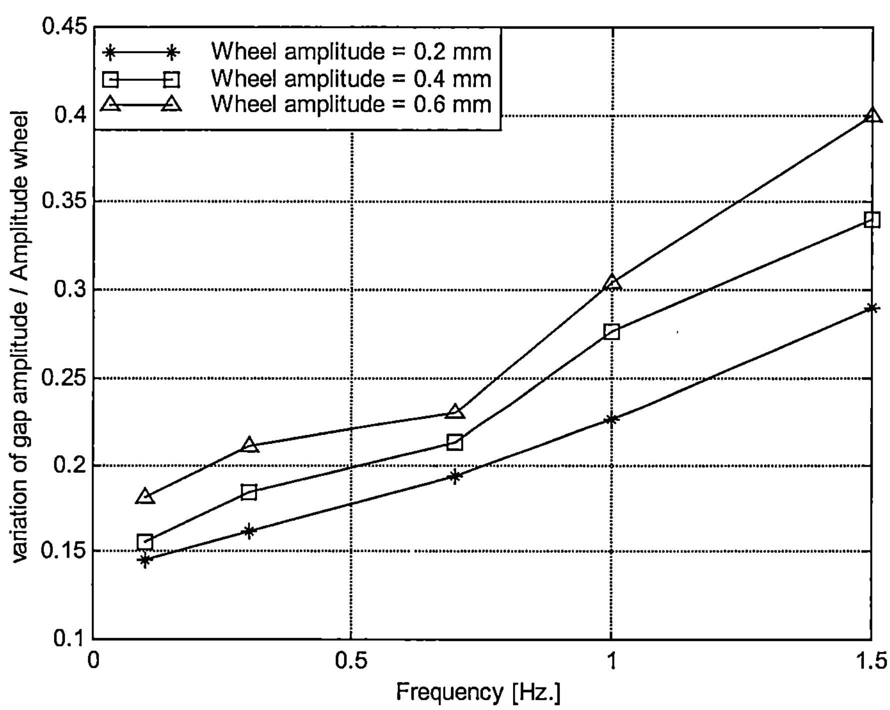

Figure 14 Gap Variation at the Prototype Model

The phase angles were measured and the results obtained are presented in Figure 15. As we can clearly see from this figure, the results obtained for the phase angles are very different from those obtained at the analytical analysis, specifically the phase angles are higher especially at higher rotation frequencies when the pneumatic transducer cannot keep the pace with the aluminum wheel. A comparison between the analytical and experimental results of the gap variation can be seen in Figure 16, Figure 17 and Figure 18.

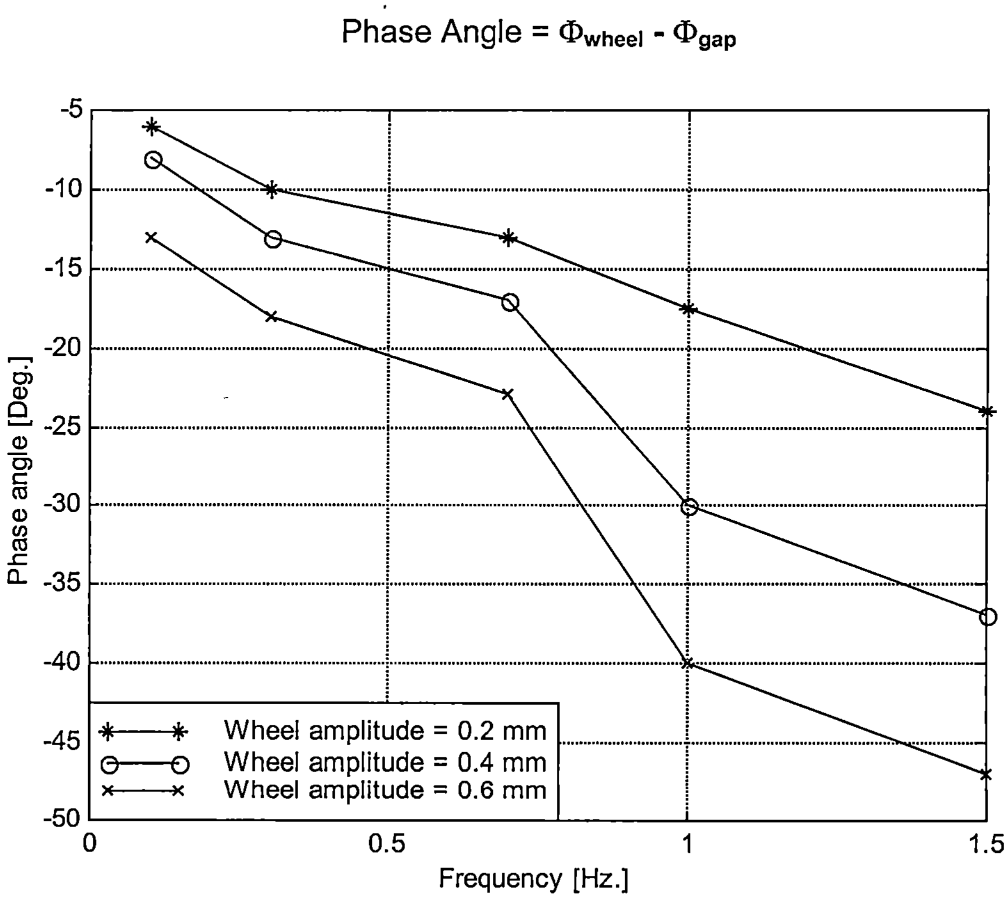

Figure 15 Experimental Phase Angle Variation

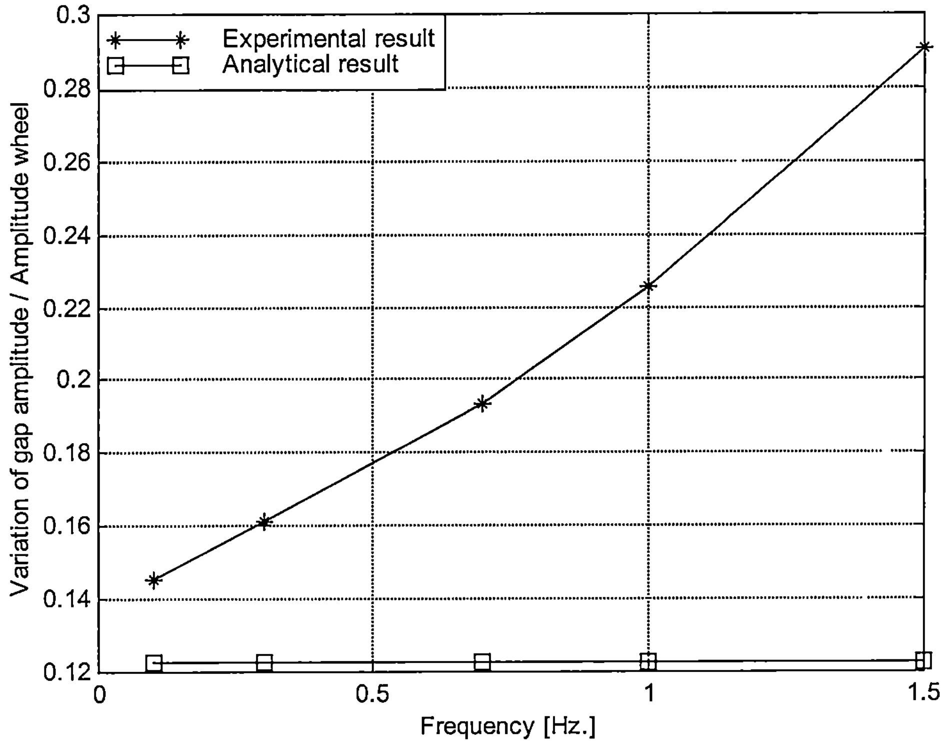

Figure 16 Comparison of Gap Variation - Amplitude 0.2 mm

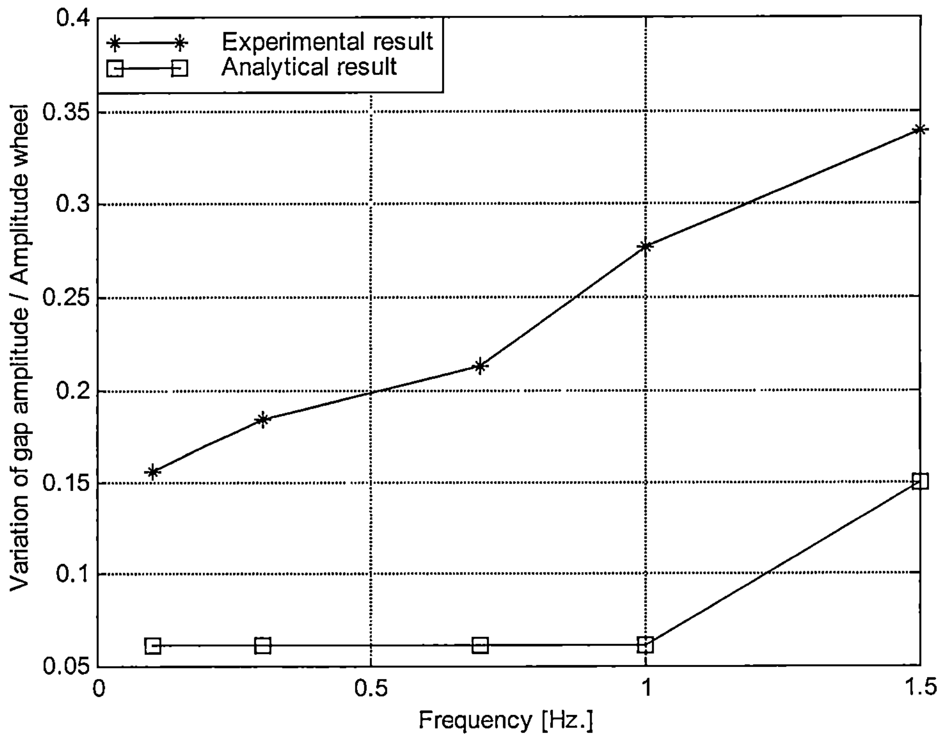

Figure 17 Comparison of Gap Variation - Amplitude 0.4 mm

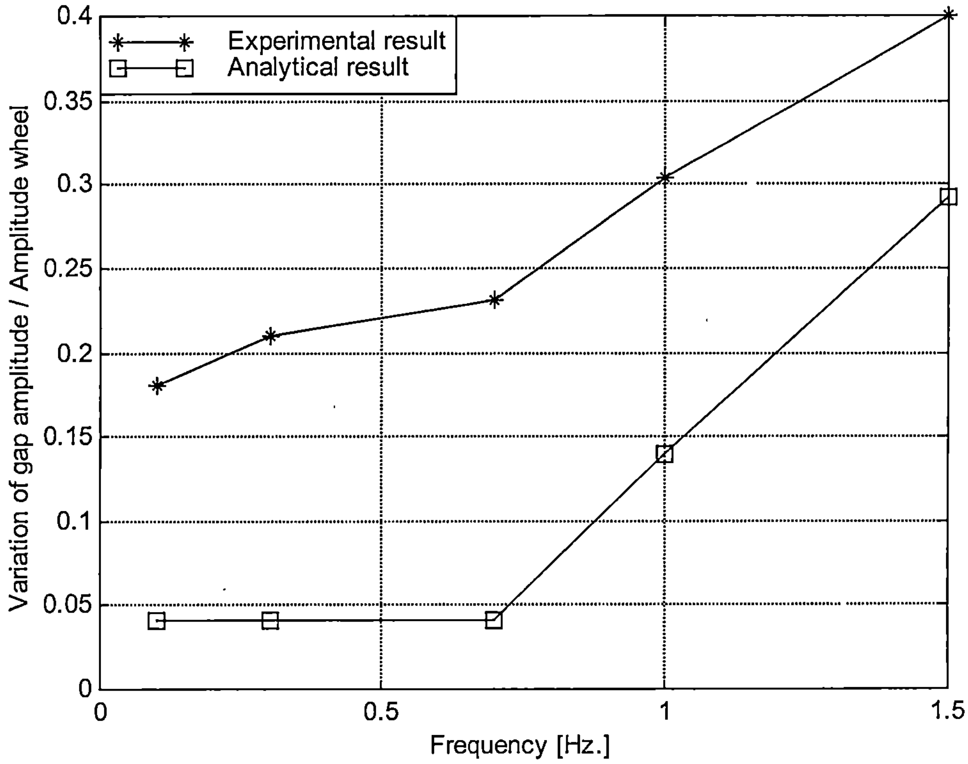

Figure 18 Comparison of Gap Variation - Amplitude 0.6 mm

CHAPTER 4

CONCLUSIONS AND RECOMMENDATIONS

The results of both computer simulation and prototype model testing suggest that the feedback position control system provides significant reduction in gap variation. A typical reduction factor obtained for average paper thickness variation was ¼.

It has to be noted that at higher frequencies and amplitudes the efficiency in gap reduction decreases and the phase angle increases. The performance at high frequency can be improved by decreasing the equivalent volume of the chamber 2 (hose, chamber 2 and diaphragm cavity).

The feedback position control system concept presented by this thesis can be implemented at the inkjet printers to obtain a higher printing quality by reducing the gap between the printing head and paper. The printing head will be attached to the pneumatic transducer such that printing head movement and pneumatic transducer movement will be the same. The diaphragm can be placed on the printing head, this way minimizing the chamber volume.

To use this feedback position control system in reducing the gap between the printing head and paper at an inkjet printer further study would be needed. The diaphragm shape should be optimized using a finite elements analysis software package and the chamber volume should be minimized. It is suggested that the stepping motor have micro stepping capabilities.

Another idea would be to use a rubber bellow instead of the diaphragm. It would be probably more expensive to manufacture but the axial deflection could be significantly higher than at the diaphragm, at the same pressure.

The diaphragm should be designed to permit significant axial movement with essentially zero resistance. In order to obtain linear and repeatable movement with little hysteresis, the resistance to axial movement should be provided by a linear spring (such as the brass cantilever spring) and not by the diaphragm. Because of the forces involved, the rate of the spring will be extremely small

BIBLIOGRAPHY

BIBLIOGRAPHY

Shames, Irving H., *Mechanics of Fluids,* Second Edition, McGraw-Hill Book Co., 1982

Oberg, Erik, Franklin D. Jones, Holbrook L. Horton and Henry H. Ryffel, *Machinery's Handbook 26,* 26^{th} Edition, Industrial Press Inc., New York, 2000

Hahn, Brian D., *Essential MATLAB for Scientists and Enginers,* John Wiley & Sons Inc., New York, 1997

Speckhart, Frank H. and Walter L. green, *A Guide to Using CSMP – The Continuous System Modeling Program,* Prentice-Hall, Englewood Cliffs, NJ, 1976

Shigley, Joseph Edward and Charles R. Mishke, *Mechanical Engineering Design,* 5^{th} Edition, McGraw-Hill Book Co., New York, 1992

APPENDICES

APPENDIX A

DERIVATION OF MASS FLOW EQUATIONS

The Figure A1 repeats the schematic of the pneumatic transducer and shows the notations used in this derivation.

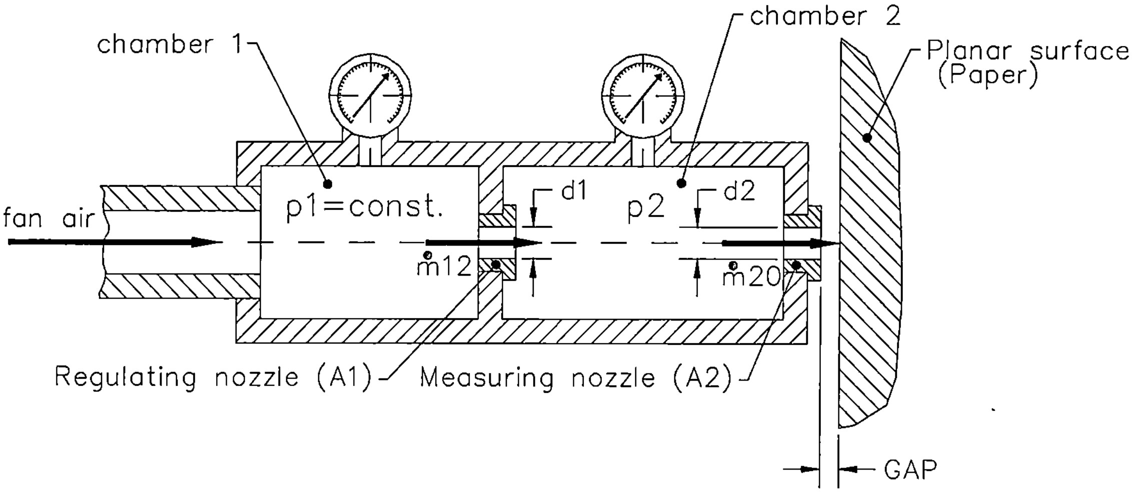

Figure A1 Schematic of Pneumatic Transducer

Several assumptions were made concerning the derivation of the mass flow equations. The flow through the pneumatic transducer is subsonic, adiabatic and compressible. We neglect the losses that occur in the system, namely a sum of the major losses due to frictional effects in the fully developed flow in constant area pipes and the minor losses due to entrances, fittings and cross area changes.

Using the assumptions listed previously the air velocity at the exit of the measuring nozzle is determined by the expression:

$$\frac{v_2^2}{2 \cdot g} = \frac{v_1^2}{2 \cdot g} + \int_{p2}^{p1} V_s \cdot dp \tag{A1}$$

To compute the integral we have to take into account the adiabatic equation and find the specific volume Vs:

$$p \cdot V_s^{\alpha} = p_1 \cdot V_{s1}^{\alpha}$$

$$\Rightarrow V_s^{\alpha} = p_1^{1/\alpha} \cdot V_{s1} \tag{A2}$$

Using equation (A2) the integral will be written successively as following:

$$\int_{p2}^{p1} V_S \cdot dp = \int_{p2}^{p1} \frac{p_1^{1/\alpha} \cdot V_{s1}}{p^{1/\varepsilon}} = p_1^{1/\alpha} \cdot V_{s1} \cdot \int_{p2}^{p1} p^{-1/\alpha} \cdot dp = p_1^{1/\alpha} \cdot V s_1 \cdot \frac{\alpha}{\alpha - 1} \cdot p^{\frac{\alpha}{\alpha-1}} \Bigg|_{p2}^{p1}$$

$$\int_{p2}^{p1} V_S \cdot dp = p_1^{1/\alpha} \cdot V_{s1} \cdot \frac{\alpha}{\alpha - 1} \cdot \left(p_1^{\frac{\alpha-1}{\alpha}} - p_2^{\frac{\alpha-1}{\alpha}} \right) = \frac{\alpha}{\alpha - 1} \cdot p_1^{1/\alpha} \cdot p_1^{\frac{\alpha-1}{\alpha}} \cdot V_{s1} \cdot \left[1 - \left(\frac{p_2}{p_1} \right)^{\frac{\alpha-1}{\alpha}} \right]$$

And finally the integral becomes:

$$\int_{p2}^{p1} V_S \cdot dp = \frac{\alpha}{\alpha - 1} \cdot p_1 \cdot V_{s1} \cdot \left[1 - \left(\frac{p_2}{p_1} \right)^{\frac{\alpha-1}{\alpha}} \right] \tag{A3}$$

Substituting the equation (A3) into equation (A1), and knowing the initial air velocity $v_1 \cong 0$, we obtain the air velocity through regulating nozzle:

$$v_2 = \sqrt{\frac{2 \cdot g \cdot \alpha}{\alpha - 1} \cdot p_1 \cdot V_{s1} \cdot \left[1 - \left(\frac{p_2}{p_1}\right)^{\frac{\alpha-1}{\alpha}}\right]} \tag{A4}$$

The mathematical expression of the mass flow rate through the regulating nozzle is:

$$\dot{m}_{12} = \frac{A_1 \cdot v_2}{V_{s2}} \tag{A5}$$

Also, using the adiabatic equation we obtain the expression for the specific volume:

$$p_1 \cdot V_{s1}{}^{\alpha} = p_2 \cdot V_{s2}^{\alpha}$$

$$\Rightarrow V_{s2} = V_{s1} \cdot \left(\frac{p_1}{p_2}\right)^{1/\alpha} \tag{A6}$$

The perfect gas law and is:

$$p_1 \cdot Vs_1 = R \cdot T \tag{A7}$$

Substituting (A4), (A6), (A7) in (A5) and doing the algebra we obtain the mass flow through the regulating nozzle:

$$\dot{m}_{12} = A_1 \cdot p_1 \cdot \sqrt{\frac{2 \cdot g \cdot \alpha}{(\alpha - 1) \cdot R \cdot T}\left[\left(\frac{p_2}{p_1}\right)^{2/\alpha} - \left(\frac{p_2}{p_1}\right)^{\frac{\alpha+1}{\alpha}}\right]} \tag{A8}$$

The flow area A_2 between the measuring nozzle and the paper is:

$$A_2 = \pi \cdot d_2 \cdot gap \tag{A9}$$

Using the similitude of the mass flow expressions and the expression (A9) we can write the equation of the mass flow rate (A10) through the measuring nozzle:

$$\dot{m}_{20} = \pi \cdot d_2 \cdot gap \cdot p_2 \cdot \sqrt{\frac{2 \cdot g \cdot \alpha}{(\alpha - 1) \cdot R \cdot T}\left[\left(\frac{p_0}{p_2}\right)^{2/\alpha} - \left(\frac{p_0}{p_2}\right)^{\frac{\alpha+1}{\alpha}}\right]} \qquad \textbf{(A10)}$$

APPENDIX B

NEWTON'S METHOD TO SOLVE THE STEADY-STATE EQUATION

Using the mass flow expressions derived in Appendix A and the fact that at steady state the mass flow through the nozzles is the same:

$$\dot{m}_{12} = A_1 \cdot p_1 \cdot \sqrt{\frac{2 \cdot g \cdot \alpha}{(\alpha - 1) \cdot R \cdot T}\left[\left(\frac{p_2}{p_1}\right)^{2/\alpha} - \left(\frac{p_2}{p_1}\right)^{\frac{\alpha+1}{\alpha}}\right]} \qquad \textbf{(B1)}$$

$$\dot{m}_{20} = A_2 \cdot p_2 \cdot \sqrt{\frac{2 \cdot g \cdot \alpha}{(\alpha - 1) \cdot R \cdot T}\left[\left(\frac{p_0}{p_2}\right)^{2/\alpha} - \left(\frac{p_0}{p_2}\right)^{\frac{\alpha+1}{\alpha}}\right]} \qquad \textbf{(B2)}$$

$$\dot{m}_{12} = \dot{m}_{20} \qquad \textbf{(B3)}$$

we can derive the following equation:

$$A_1 \cdot p_1 \sqrt{\frac{2g\alpha}{(\alpha - 1)RT}\left[\left(\frac{p_2}{p_1}\right)^{2/\alpha} - \left(\frac{p_2}{p_1}\right)^{\frac{\alpha+1}{\alpha}}\right]} = A_2 \cdot p_2 \sqrt{\frac{2g\alpha}{(\alpha - 1)RT}\left[\left(\frac{p_0}{p_2}\right)^{2/\alpha} - \left(\frac{p_0}{p_2}\right)^{\frac{\alpha+1}{\alpha}}\right]} \qquad \textbf{(B4)}$$

Squaring the expression (B4) and simplifying the identities we obtain successively:

$$\left(\frac{p_0}{p_2}\right)^{2/\alpha} - \left(\frac{p_0}{p_2}\right)^{\frac{\alpha+1}{\alpha}} = \frac{A_1^2 \cdot p_1^2}{A_2^2 \cdot p_2^2} \cdot \left(\frac{p_2}{p_1}\right)^{2/\alpha} - \frac{A_1^2 \cdot p_1^2}{A_2^2 \cdot p_2^2} \cdot \left(\frac{p_2}{p_1}\right)^{\frac{\alpha+1}{\alpha}}$$

$$A_1^2 \cdot p_1^2 \cdot \left[\left(\frac{p_2}{p_1}\right)^{2/\alpha} - \left(\frac{p_2}{p_1}\right)^{\frac{\alpha+1}{\alpha}}\right] = A_2^2 \cdot p_2^2 \cdot \left[\left(\frac{p_0}{p_2}\right)^{2/\alpha} - \left(\frac{p_0}{p_2}\right)^{\frac{\alpha+1}{\alpha}}\right]$$

$$\left(\frac{p_0}{p_2}\right)^{2/\alpha}\cdot\frac{\left(\frac{p_2}{p_1}\right)^{2/\alpha}}{\left(\frac{p_2}{p_1}\right)^{2/\alpha}}-\left(\frac{p_0}{p_2}\right)^{\frac{\alpha+1}{\alpha}}\cdot\frac{\left(\frac{p_2}{p_1}\right)^{\frac{\alpha+1}{\alpha}}}{\left(\frac{p_2}{p_1}\right)^{\frac{\alpha+1}{\alpha}}}=\frac{A_1^2}{A_2^2}\cdot\left(\frac{p_1}{p_2}\right)^2\cdot\left(\frac{p_2}{p_1}\right)^{2/\alpha}-\frac{A_1^2}{A_2^2}\cdot\left(\frac{p_1}{p_2}\right)^2\cdot\left(\frac{p_2}{p_1}\right)^{\frac{\alpha+1}{\alpha}}$$

$$\left(\frac{p_0}{p_1}\right)^{2/\alpha}\cdot\left(\frac{p_2}{p_1}\right)^{-(2/\alpha)}-\left(\frac{p_0}{p_1}\right)^{\frac{\alpha+1}{\alpha}}\cdot\left(\frac{p_2}{p_1}\right)^{-\left(\frac{\alpha+1}{\alpha}\right)}-\frac{A_1^2}{A_2^2}\cdot\left(\frac{p_1}{p_2}\right)^2\cdot\left(\frac{p_2}{p_1}\right)^{2/\alpha}+\frac{A_1^2}{A_2^2}\cdot\left(\frac{p_1}{p_2}\right)^2\cdot\left(\frac{p_2}{p_1}\right)^{\frac{\alpha+1}{\alpha}}=0$$

$$\left(\frac{p_0}{p_1}\right)^{2/\alpha}\cdot\left(\frac{p_2}{p_1}\right)^{-(2/\alpha)}-\left(\frac{p_0}{p_1}\right)^{\frac{\alpha+1}{\alpha}}\cdot\left(\frac{p_2}{p_1}\right)^{-\left(\frac{\alpha+1}{\alpha}\right)}-\frac{A_1^2}{A_2^2}\cdot\left(\frac{p_2}{p_1}\right)^{(2-2\cdot\alpha)/\alpha}+\frac{A_1^2}{A_2^2}\cdot\left(\frac{p_2}{p_1}\right)^{\frac{1-\alpha}{\alpha}}=0$$

$$\left(\frac{p_0}{p_1}\right)^{2/\alpha}\left(\frac{p_2}{p_1}\right)^{-(2/\alpha)}-\left(\frac{p_0}{p_1}\right)^{\frac{\alpha+1}{\alpha}}\left(\frac{p_2}{p_1}\right)^{-\left(\frac{\alpha+1}{\alpha}\right)}-\frac{A_1^2}{A_2^2}\left(\frac{p_2}{p_1}\right)^{-2}\left(\frac{p_2}{p_1}\right)^{2/\alpha}+\frac{A_1^2}{A_2^2}\left(\frac{p_2}{p_1}\right)^{-2}\left(\frac{p_2}{p_1}\right)^{\frac{\alpha+1}{\alpha}}=0$$

Finally:

$$A_2^2\left(\frac{p_0}{p_1}\right)^{2/\alpha}\left(\frac{p_2}{p_1}\right)^{-(2/\alpha)}-A_2^2\left(\frac{p_0}{p_1}\right)^{\frac{\alpha+1}{\alpha}}\left(\frac{p_2}{p_1}\right)^{-\left(\frac{\alpha+1}{\alpha}\right)}-A_1^2\left(\frac{p_2}{p_1}\right)^{(2-2\cdot\alpha)/\alpha}+A_1^2\left(\frac{p_2}{p_1}\right)^{\frac{1-\alpha}{\alpha}}=0 \qquad \textbf{(B5)}$$

with $A_2 = \pi \cdot d_2 \cdot gap$.

To solve for the quotient p_2 / p_1 from equation (B5) we use the Newton's method. This method is based on a linear approximation of the function using a tangent to the curve. Figure A1 gives a graphical description of the method. Starting from a single initial estimate, x_0 , that is not too far from a root, we move along the tangent to its intersection with the x-axis, and take that as the next approximation.

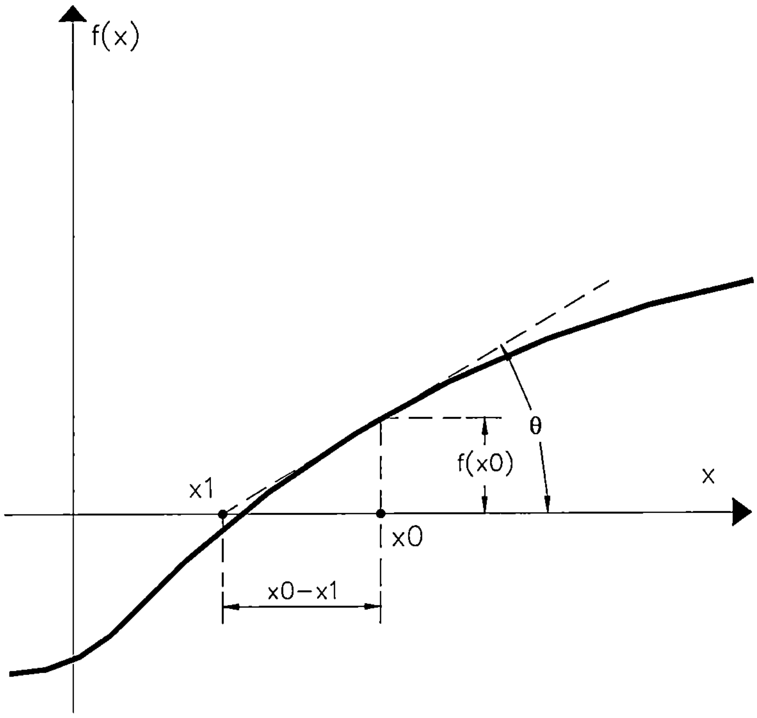

Figure B1 Newton's method schematic

This is continued until either the successive close or the value of the function is sufficiently near zero. The calculation scheme follows immediately from the right triangle shown in Figure B1, which has the angle of inclination of the tangent line to the curve at x = x_0 as one of its acute angles:

$$\tan\theta = f'(x_0) = \frac{f(x_0)}{x_0 - x_1} \Rightarrow x_1 = x_0 - \frac{f(x_0)}{f'(x_0)}$$

We continue the calculation scheme by computing:

$$x_2 = x_1 - \frac{f(x_1)}{f'(x_1)}$$

If we consider the expression (B5) and our function being $f(p_2/p_1)$, to use the Newton's method we have to calculate the first derivative of this function which will be:

$$f'\left(\frac{p_2}{p_1}\right)=-A_2^2\left(\frac{2}{\alpha}\right)\left(\frac{p_0}{p_1}\right)^{2/\alpha}\left(\frac{p_2}{p_1}\right)^{-\left(\frac{2+\alpha}{\alpha}\right)}+A_2^2\left(\frac{\alpha+1}{\alpha}\right)\left(\frac{p_0}{p_1}\right)^{\frac{\alpha+1}{\alpha}}\left(\frac{p_2}{p_1}\right)^{-\left(\frac{2\cdot\alpha+1}{\alpha}\right)}-A_1^2\left(\frac{2-2\cdot\alpha}{\alpha}\right)\left(\frac{p_2}{p_1}\right)^{(2-3\cdot\alpha)/\alpha}+A_1^2\left(\frac{1-\alpha}{\alpha}\right)\left(\frac{p_2}{p_1}\right)^{\frac{1-2\cdot\alpha}{\alpha}}$$

The solution of equation (B6), following Newton's method, was obtained using a Matlab program, which can be seen in Appendix D. The MatLab program performs 21 iterations and uses a tolerance of 0.0000000000001 when comparing the values resulted from iterations.

APPENDIX C

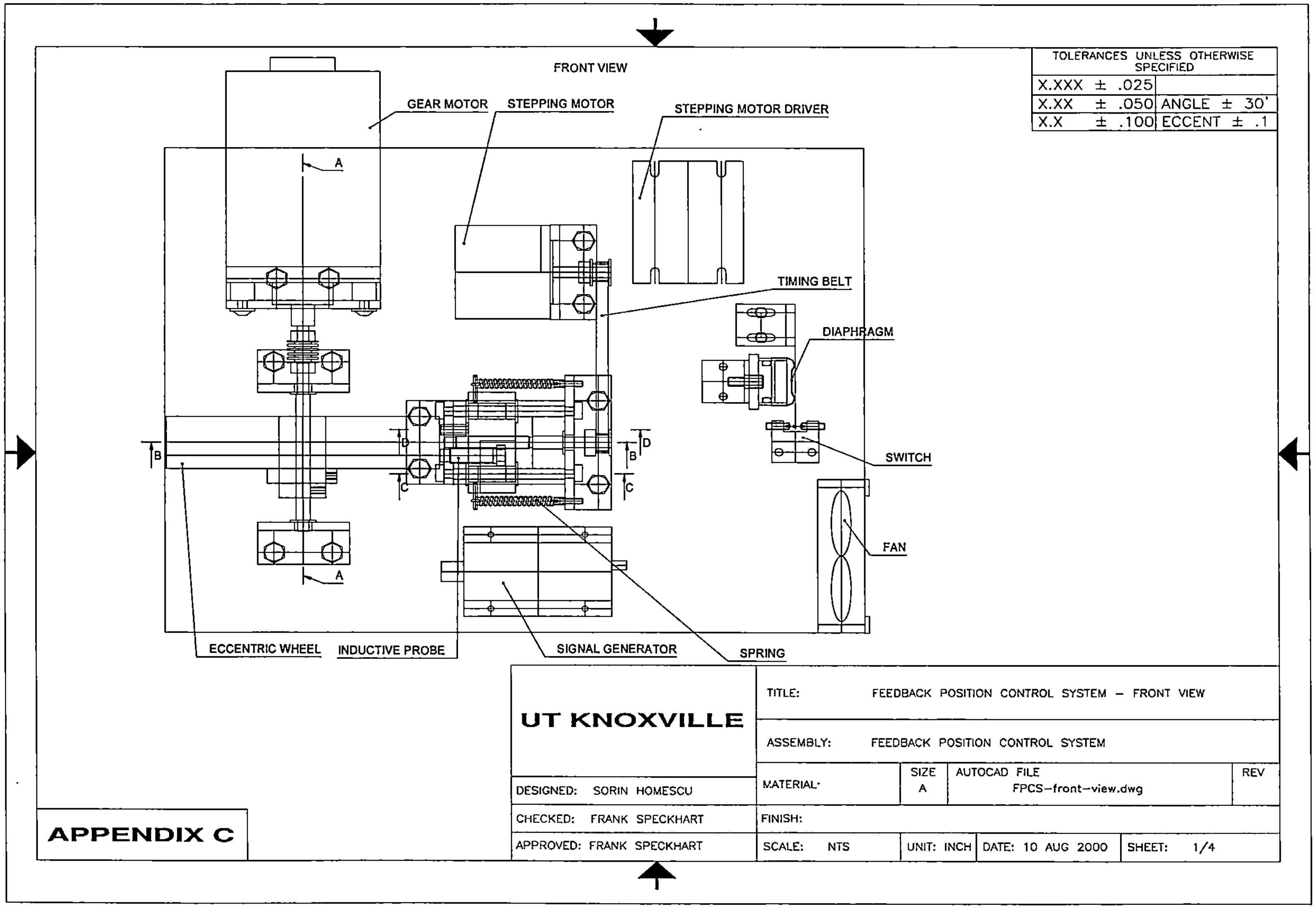
FRONT VIEW
GEAR MOTOR
STEPPING MOTOR
STEPPING MOTOR DRIVER
TIMING BELT
DIAPHRAGM
SWITCH
FAN
ECCENTRIC WHEEL
INDUCTIVE PROBE
SIGNAL GENERATOR
SPRING
A
A
B
B
C
C
D
D
TOLERANCES UNLESS OTHERWISE SPECIFIED
X.XXX ± .025
X.XX ± .050 ANGLE ± 30'
X.X ± .100 ECCENT ± .1
UT KNOXVILLE
TITLE: FEEDBACK POSITION CONTROL SYSTEM – FRONT VIEW
ASSEMBLY: FEEDBACK POSITION CONTROL SYSTEM
DESIGNED: SORIN HOMESCU
MATERIAL:
SIZE A
AUTOCAD FILE FPCS–front–view.dwg
REV
CHECKED: FRANK SPECKHART
FINISH:
APPROVED: FRANK SPECKHART
SCALE: NTS
UNIT: INCH
DATE: 10 AUG 2000
SHEET: 1/4
APPENDIX C

TOLERANCES UNLESS OTHERWISE SPECIFIED	
X.XXX ± .025	
X.XX ± .050	ANGLE ± 30'
X.X ± .100	ECCENT ± .1

SECTION A-A

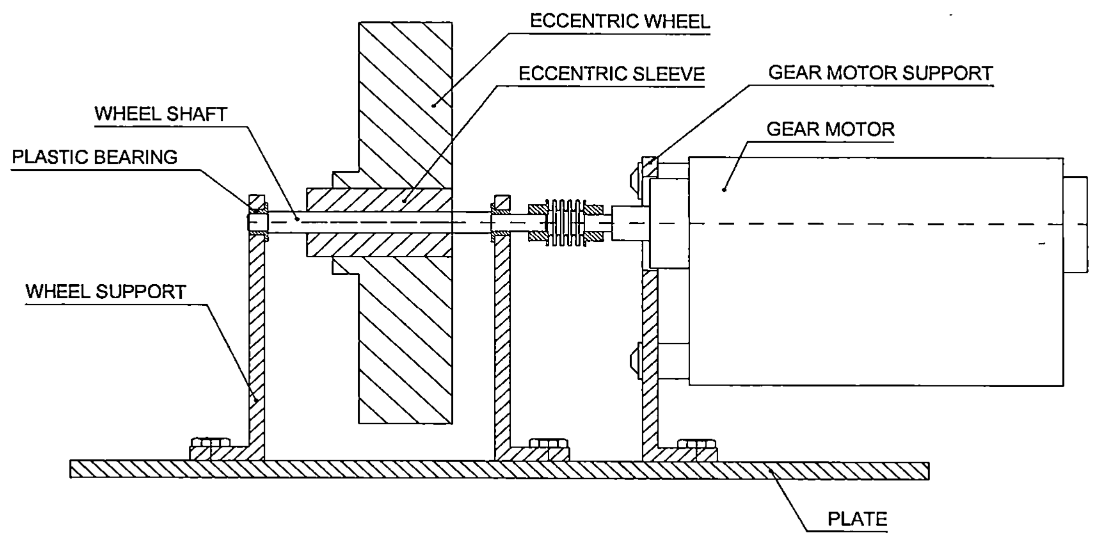

UT KNOXVILLE

TITLE: SECTION A–A				
ASSEMBLY: FEEDBACK POSITION CONTROL SYSTEM				
DESIGNED: SORIN HOMESCU	MATERIAL:	SIZE A	AUTOCAD FILE sectionA–A.dwg	REV
CHECKED: FRANK SPECKHART	FINISH:			
APPROVED: FRANK SPECKHART	SCALE: 1:2	UNIT: INCH	DATE: 10 AUG 2000	SHEET: 2/4

APPENDIX C

TOLERANCES UNLESS OTHERWISE SPECIFIED	
X.XXX ± 025	
X.XX ± .050	ANGLE ± 30'
X.X ± .100	ECCENT ± .1

SECTION B-B

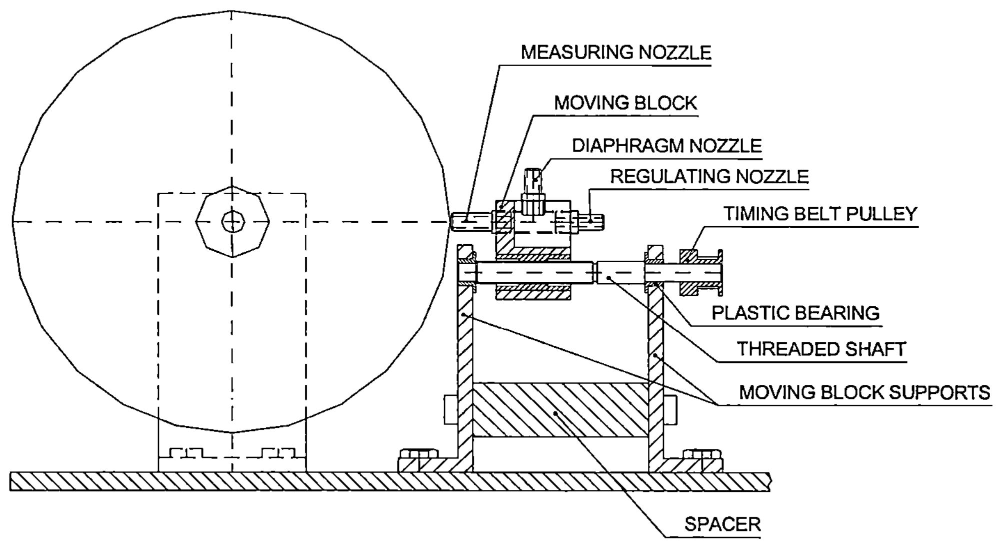

APPENDIX C

UT KNOXVILLE	TITLE: SECTION B-B			
	ASSEMBLY: FEEDBACK POSITION CONTROL SYSTEM			
DESIGNED: SORIN HOMESCU	MATERIAL:	SIZE A	AUTOCAD FILE sectionB-B.dwg	REV
CHECKED: FRANK SPECKHART	FINISH:			
APPROVED: FRANK SPECKHART	SCALE: 1:2	UNIT: INCH	DATE: 10 AUG 2000	SHEET: 3/4

TOLERANCES UNLESS OTHERWISE SPECIFIED	
X.XXX ± .025	
X.XX ± .050	ANGLE ± 30'
X.X ± .100	ECCENT ± .1

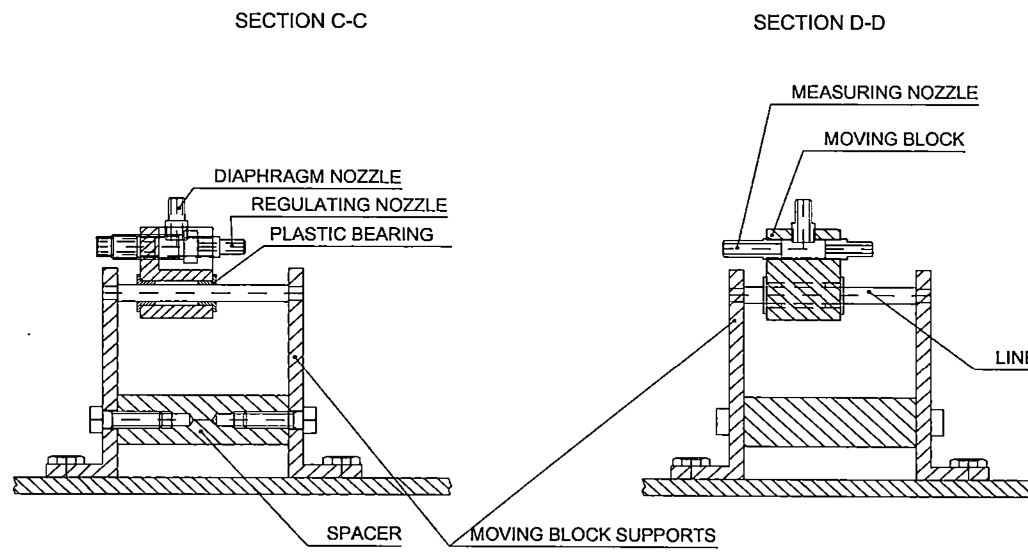

UT KNOXVILLE	TITLE: SECTION C–C / SECTION D–D			
	ASSEMBLY: FEEDBACK POSITION CONTROL SYSTEM			
DESIGNED SORIN HOMESCU	MATERIAL:	SIZE A	AUTOCAD FILE sectionC–C_D–D.dwg	REV
CHECKED: FRANK SPECKHART	FINISH:			
APPROVED: FRANK SPECKHART	SCALE: 1:2	UNIT: INCH	DATE: 10 AUG 2000	SHEET: 4/4

APPENDIX C

TOLERANCES UNLESS OTHERWISE SPECIFIED	
X.XXX ± .025	
X.XX ± .050	ANGLE ± 30'
X.X ± .100	ECCENT ± .1

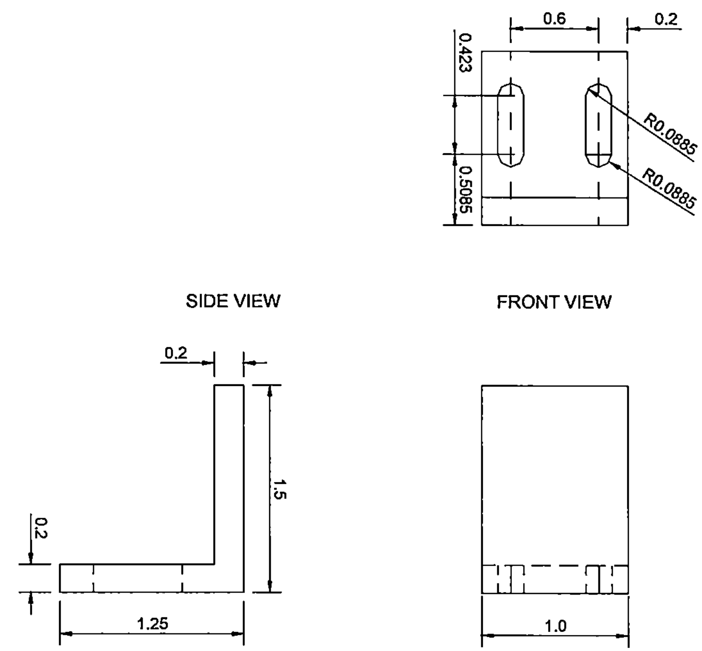

UT KNOXVILLE	TITLE CANTILEVER BEAM SUPPORT			
	ASSEMBLY: FEEDBACK POSITION CONTROL SYSTEM			
DESIGNED: SORIN HOMESCU	MATERIAL: STEEL	SIZE A	AUTOCAD FILE cantilever-beam-support.dwg	REV
CHECKED: FRANK SPECKHART	FINISH:			
APPROVED: FRANK SPECKHART	SCALE: 1:1	UNIT: INCH	DATE: 10 AUG 2000	SHEET: 1/1

APPENDIX C

APPENDIX C

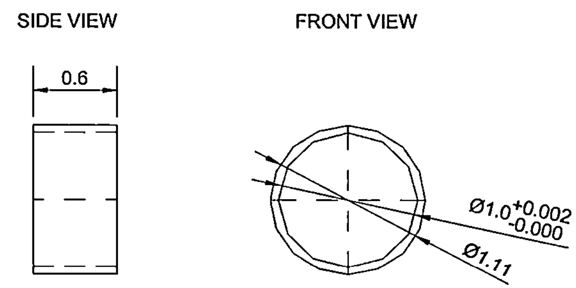

TOLERANCES UNLESS OTHERWISE SPECIFIED	
X.XXX ± .025	
X.XX ± .050	ANGLE ± 30'
X.X ± .100	ECCENT ± .1

UT KNOXVILLE	TITLE: CYLINDER			
	ASSEMBLY: FEEDBACK POSITION CONTROL SYSTEM			
DESIGNED: SORIN HOMESCU	MATERIAL: ALUMINUM	SIZE A	AUTOCAD FILE cylinder.dwg	REV
CHECKED: FRANK SPECKHART	FINISH:			
APPROVED: FRANK SPECKHART	SCALE: 1:1	UNIT. INCH	DATE: 10 AUG 2000	SHEET: 1/1

TOLERANCES UNLESS OTHERWISE SPECIFIED	
X.XXX ± .025	
X.XX ± .050	ANGLE ± 30'
X.X ± .100	ECCENT ± .1

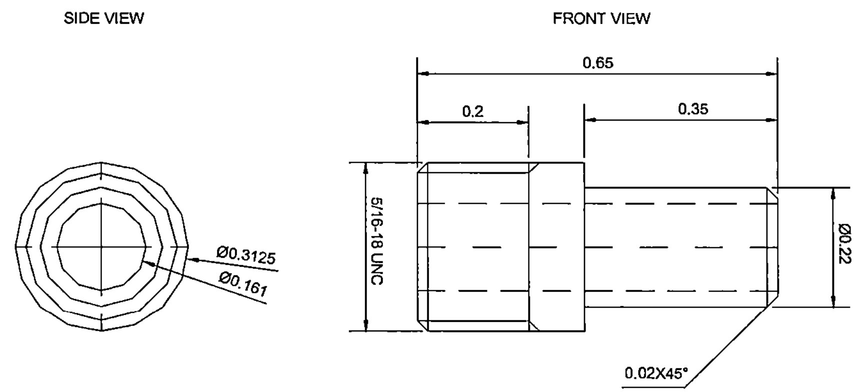

UT KNOXVILLE	TITLE: DIAPHRAGM NOZZLE				
	ASSEMBLY: FEEDBACK POSITION CONTROL SYSTEM				
DESIGNED: SORIN HOMESCU	MATERIAL: STEEL	SIZE A	AUTOCAD FILE diaphragm-nozzle.dwg		REV
CHECKED: FRANK SPECKHART	FINISH:				
APPROVED: FRANK SPECKHART	SCALE: 4:1	UNIT: INCH	DATE: 10 AUG 2000	SHEET: 1/1	

APPENDIX C

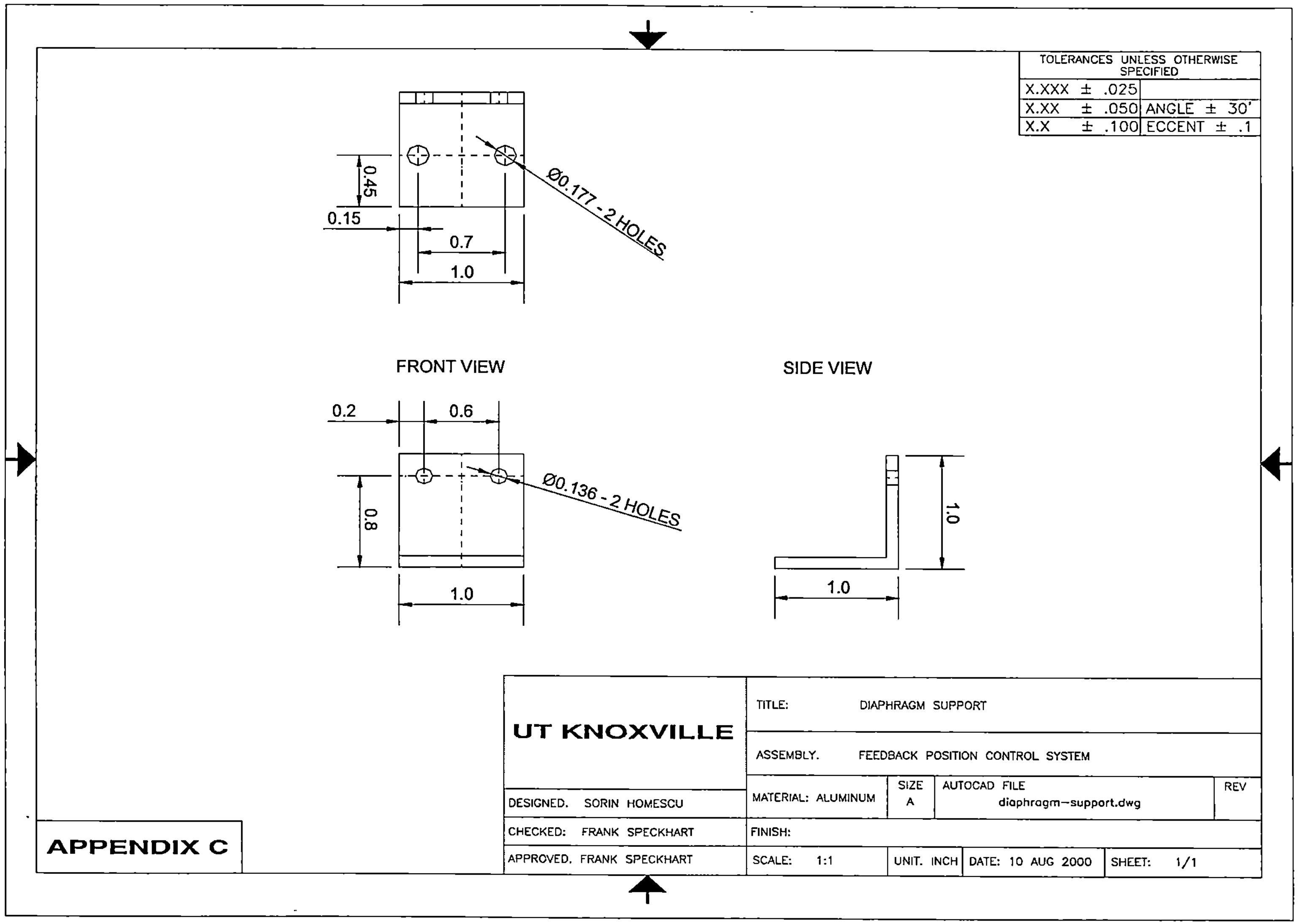
TOLERANCES UNLESS OTHERWISE SPECIFIED
X.XXX ± .025
X.XX ± .050
ANGLE ± 30'
X.X ± .100
ECCENT ± .1
Ø0.177 - 2 HOLES
0.45
0.15
0.7
1.0
FRONT VIEW
SIDE VIEW
0.2
0.6
Ø0.136 - 2 HOLES
0.8
1.0
1.0
1.0
UT KNOXVILLE
TITLE: DIAPHRAGM SUPPORT
ASSEMBLY. FEEDBACK POSITION CONTROL SYSTEM
MATERIAL: ALUMINUM
SIZE A
AUTOCAD FILE diaphragm-support.dwg
REV
DESIGNED. SORIN HOMESCU
CHECKED: FRANK SPECKHART
APPROVED. FRANK SPECKHART
FINISH:
SCALE: 1:1
UNIT. INCH
DATE: 10 AUG 2000
SHEET: 1/1
APPENDIX C

TOLERANCES UNLESS OTHERWISE SPECIFIED	
X.XXX ± .025	
X.XX ± .050	ANGLE ± 30'
X.X ± .100	ECCENT ± .1

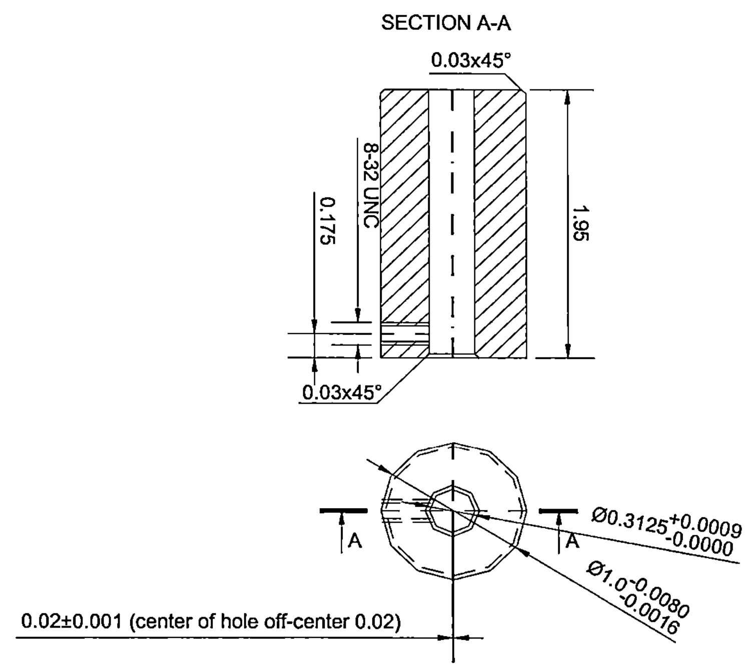

UT KNOXVILLE	TITLE: ECCENTRIC SLEEVE				
	ASSEMBLY: FEEDBACK POSITION CONTROL SYSTEM				
DESIGNED: SORIN HOMESCU	MATERIAL: ALUMINUM	SIZE A	AUTOCAD FILE eccentric–sleeve.dwg		REV
CHECKED: FRANK SPECKHART	FINISH:				
APPROVED: FRANK SPECKHART	SCALE: 1:1	UNIT: INCH	DATE: 10 AUG 2000	SHEET: 1/1	

APPENDIX C

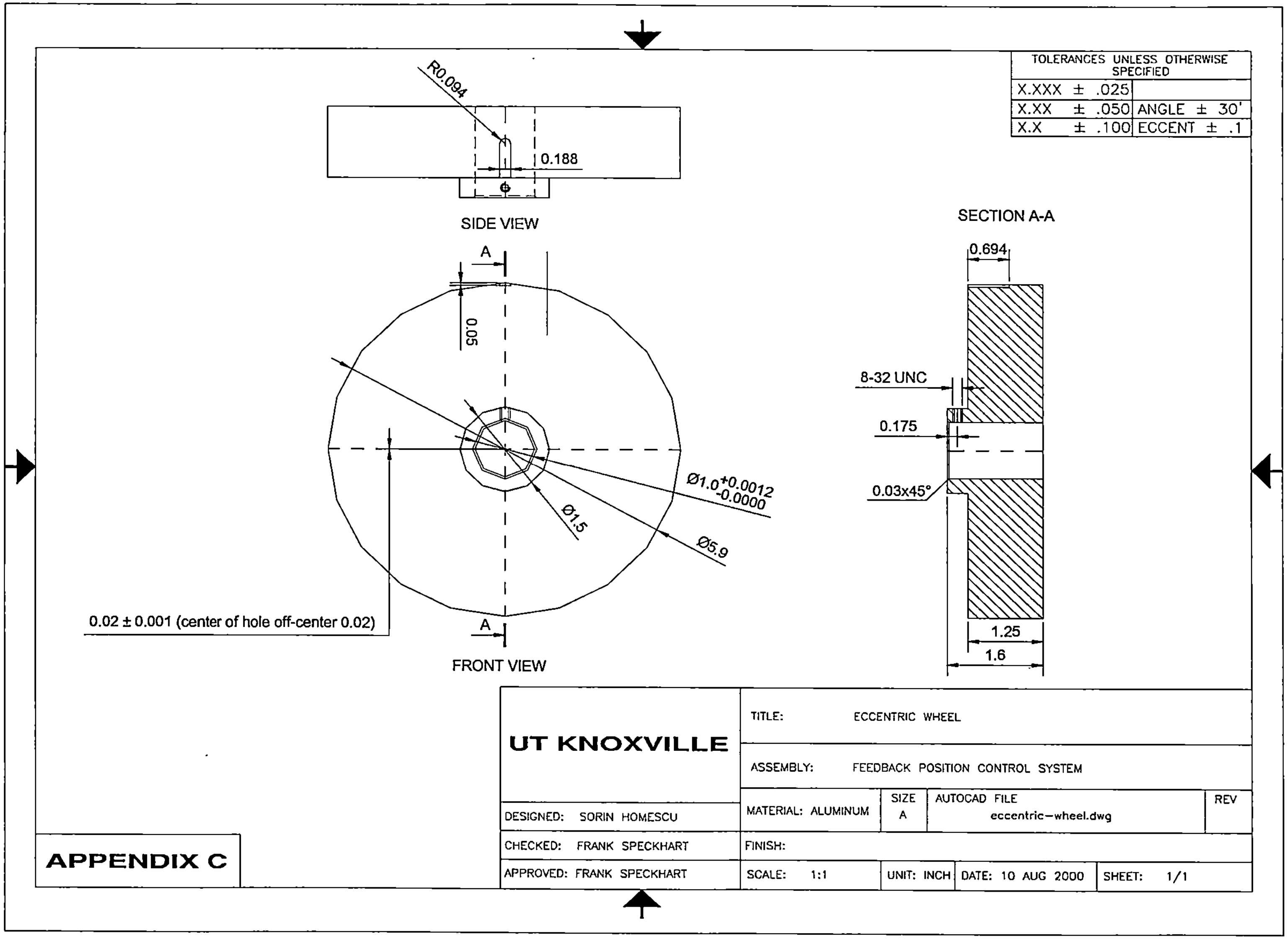
TOLERANCES UNLESS OTHERWISE SPECIFIED
X.XXX ± .025
X.XX ± .050 ANGLE ± 30'
X.X ± .100 ECCENT ± .1
R0.094
0.188
SIDE VIEW
A
0.05
Ø1.0+0.0012 -0.0000
Ø1.5
Ø5.9
0.02 ± 0.001 (center of hole off-center 0.02)
A
FRONT VIEW
SECTION A-A
0.694
8-32 UNC
0.175
0.03x45°
1.25
1.6
UT KNOXVILLE
TITLE: ECCENTRIC WHEEL
ASSEMBLY: FEEDBACK POSITION CONTROL SYSTEM
DESIGNED: SORIN HOMESCU
MATERIAL: ALUMINUM
SIZE A
AUTOCAD FILE eccentric-wheel.dwg
REV
CHECKED: FRANK SPECKHART
FINISH:
APPROVED: FRANK SPECKHART
SCALE: 1:1
UNIT: INCH
DATE: 10 AUG 2000
SHEET: 1/1
APPENDIX C

TOLERANCES UNLESS OTHERWISE SPECIFIED	
X.XXX ± .025	
X.XX ± .050	ANGLE ± 30'
X.X ± .100	ECCENT ± .1

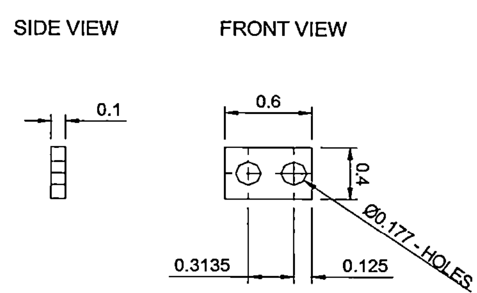

UT KNOXVILLE	TITLE. FAN MOUNTING			
	ASSEMBLY: FEEDBACK POSITION CONTROL SYSTEM			
DESIGNED: SORIN HOMESCU	MATERIAL: STEEL	SIZE A	AUTOCAD FILE fan-mounting.dwg	REV
CHECKED: FRANK SPECKHART	FINISH.			
APPROVED· FRANK SPECKHART	SCALE. 1:1	UNIT: INCH	DATE: 10 AUG 2000	SHEET: 1/1

APPENDIX C

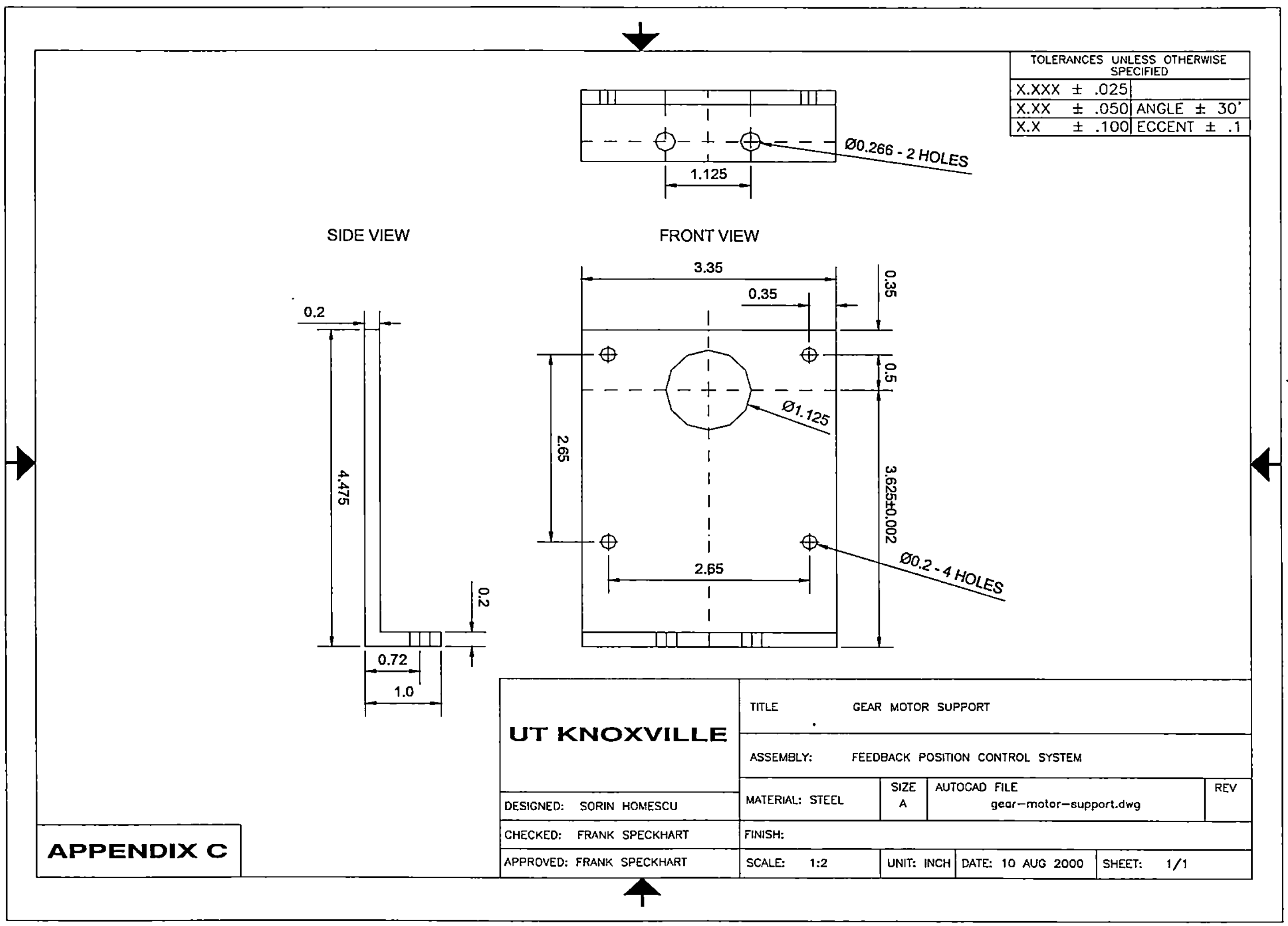

TOLERANCES UNLESS OTHERWISE SPECIFIED
X.XXX ± .025
X.XX ± .050 ANGLE ± 30'
X.X ± .100 ECCENT ± .1
Ø0.266 - 2 HOLES
1.125
SIDE VIEW
FRONT VIEW
3.35
0.35
0.35
0.5
Ø1.125
2.65
3.625±0.002
2.65
Ø0.2 - 4 HOLES
0.2
4.475
0.2
0.72
1.0
UT KNOXVILLE
TITLE GEAR MOTOR SUPPORT
ASSEMBLY: FEEDBACK POSITION CONTROL SYSTEM
DESIGNED: SORIN HOMESCU
MATERIAL: STEEL
SIZE A
AUTOCAD FILE gear-motor-support.dwg
REV
CHECKED: FRANK SPECKHART
FINISH:
APPROVED: FRANK SPECKHART
SCALE: 1:2
UNIT: INCH
DATE: 10 AUG 2000
SHEET: 1/1
APPENDIX C

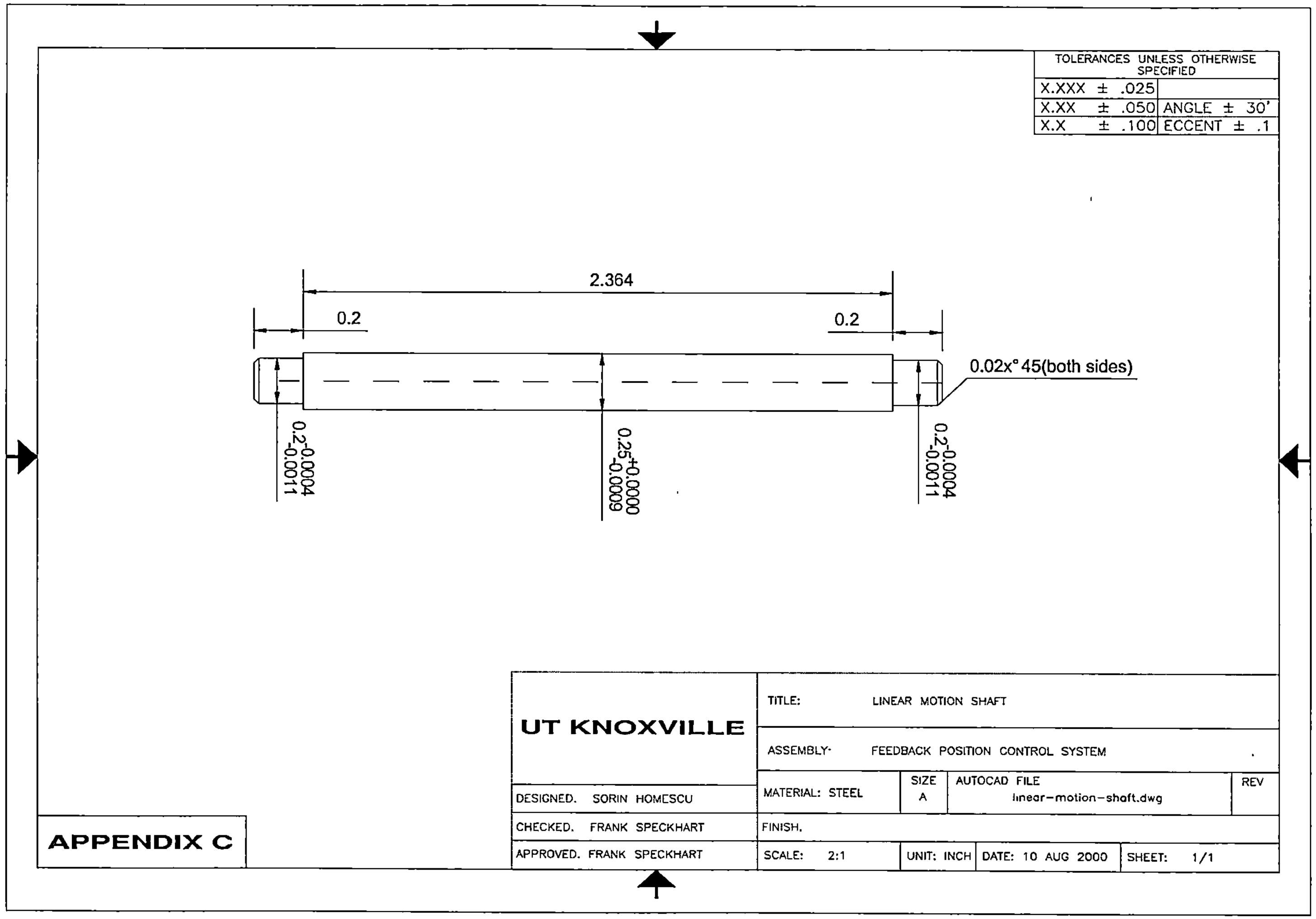
TOLERANCES UNLESS OTHERWISE SPECIFIED
X.XXX ± .025
X.XX ± .050
ANGLE ± 30'
X.X ± .100
ECCENT ± .1
2.364
0.2
0.2
0.02x° 45(both sides)
0.2 -0.0004 -0.0011
0.25 +0.0000 -0.0009
0.2 -0.0004 -0.0011
UT KNOXVILLE
TITLE: LINEAR MOTION SHAFT
ASSEMBLY: FEEDBACK POSITION CONTROL SYSTEM
DESIGNED. SORIN HOMESCU
CHECKED. FRANK SPECKHART
APPROVED. FRANK SPECKHART
MATERIAL: STEEL
SIZE A
AUTOCAD FILE linear-motion-shaft.dwg
REV
FINISH.
SCALE: 2:1
UNIT: INCH
DATE: 10 AUG 2000
SHEET: 1/1
APPENDIX C

TOLERANCES UNLESS OTHERWISE SPECIFIED	
X.XXX ± .025	
X.XX ± .050	ANGLE ± 30'
X.X ± .100	ECCENT ± .1

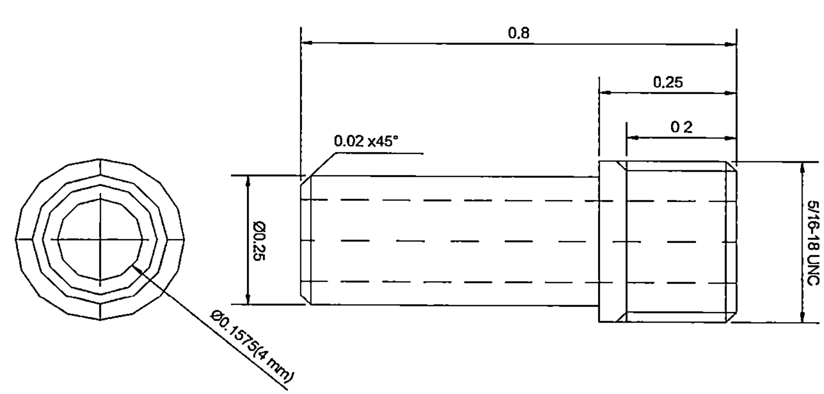

UT KNOXVILLE	TITLE: MEASURING NOZZLE				
	ASSEMBLY: FEEDBACK POSITION CONTROL SYSTEM				
DESIGNED: SORIN HOMESCU	MATERIAL: STEEL	SIZE A	AUTOCAD FILE measuring-nozzle.dwg		REV
CHECKED: FRANK SPECKHART	FINISH:				
APPROVED: FRANK SPECKHART	SCALE: 4:1	UNIT: INCH	DATE: 10 AUG 2000	SHEET: 1/1	

APPENDIX C

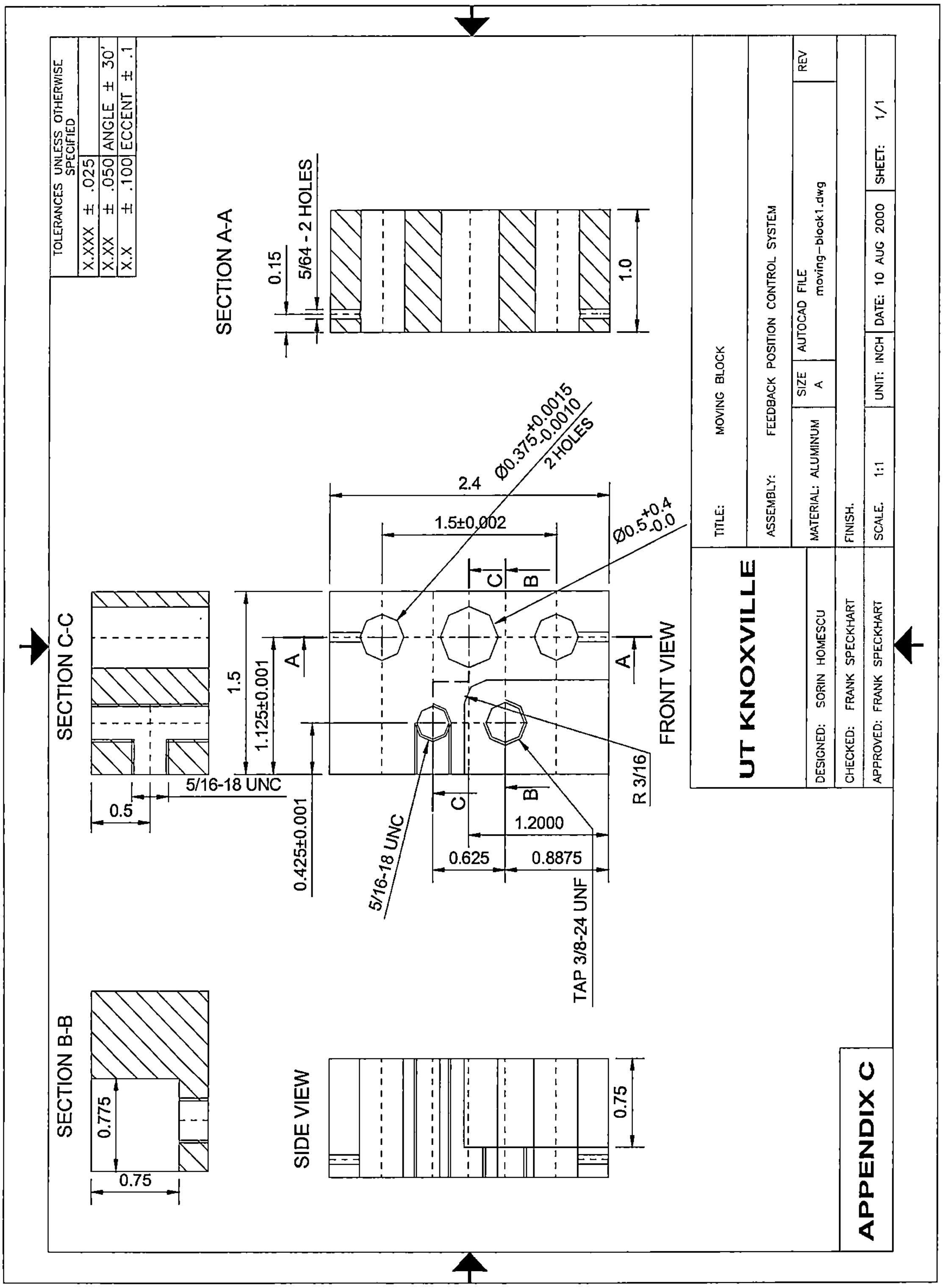
TOLERANCES UNLESS OTHERWISE SPECIFIED
X.XXX ± .025
X.XX ± .050
X.X ± .100
ANGLE ± 30'
ECCENT ± .1
SECTION A-A
0.15
5/64 - 2 HOLES
1.0
SECTION C-C
SECTION B-B
SIDE VIEW
FRONT VIEW
2.4
1.5±0.002
Ø0.375+0.0015 -0.0010
2 HOLES
Ø0.5+0.4 -0.0
1.5
1.125±0.001
0.425±0.001
5/16-18 UNC
0.5
5/16-18 UNC
R 3/16
1.2000
0.625
0.8875
TAP 3/8-24 UNF
0.775
0.75
0.75
A
B
C
UT KNOXVILLE
TITLE: MOVING BLOCK
ASSEMBLY: FEEDBACK POSITION CONTROL SYSTEM
DESIGNED: SORIN HOMESCU
CHECKED: FRANK SPECKHART
APPROVED: FRANK SPECKHART
MATERIAL: ALUMINUM
SIZE A
AUTOCAD FILE moving-block1.dwg
REV
FINISH.
SCALE. 1:1
UNIT: INCH
DATE: 10 AUG 2000
SHEET: 1/1
APPENDIX C

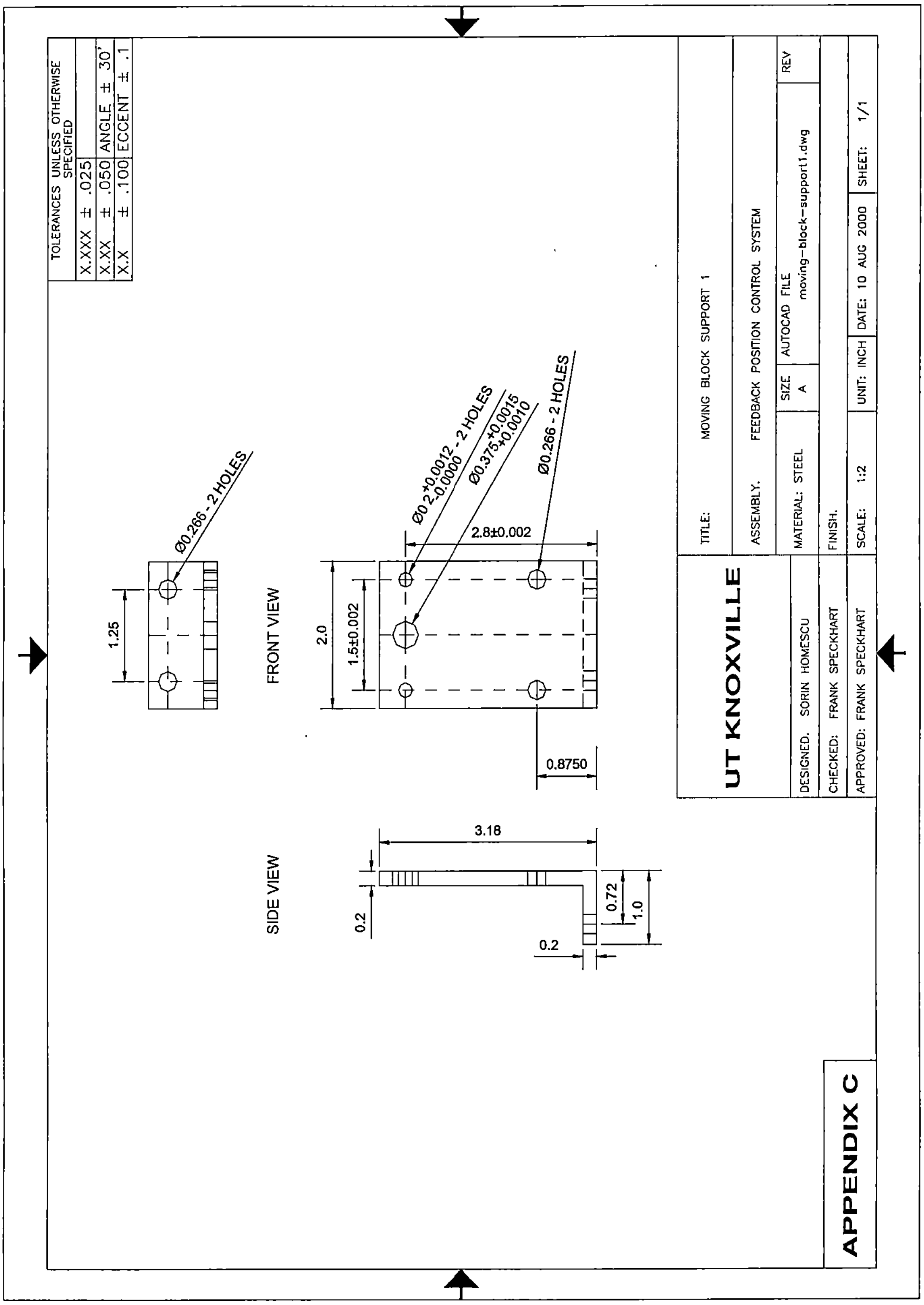
TOLERANCES UNLESS OTHERWISE SPECIFIED
X.XXX ± .025
X.XX ± .050
ANGLE ± 30'
X.X ± .100
ECCENT ± .1
Ø0.266 - 2 HOLES
1.25
FRONT VIEW
Ø0.2+0.0012 -0.0000 - 2 HOLES
Ø0.375+0.0015 +0.0010
Ø0.266 - 2 HOLES
2.8±0.002
2.0
1.5±0.002
0.8750
SIDE VIEW
3.18
0.2
0.72
1.0
0.2
UT KNOXVILLE
TITLE: MOVING BLOCK SUPPORT 1
ASSEMBLY. FEEDBACK POSITION CONTROL SYSTEM
DESIGNED. SORIN HOMESCU
MATERIAL: STEEL
SIZE A
AUTOCAD FILE moving-block-support1.dwg
REV
CHECKED: FRANK SPECKHART
FINISH.
APPROVED: FRANK SPECKHART
SCALE: 1:2
UNIT: INCH
DATE: 10 AUG 2000
SHEET: 1/1
APPENDIX C

TOLERANCES UNLESS OTHERWISE SPECIFIED	
X.XXX ± .025	
X.XX ± .050	ANGLE ± 30'
X.X ± .100	ECCENT ± .1

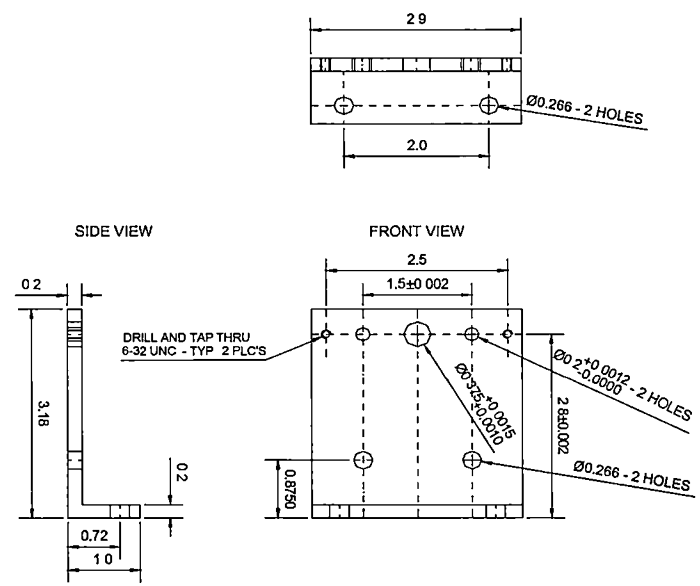

UT KNOXVILLE	TITLE: MOVING BLOCK SUPPORT 2				
	ASSEMBLY: FEEDBACK POSITION CONTROL SYSTEM				
DESIGNED: SORIN HOMESCU	MATERIAL: STEEL	SIZE A	AUTOCAD FILE moving-block-support2.dwg		REV
CHECKED: FRANK SPECKHART	FINISH:				
APPROVED. FRANK SPECKHART	SCALE: 1:2	UNIT· INCH	DATE: 10 AUG 2000	SHEET· 1/1	

APPENDIX C

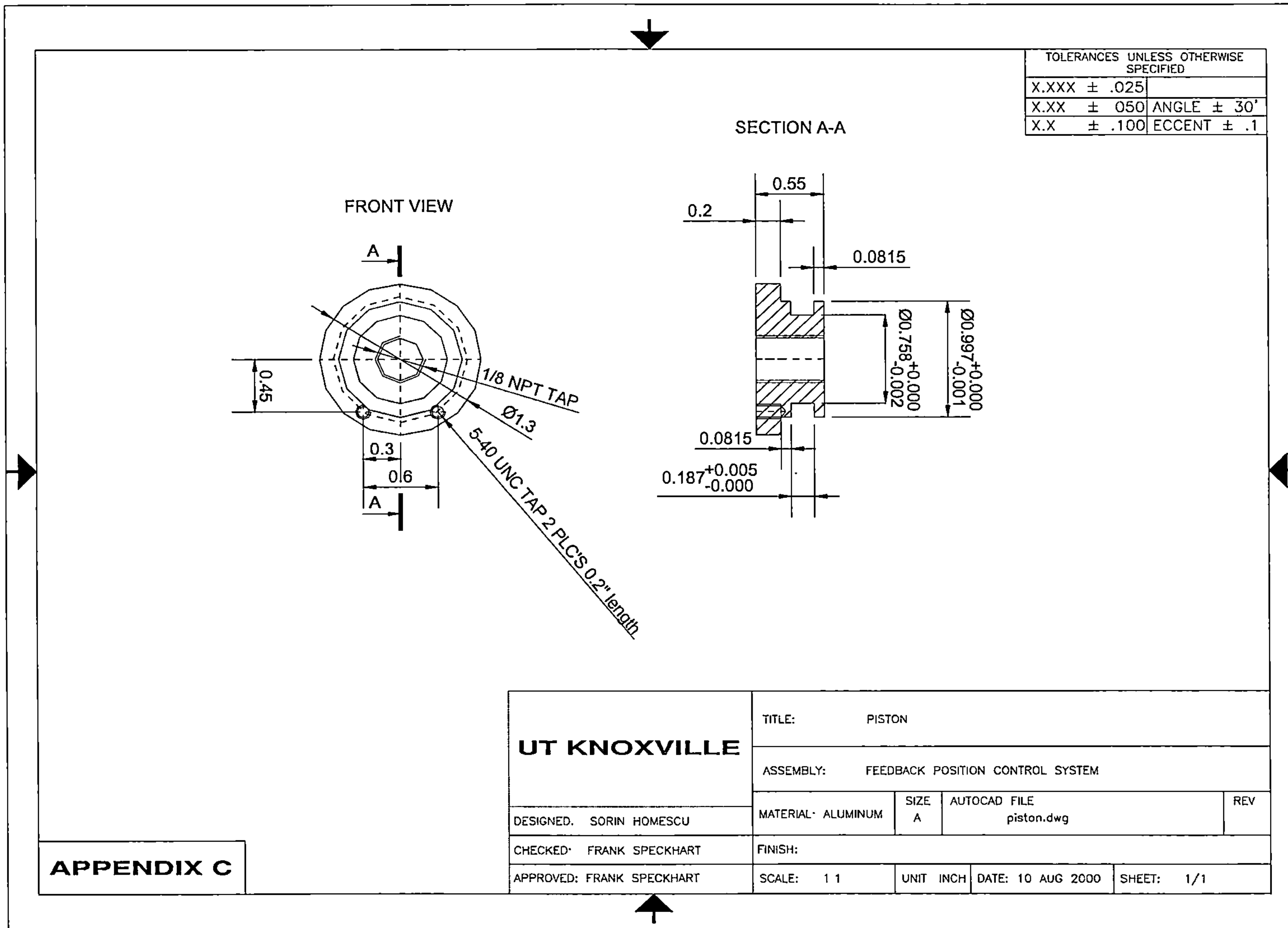
TOLERANCES UNLESS OTHERWISE SPECIFIED
X.XXX ± .025
X.XX ± 050 ANGLE ± 30'
X.X ± .100 ECCENT ± .1
FRONT VIEW
SECTION A-A
A
0.45
0.3
0.6
1/8 NPT TAP
Ø1.3
5-40 UNC TAP 2 PLC'S 0.2" length
0.55
0.2
0.0815
Ø0.758 +0.000 -0.002
Ø0.997 +0.000 -0.001
0.0815
0.187 +0.005 -0.000
UT KNOXVILLE
TITLE: PISTON
ASSEMBLY: FEEDBACK POSITION CONTROL SYSTEM
MATERIAL· ALUMINUM
SIZE A
AUTOCAD FILE piston.dwg
REV
DESIGNED. SORIN HOMESCU
CHECKED· FRANK SPECKHART
APPROVED: FRANK SPECKHART
FINISH:
SCALE: 1 1
UNIT INCH
DATE: 10 AUG 2000
SHEET: 1/1
APPENDIX C

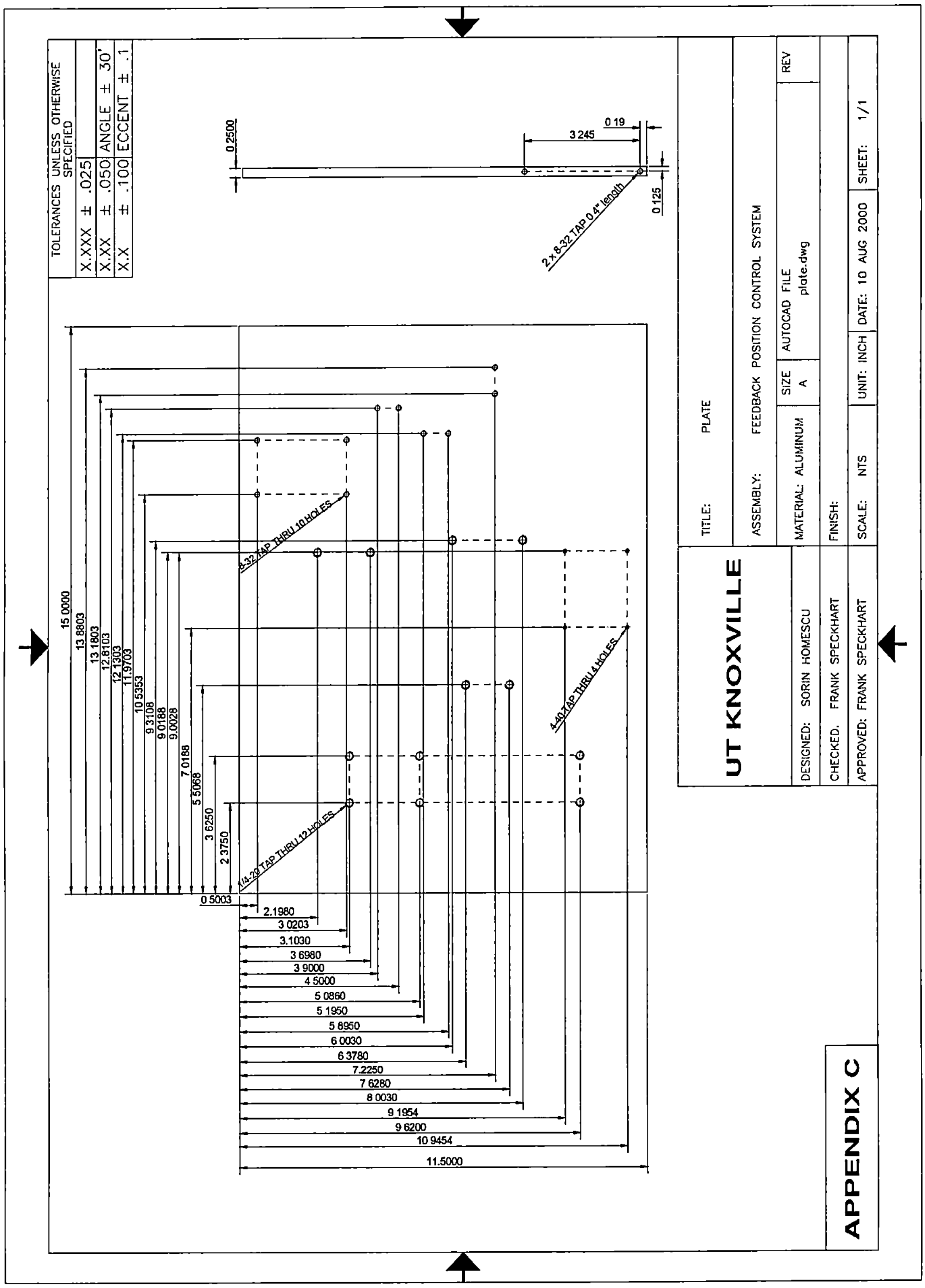
TOLERANCES UNLESS OTHERWISE SPECIFIED
X.XXX ± .025
X.XX ± .050
X.X ± .100
ANGLE ± 30'
ECCENT ± .1
0.2500
3.245
0.19
0.125
2 x 8-32 TAP 0.4" length
8-32 TAP THRU 10 HOLES
4-40 TAP THRU 4 HOLES
1/4-20 TAP THRU 12 HOLES
15.0000
13.8803
13.1803
12.8103
12.1303
11.9703
10.5353
9.3108
9.0188
9.0028
7.0188
5.5068
3.6250
2.3750
0.5003
2.1980
3.0203
3.1030
3.6980
3.9000
4.5000
5.0860
5.1950
5.8950
6.0030
6.3780
7.2250
7.6280
8.0030
9.1954
9.6200
10.9454
11.5000
UT KNOXVILLE
TITLE: PLATE
ASSEMBLY: FEEDBACK POSITION CONTROL SYSTEM
MATERIAL: ALUMINUM
SIZE A
AUTOCAD FILE plate.dwg
REV
FINISH:
DESIGNED: SORIN HOMESCU
CHECKED: FRANK SPECKHART
APPROVED: FRANK SPECKHART
SCALE: NTS
UNIT: INCH
DATE: 10 AUG 2000
SHEET: 1/1
APPENDIX C

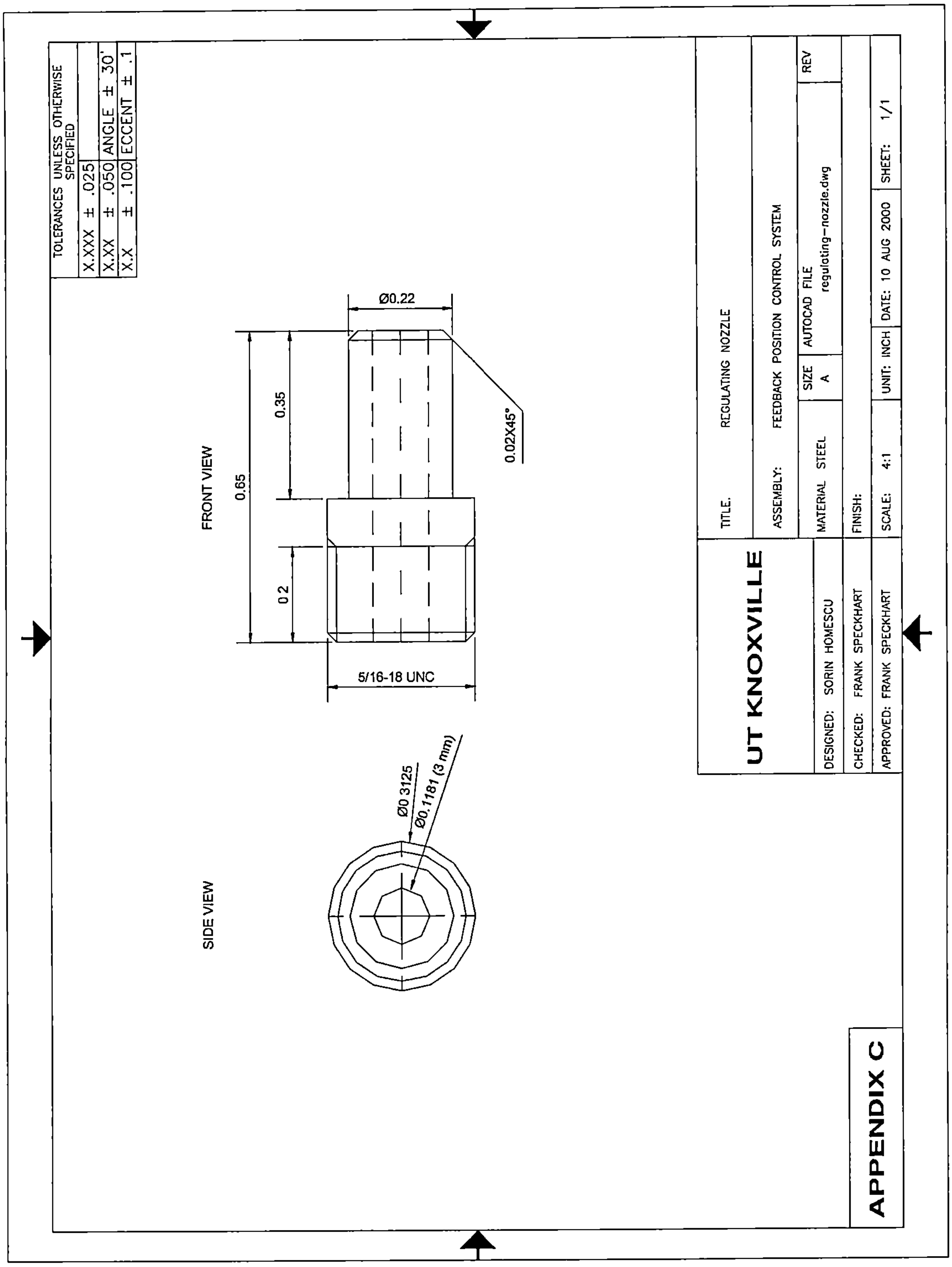

APPENDIX C
SIDE VIEW
FRONT VIEW
Ø0 3125
Ø0.1181 (3 mm)
5/16-18 UNC
0.65
0.35
0 2
Ø0.22
0.02X45°
TOLERANCES UNLESS OTHERWISE SPECIFIED
X.XXX ± .025
X.XX ± .050 ANGLE ± 30'
X.X ± .100 ECCENT ± .1
UT KNOXVILLE
TITLE. REGULATING NOZZLE
ASSEMBLY: FEEDBACK POSITION CONTROL SYSTEM
DESIGNED: SORIN HOMESCU
MATERIAL STEEL
SIZE A
AUTOCAD FILE regulating-nozzle.dwg
REV
CHECKED: FRANK SPECKHART
FINISH:
APPROVED: FRANK SPECKHART
SCALE: 4:1
UNIT: INCH
DATE: 10 AUG 2000
SHEET: 1/1

TOLERANCES UNLESS OTHERWISE SPECIFIED	
X.XXX ± .025	
X.XX ± .050	ANGLE ± 30'
X.X ± .100	ECCENT ± .1

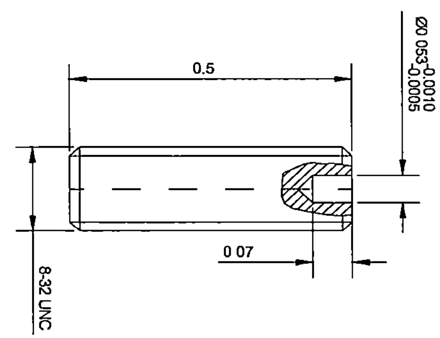

UT KNOXVILLE	TITLE. SCREW			
	ASSEMBLY: FEEDBACK POSITION CONTROL SYSTEM			
DESIGNED: SORIN HOMESCU	MATERIAL: BRASS	SIZE A	AUTOCAD FILE screw.dwg	REV
CHECKED: FRANK SPECKHART	FINISH:			
APPROVED: FRANK SPECKHART	SCALE: 4·1	UNIT: INCH	DATE: 10 AUG 2000	SHEET: 1/1

APPENDIX C

APPENDIX C

TOLERANCES UNLESS OTHERWISE SPECIFIED	
X.XXX ± .025	
X.XX ± .050	ANGLE ± 30'
X.X ± .100	ECCENT ± .1

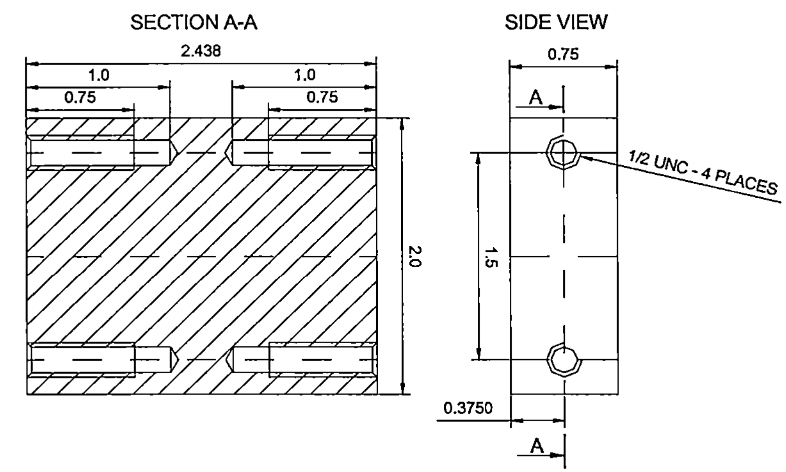

UT KNOXVILLE	TITLE: SPACER				
	ASSEMBLY: FEEDBACK POSITION CONTROL SYSTEM				
DESIGNED: SORIN HOMESCU	MATERIAL: ALUMINUM	SIZE A	AUTOCAD FILE spacer.dwg		REV
CHECKED. FRANK SPECKHART	FINISH:				
APPROVED: FRANK SPECKHART	SCALE: 1:1	UNIT: INCH	DATE: 10 AUG 2000	SHEET: 1/1	

APPENDIX C

TOLERANCES UNLESS OTHERWISE SPECIFIED			
X.XXX	± .025		
X.XX	± .050	ANGLE	± 30'
X.X	± .100	ECCENT	± .1

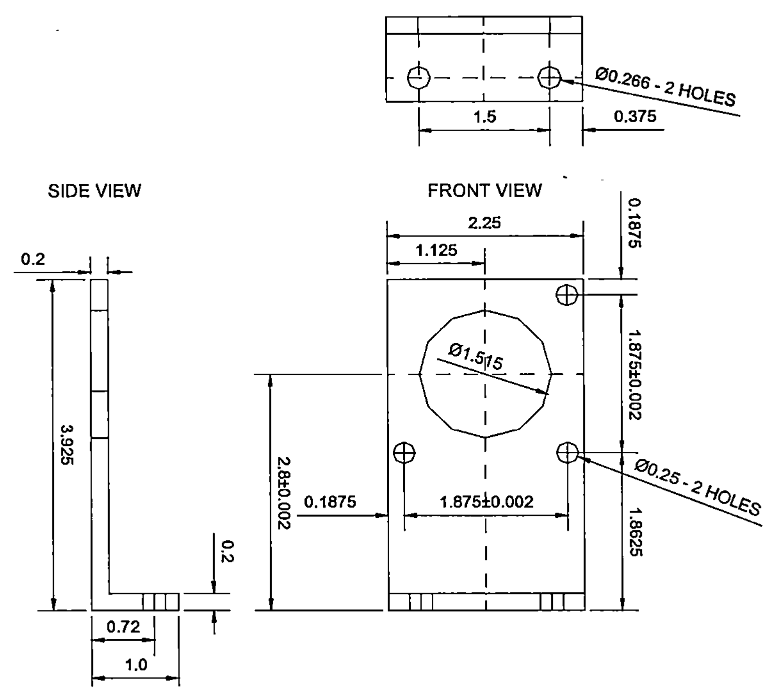

UT KNOXVILLE	TITLE: STEP MOTOR SUPPORT			
	ASSEMBLY: FEEDBACK POSITION CONTROL SYSTEM			
DESIGNED: SORIN HOMESCU	MATERIAL: STEEL	SIZE A	AUTOCAD FILE step-motor-support.dwg	REV
CHECKED. FRANK SPECKHART	FINISH:			
APPROVED: FRANK SPECKHART	SCALE: 1:2	UNIT: INCH	DATE. 10 AUG 2000	SHEET: 1/1

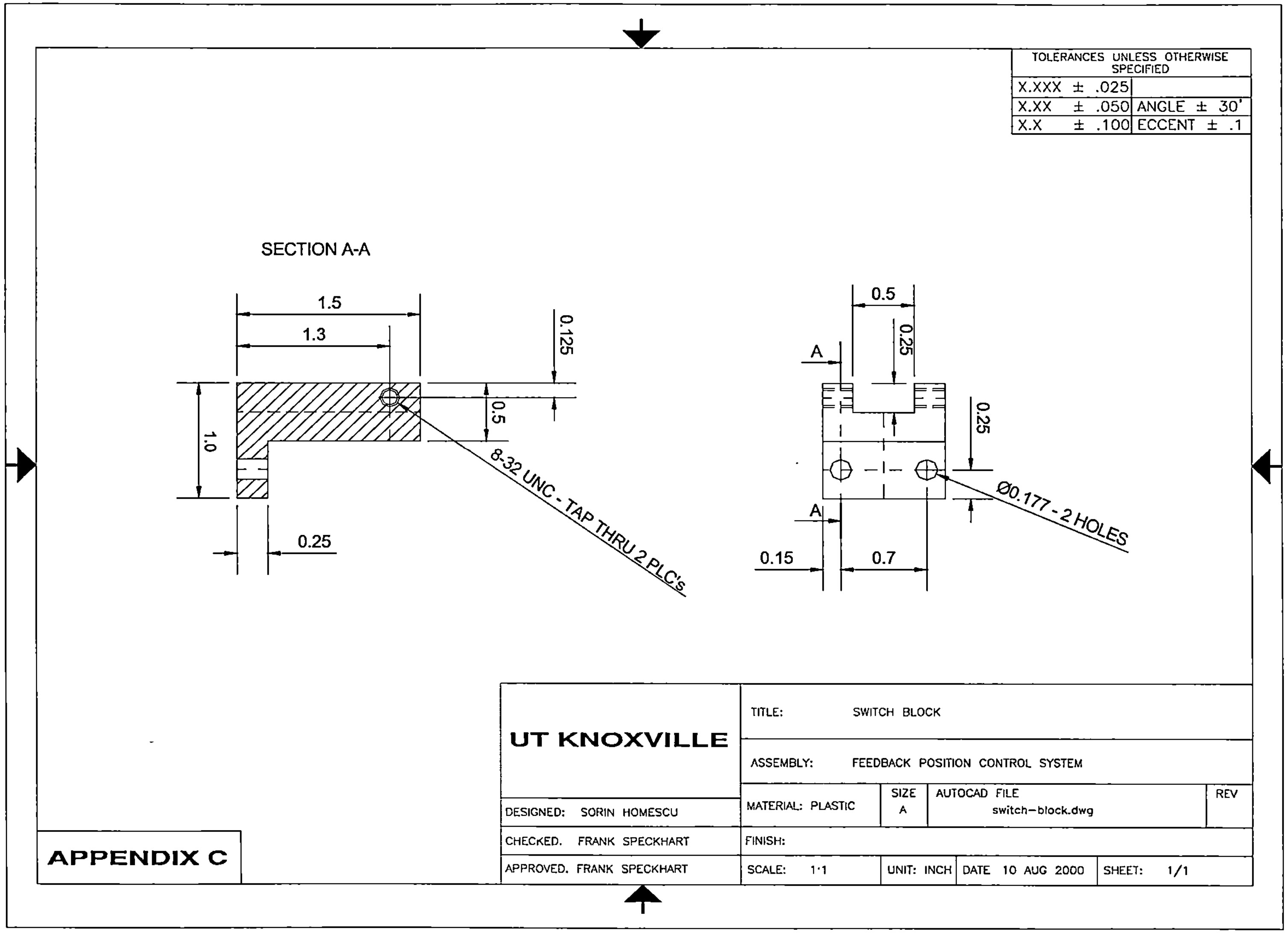
TOLERANCES UNLESS OTHERWISE SPECIFIED
X.XXX ± .025
X.XX ± .050
ANGLE ± 30'
X.X ± .100
ECCENT ± .1
SECTION A-A
1.5
1.3
1.0
0.125
0.5
0.25
8-32 UNC - TAP THRU 2 PLC's
0.5
0.25
A
A
0.25
Ø0.177 - 2 HOLES
0.15
0.7
UT KNOXVILLE
TITLE: SWITCH BLOCK
ASSEMBLY: FEEDBACK POSITION CONTROL SYSTEM
DESIGNED: SORIN HOMESCU
MATERIAL: PLASTIC
SIZE A
AUTOCAD FILE switch-block.dwg
REV
CHECKED. FRANK SPECKHART
FINISH:
APPROVED. FRANK SPECKHART
SCALE: 1:1
UNIT: INCH
DATE 10 AUG 2000
SHEET: 1/1
APPENDIX C

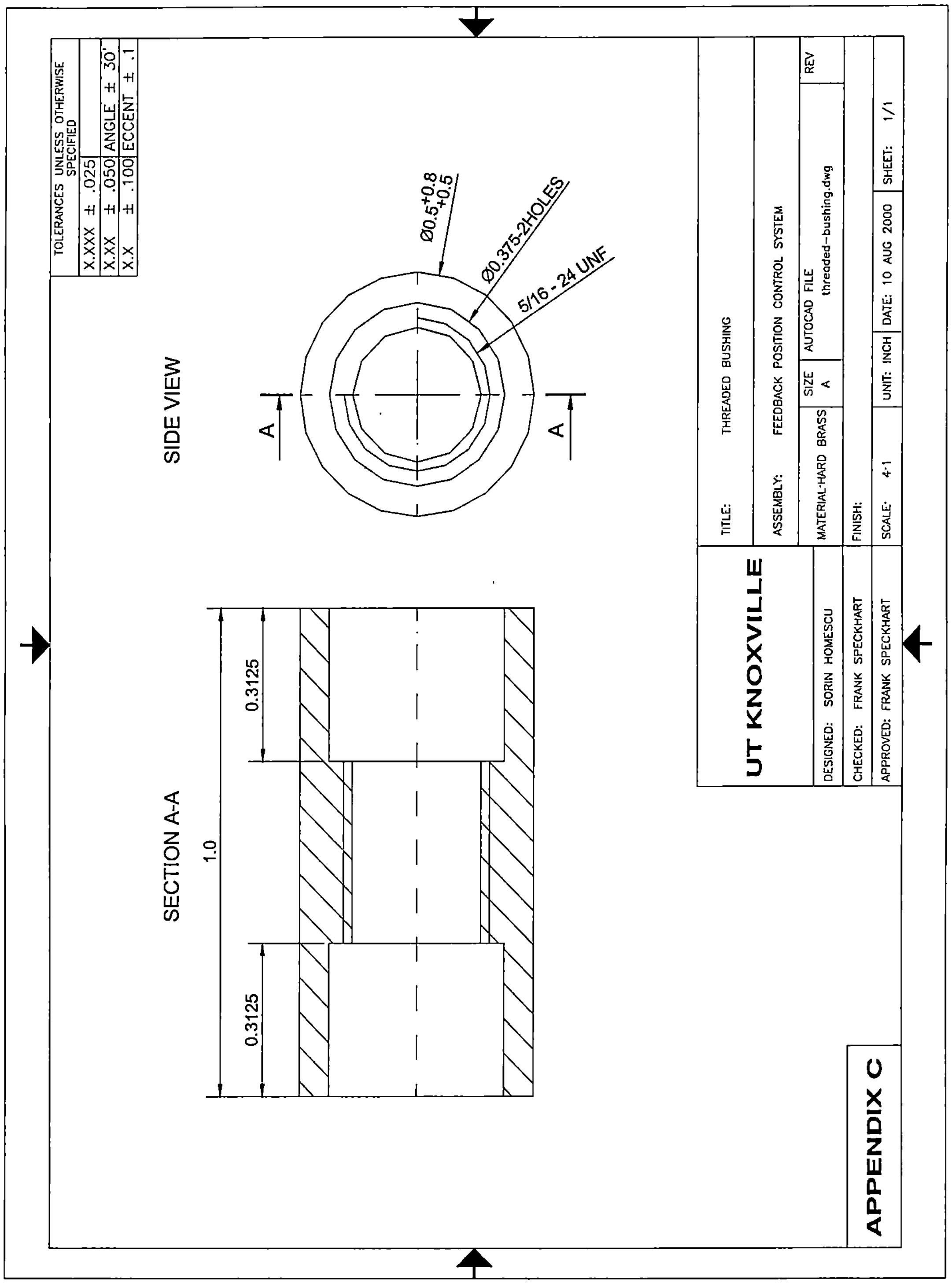
APPENDIX C
SECTION A-A
1.0
0.3125
0.3125
SIDE VIEW
A
A
Ø0.5+0.8 +0.5
Ø0.375-2HOLES
5/16 - 24 UNF
TOLERANCES UNLESS OTHERWISE SPECIFIED
X.XXX ± .025
X.XX ± .050 ANGLE ± 30'
X.X ± .100 ECCENT ± .1
UT KNOXVILLE
TITLE: THREADED BUSHING
ASSEMBLY: FEEDBACK POSITION CONTROL SYSTEM
MATERIAL: HARD BRASS
SIZE A
AUTOCAD FILE threaded-bushing.dwg
REV
FINISH:
SCALE: 4:1
UNIT: INCH
DATE: 10 AUG 2000
SHEET: 1/1
DESIGNED: SORIN HOMESCU
CHECKED: FRANK SPECKHART
APPROVED: FRANK SPECKHART

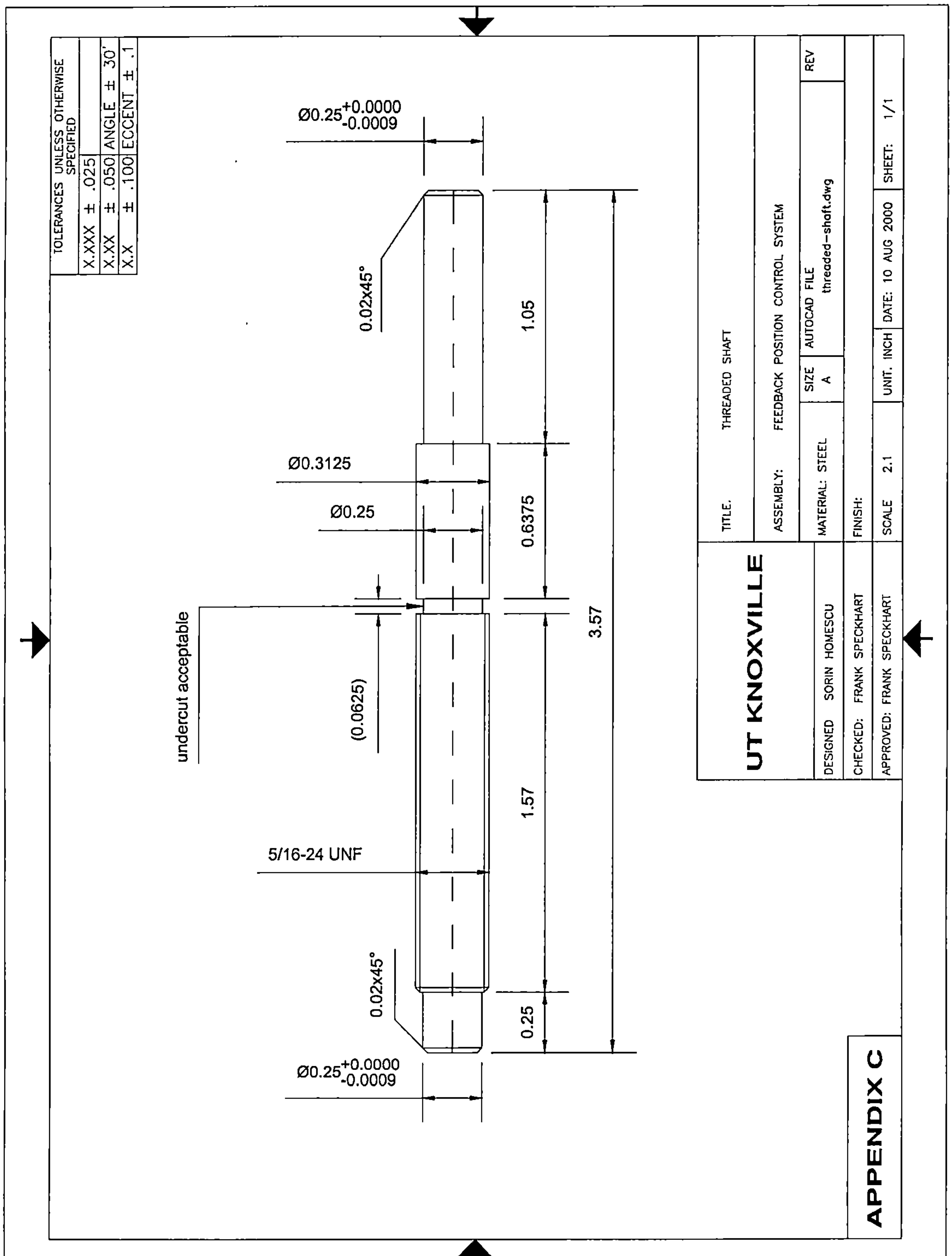
TOLERANCES UNLESS OTHERWISE SPECIFIED
X.XXX ± .025
X.XX ± .050
X.X ± .100
ANGLE ± 30'
ECCENT ± .1
Ø0.25 +0.0000 -0.0009
0.02x45°
1.05
Ø0.3125
Ø0.25
0.6375
undercut acceptable
(0.0625)
3.57
1.57
5/16-24 UNF
0.02x45°
0.25
Ø0.25 +0.0000 -0.0009
TITLE. THREADED SHAFT
ASSEMBLY: FEEDBACK POSITION CONTROL SYSTEM
MATERIAL: STEEL
SIZE A
AUTOCAD FILE threaded-shaft.dwg
REV
FINISH:
SCALE 2:1
UNIT: INCH
DATE: 10 AUG 2000
SHEET: 1/1
UT KNOXVILLE
DESIGNED SORIN HOMESCU
CHECKED: FRANK SPECKHART
APPROVED: FRANK SPECKHART
APPENDIX C

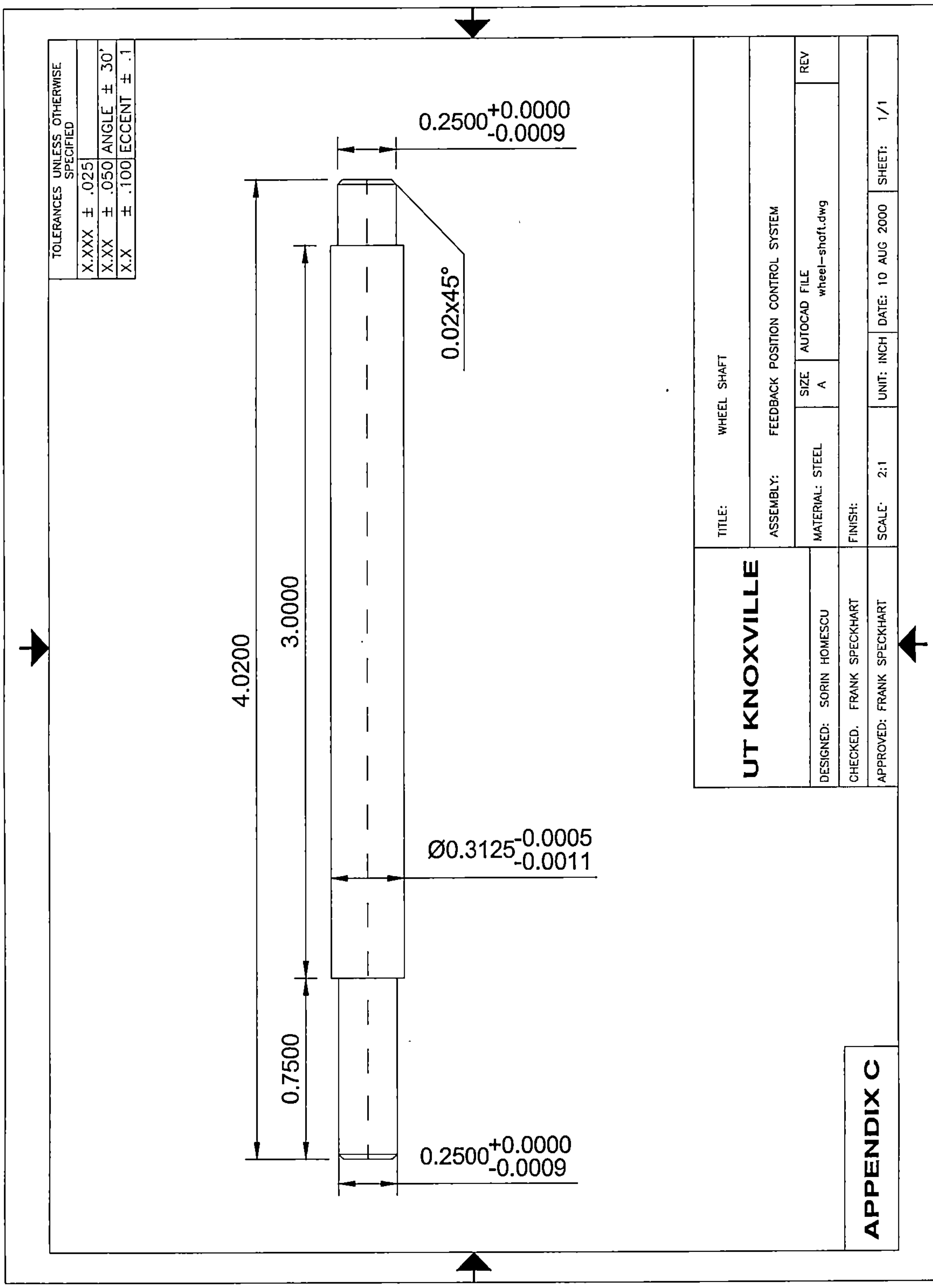
TOLERANCES UNLESS OTHERWISE SPECIFIED
X.XXX ± .025
X.XX ± .050
X.X ± .100
ANGLE ± 30'
ECCENT ± .1
0.2500 +0.0000 -0.0009
0.02x45°
4.0200
3.0000
Ø0.3125 -0.0005 -0.0011
0.7500
0.2500 +0.0000 -0.0009
UT KNOXVILLE
TITLE: WHEEL SHAFT
ASSEMBLY: FEEDBACK POSITION CONTROL SYSTEM
MATERIAL: STEEL
SIZE A
AUTOCAD FILE wheel-shaft.dwg
REV
FINISH:
SCALE: 2:1
UNIT: INCH
DATE: 10 AUG 2000
SHEET: 1/1
DESIGNED: SORIN HOMESCU
CHECKED. FRANK SPECKHART
APPROVED: FRANK SPECKHART
APPENDIX C

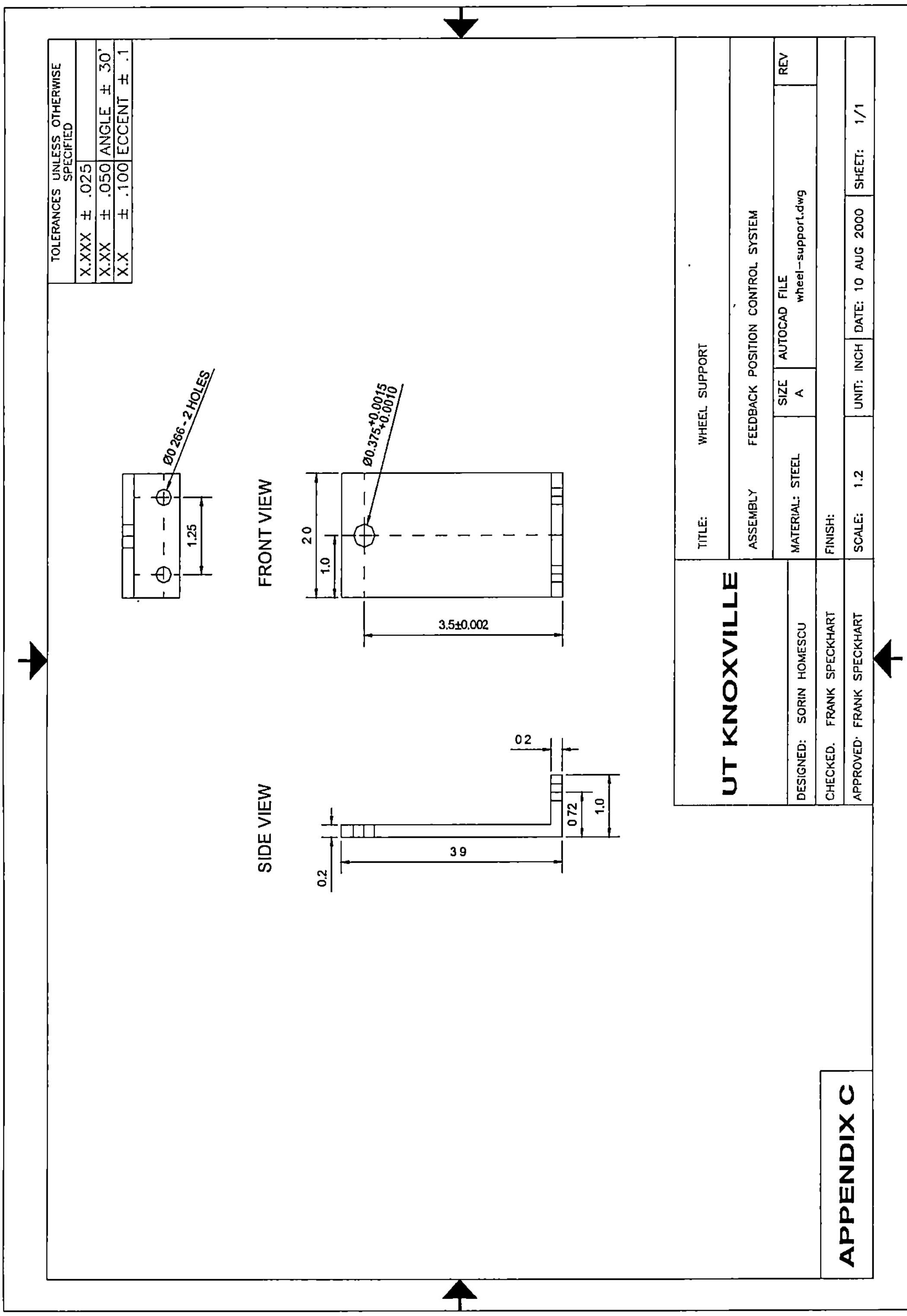
TOLERANCES UNLESS OTHERWISE SPECIFIED
X.XXX ± .025
X.XX ± .050 ANGLE ± 30'
X.X ± .100 ECCENT ± .1
Ø0.266 - 2 HOLES
1.25
FRONT VIEW
Ø0.375+0.0015 +0.0010
2.0
1.0
3.5±0.002
SIDE VIEW
0.2
0.72
1.0
3.9
0.2
UT KNOXVILLE
TITLE: WHEEL SUPPORT
ASSEMBLY FEEDBACK POSITION CONTROL SYSTEM
MATERIAL: STEEL
SIZE A
AUTOCAD FILE wheel-support.dwg
REV
DESIGNED: SORIN HOMESCU
CHECKED: FRANK SPECKHART
APPROVED: FRANK SPECKHART
FINISH:
SCALE: 1:2
UNIT: INCH
DATE: 10 AUG 2000
SHEET: 1/1
APPENDIX C

APPENDIX D

MATLAB PROGRAM TO SOLVE THE STEADY-STATE EQUATION

```
%          **************************************************************************
%          *                        SORIN HOMESCU                                   *
%          * MATLAB CODE TO SOLVE THE STEADY-STATE ANALYSIS*
%          *                              UTK                                        *
%          **************************************************************************
clear all
steps = 0;
%atmospheric pressure [mmH2O]
p0 = (101325*101.9745)/1000;
%fan pressure (absolute pressure) [mmH2O]
p1 = 0.1*25.4 + p0;
%initial estimate of the unknown quotient p2/p1
p21 = 1;
%diameters of the regulating nozzle [mm]
d1 = [2 ; 2.5 ; 3 ; 3.5 ; 4];
%diameter of the measuring nozzle [mm]
d2 = 4;
%tolerance imposed in computing the quotient p2/p1
tol = 0.0000000000001;
k = 0;
i = 0;
%Netwon's method to solve the nonlinear equation in p2/p1
for i = 1 : length ( d1 );
  for z = 0 : 0.1 : 1;
    k = k + 1;
    while ( abs (f (p21,z,d1(i),d2) ) >= tol )
      p21 = p21 - ( f(p21,z,d1(i),d2) / df(p21,z,d1(i),d2) );
      steps = steps + 1;
```

```
      disp( [ p21 f(p21,z,d1(i),d2)] );
    end;
    %quotient p2/p1
    p2overp1( k ) = p21;
    %pressure p2 [mmH2O] (absolute pressure)
    p2 = p2overp1 * p1;
    %pressure p2 [mmH2O] (gauge pressure)
    p2gauge = p2 - p0;
    %pressure p2 [inchH2O] (gauge pressure)
    p2gaugeinch = p2gauge / 25.4;
  end
  k=0;
  z = [0 : 0.1 : 1];
  if i == 1
    plot(z,p2gaugeinch,'ko-')
  elseif i == 2
    plot(z,p2gaugeinch,'kd-')
  elseif i == 3
    plot(z,p2gaugeinch,'ks-')
  elseif i == 4
    plot(z,p2gaugeinch,'k^-')
  else i == 5
    plot(z,p2gaugeinch,'k*-')
  end
title('d2=4mm')
xlabel('Gap [mm]')
ylabel('Measuring pressure p2 [in.H2O]')
legend('d1=2mm','d1=2.5mm','d1=3mm','d1=3.5mm','d1=4mm')
grid
hold on
```

```
end

%        *********************************************************************
%        *                    SORIN HOMESCU                                  *
%        * MATLAB FUNCTION WHICH CONTAIN THE EQUATION                        *
%        *    TO BE SOLVED WITH THE NEWTON'S METHOD                          *
%        *                         UTK                                       *
%        *********************************************************************
function y = f ( p21 , z , d1 , d2 )
%atmospheric pressure [mmH2O]
p0 = (101325*101.9745)/1000;
%fan pressure (absolute pressure) [mmH2O]
p1 = 0.1*25.4 + p0;
%adiabatic constant for air
alpha = 1.41;
%flow area of the regulating nozzle   [m2]
A1 = (pi*(d1^2))/4;
%flow area of the measuring nozzle [m2]
A2 = pi*d2*z;
%equation which has to be solved with the Newton's method
y =  (A2^2)*((p0/p1) ^ ( 2 / alpha )) * ( (p21) ^ (-2/alpha) ) ...
  - (A2^2)*((p0/p1)^((alpha+1)/alpha))*(p21^(-(alpha+1)/alpha))...
  - (A1^2)  * (p21 ^ ( (2-2*alpha) /alpha )) ...
  + (A1 ^ 2)  * ( p21 ^ ( (1-alpha) / alpha));
```

```
%    ***************************************************************************************
%    *                          SORIN HOMESCU                                              *
%    *   MATLAB FUNCTION WHICH CONTAIN THE FIRST DERIVATIVE                                *
%    *OF THE EQUATION TO BE SOLVED WITH THE NEWTON'S METHOD *
%    *                               UTK                                                   *
%    ***************************************************************************************
function y = df ( p21 , z , d1 , d2)
%atmospheric pressure [mmH2O]
p0 = (101325*101.9745)/1000;
%fan pressure (absolute pressure) [mH2O]
p1 = 0.1*25.4 + p0;
%adiabatic constant for air
alpha = 1.41;
%flow area of the regulating nozzle   [m2]
A1 = (pi*(d1^2))/4;
%flow area of the measuring nozzle [m2]
A2 = pi*d2*z;
%first derivative of the equation which has
%to be solved with the Newton's method
y = (A2^2) * ((p0/p1) ^ (2/alpha))  *  (-2/alpha) *  ((p21) ^ ((-2-alpha)/alpha))...
  + (A2^2)*((p0/p1) ^ ((alpha+1)/alpha))  * ((alpha+1)/alpha) * (p21^(-
(2*alpha+1)/alpha))...
  - (A1^2)* ((2-2*alpha)/alpha) *   (p21^( (2-3*alpha)/alpha ))...
  + (A1^2)  *  ((1-alpha)/alpha)  *  ( p21^ ( (1-2*alpha)/alpha));
```

APPENDIX E

TRANSIENT ANALYSIS DERIVATION

The mass flow rates expressions derived at the steady-state analysis and shown in Appendix A were used for the transient analysis:

$$\dot{m}_{12} = A_1 \cdot p_1 \cdot \sqrt{\frac{2 \cdot g \cdot \alpha}{(\alpha - 1) \cdot R \cdot T} \cdot \left[\left(\frac{p_2}{p_1} \right)^{\frac{2}{\alpha}} - \left(\frac{p_2}{p_1} \right)^{\frac{\alpha - 1}{\alpha}} \right]} \quad \textbf{(E1)}$$

$$\dot{m}_{20} = \pi \cdot d_2 \cdot gap \cdot p_2 \cdot \sqrt{\frac{2 \cdot g \cdot \alpha}{(\alpha - 1) \cdot R \cdot T} \cdot \left[\left(\frac{p_0}{p_2} \right)^{\frac{2}{\alpha}} - \left(\frac{p_0}{p2} \right)^{\frac{\alpha - 1}{\alpha}} \right]} \quad \textbf{(E2)}$$

The transient equation shown in Chapter 2 is:

$$\dot{m}_{12} - \dot{m}_{20} = \frac{dm_2}{dt} = \dot{m}_2 \quad \textbf{(E3)}$$

From equations (E1), (E2) and (E3) we can derive the expression:

$$\dot{m}_2 = A_1 p_1 \sqrt{\frac{2 \cdot g \cdot \alpha}{(\alpha - 1) \cdot R \cdot T} \left[\left(\frac{p_2}{p_1} \right)^{2/\alpha} - \left(\frac{p_2}{p_1} \right)^{\frac{\alpha + 1}{\alpha}} \right]} - \pi d_2 \cdot gap \cdot p_2 \sqrt{\frac{2 \cdot g \cdot \alpha}{(\alpha - 1) \cdot R \cdot T} \left[\left(\frac{p_0}{p_2} \right)^{2/\alpha} - \left(\frac{p_0}{p_2} \right)^{\frac{\alpha + 1}{\alpha}} \right]} \quad \textbf{(E4)}$$

The measuring pressure p_2 will be calculated by using the perfect gas law:

$$p_2 = \frac{m_2 \cdot R \cdot T}{V_2} \quad \textbf{(E5)}$$

and equation (E4) will become:

$$\dot{m}_2 = A_1 p_1 \sqrt{\frac{2 \cdot g \cdot \alpha}{(\alpha - 1) \cdot R \cdot T} \left[\left(\frac{m_2 RT}{p_1 V_2} \right)^{2/\alpha} - \left(\frac{m_2 RT}{p_1 V_2} \right)^{\frac{\alpha + 1}{\alpha}} \right]} - \pi d_2 \cdot gap \cdot \frac{m_2 RT}{V_2} \sqrt{\frac{2 \cdot g \cdot \alpha}{(\alpha - 1) \cdot R \cdot T} \left[\left(\frac{p_0 V_2}{m_2 RT} \right)^{2/\alpha} - \left(\frac{p_0 V_2}{m_2 RT} \right)^{\frac{\alpha + 1}{\alpha}} \right]} \quad \textbf{(E6)}$$

APPENDIX F

COMPUTER PROGRAMS TO SOLVE THE TRANSIENT ANALYSIS

```
10 ' save"runkut3"
20 PP = 1: 'set pp = 1 to print
30 PI = 4*ATN(1)
40 REM  This program uses a 4th order Runge-Kutta integration method to solve
50 ' systems of first-order ordinary differential equations  F. H. Speckhart
60 ' April 6, 2001   Program to simulate the response of the Lexmark Inkjet
70 DIM K(4, 80), Y(80), Z(80), YD(80)
80 'FOR I = 1 TO 80:  Y(I) = 0:  NEXT I
90 '   Enter constants, parameters, and one time calculations
100 ' Unit are in feet and lb/ft^2
110  '  1 ft of H20 = 62.4 lb/ft^2, 1 inch of H2O = 62.4/12 lb/ft^2
120 YBEAMHIGH= 1.48/(12*25.4):   YBEAMLOW = 1.42/(12*25.4)
130 P1H20= .1  :'  input pressure in H20
140 P0 = 14.7*144:    ' pressure in lb/ft^3
150 P1 = P1H20 * 62.4/12  + P0:  ' p1 in lb/ft^2
160 RPS = 3: ' speed of screw in rev/sec
170 TAU = 10:' PERIOD OF CYCYLING RATE
180 DEFF = .2/(25.4*12):   ' half deflection of paper variation in feet
190 LEAD = 1/(24* 12): ' lead of screw in feet
200 D1 = 3/(25.4*12):   D2 = 4/(25.4*12):  A1 = PI*D1^2/4:   A2 = PI*D2
210 E= 1.59E+07:  W= .5: T=.004: EI = E*T^3*W/12:L1=1.25: L2= 1: ALPHA =
1.4
220 KI= L1^3/(3*EI) + L1*L1*L2/(2*EI): ' Lb/ft
230 K = 12/KI
240 AREA = PI/(4*144): ' area of diaphragm in ft^2
250 VOL =(.5*PI/4 + PI*8*(3/16)^2/4)/1728: ' volume in ft^3
260 R = 53.35:   TEMP = 530    : G = 32.15
```

```
270 FACTOR = 2*G*ALPHA/((ALPHA-1)*R*TEMP):  F1 = 2/ALPHA: F2 =
(ALPHA+1)/ALPHA
280 GAPMIN =999:   YBEAMMIN  =  99999!: P2MIN = 99999!
290 REM **********************************************************************
300 REM  Enter initial conditions if different than zero
310 Y(1)=   P0*VOL/(R*TEMP)
320 REM  T9 = maximum time
330 T9 =     3
340 REM  T8 is equal to the print interval
350 T8 =    .04
360 REM  D1 = Increment of integration step size
370 D1 = .00001
380 REM  N = number of first order equations
390 N =2
400 REM *********************************************************************
410 T8 = T8 / D1
420 FOR I = 1 TO 80
430 Z(I) = Y(I)
440 NEXT I
450 T7 = 9.000001E+09
460 T = 0
470 GOTO 700
480 FOR J = 1 TO 4
490 ON J GOTO 630, 500, 550, 590
500 T = T + D1 * .5
510 FOR I = 1 TO N
520 Y(I) = K(1, I) * D1 * .5 + Z(I)
530 NEXT I
540 GOTO 630
550 FOR I = 1 TO N
```

```
560 Y(I) = K(2, I) * D1 * .5 + Z(I)
570 NEXT I
580 GOTO 630
590 T = T + .5 * D1
600 FOR I = 1 TO N
610 Y(I) = K(3, I) * D1 + Z(I)
620 NEXT I
630 GOSUB 920
640 FOR JK = 1 TO N
650 K(J, JK) = YD(JK):   NEXT JK
660 NEXT J
670 FOR I = 1 TO N
680 Z(I) = Z(I) + D1 * (K(1, I) + K(4, I) + 2 * (K(3, I) + K(2, I))) / 6
690 NEXT I
700 FOR I = 1 TO N
710 Y(I) = Z(I)
720 NEXT I
730 T7 = T7 + 1
740 IF T7 <= T8 - .0002 THEN 850
750 T7 = 0
760 REM ***************************************************************************
770 PRINT USING"t=#.### P2=#.### gap=##.### ybeam=##.###  Mtr=##.###
Y=##.### Yin=##.### ";T,(P2-P0)*12/62.4,
GAP*12*25.4,YBEAM*12*25.4,OMEGAMOTOR,Y*12*25.4,YIN*12*25.4
780 'PRINT USING "t=##.### Mass=#.####### m12=#.#######
m20=#.#######   P2=###.#### in H20";T,Y(1),MD12, MD20, (P2-P0)*12/62.4
790 'PRINT USING "Gap=.#### mm  ybeam=#.#### mm  y=#.#### mm
Mmotor=##.####";GAP*12*25.4, YBEAM*12*25.4,Y(2)*12*25.4,OMEGAMOTOR
800 IF PP < .5 THEN 840
```

```
810 LPRINT USING"t=#.### P2=#.### gap=##.### ybeam=##.###
Mtr=##.### Y=##.### Yin=##.### ";T,(P2-P0)*12/62.4,
GAP*12*25.4,YBEAM*12*25.4,OMEGAMOTOR,Y*12*25.4,YIN*12*25.4
820 'LPRINT USING "t=##.### Mass=#.####### m12=#.#######
m20=#.####### P2=###.#### in H20";T,Y(1),MD12, MD20, (P2-P0)*12/62.4
830 'LPRINT USING "Gap=.#### mm ybeam=#.#### mm y=#.#### mm
Mmotor=##.####";GAP*12*25.4, YBEAM*12*25.4,Y(2)*12*25.4,OMEGAMOTOR
840 REM ********************************************************************
850 IF T <= T9 THEN 480
860 PRINT USING "Gap max = ##.### Gap min = ##.### mm Ybmax=##.####
Ybmin=#.####
mm";GAPMAX*12*25.4,GAPMIN*12*25.4,YBEAMMAX*12*25.4,YBEAMMIN*12*
25.4
870 PRINT USING "P2max = #.#### in H2O P2min = #.#### in H2O Gap
high=#.## Gap low=#.###";(P2MAX-P0)*12/62.4,(P2MIN-
P0)*12/62.4,YBEAMHIGH*12*25.4,YBEAMLOW*12*25.4
880 IF PP < .5 THEN 910
890 LPRINT USING "Gap max = ##.### Gap min = ##.### mm
Ybmax=##.#### Ybmin=#.####
mm";GAPMAX*12*25.4,GAPMIN*12*25.4,YBEAMMAX*12*25.4,YBEAMMIN*12*
25.4
900 LPRINT USING "P2max = #.#### in H2O P2min = #.#### in H2O Gap
high=#.## Gap low=#.###";(P2MAX-P0)*12/62.4,(P2MIN-
P0)*12/62.4,YBEAMHIGH*12*25.4,YBEAMLOW*12*25.4
910 END
920 REM Start of a subroutine containing N first order differential equations
930 YIN = .5/(25.4*12) + DEFF*SIN(T*2*PI/TAU)
940 GAP = YIN - Y
950 IF GAP > GAPMAX THEN GAPMAX = GAP
960 IF T < .1 THEN 980
```

```
970 IF GAP < GAPMIN THEN GAPMIN = GAP
980  P2 = Y(1)*R*TEMP/VOL
990 IF P2 > P2MAX THEN P2MAX = P2
1000 FORCE = AREA*(P2-P0):    ' force acting on diaphragm
1010 YBEAM = FORCE/K:  ' deflection in feet
1020 IF YBEAM > YBEAMMAX THEN YBEAMMAX = YBEAM
1030 IF T < .1 THEN 1060
1040 IF YBEAM < YBEAMMIN THEN YBEAMMIN = YBEAM
1050 IF P2 < P2MIN THEN P2MIN = P2
1060 MD12 = A1*P1*SQR(FACTOR*((P2/P1)^F1 - (P2/P1)^F2)): 'm dot in
1070 GAPP = GAP
1080 IF GAP > D2/4 THEN GAPP = D2/4
1090 MD20 = A2*P2*GAPP*SQR(FACTOR*((P0/P2)^F1 - (P0/P2)^F2)): 'm dot
out
1100 MD = MD12-MD20
1110 YD(1) = MD
1120 OMEGAMOTOR  = 0
1130 IF YBEAM > YBEAMHIGH THEN OMEGAMOTOR =-RPS
1140 IF YBEAM < YBEAMLOW THEN OMEGAMOTOR =RPS
1150 YD(2) = OMEGAMOTOR*LEAD:   ' linear speed of screw in ft/sec
1160 Y = Y(2)
1170 RETURN
```

```
%**********************************************************************************
%*                         SORIN HOMESCU                                          *
%*MATLAB CODE TO SOLVE THE TRANSIENT ANALYSIS – PHASE ANGLE*
%*                              UTK                                               *
%**********************************************************************************
clear all
%step size for the numerical integration
```

```
h = 0.00001;
%the period of the wheel sinusoidal rotation [sec.]
tau = [10/1;10/3;10/7;10/10;10/15];
%diameter of the regulating nozzle [ft.]
d1 = 3/(12*25.4);
%diameter of the measuring nozzle [ft.]
d2 = 4/(12*25.4);
%atmospheric pressure [psf]
p0 = 14.7*144;
%regulating pressure [psf] (absolute pressure)
p1 = (0.1*62.4)/(12) + p0;
%gas constant (air) [ft.*lb./lbm.*R]
R = 53.35;
%ambient temperature [R]
T = 530;
%length of the diaphragm chamber [in.]
length = 0.5;
%diameter of the diaphragm chamber [in.]
dia = 1;
%cantilever beam thickness [in.]
thick = 0.004;
%cantilever beam width [in.]
b = 0.325;
%Module of elasticity for brass [psi]
E = 15.9*10^6;
%cantilever beam length(s) [in.]
L1 = 1.25;
L2 = 1.0;
%diaphragm aria
Adiaph = (pi*dia^2)/4;
```

```
%hose length [in.]
hl = 8;
%hose inside diameter [in.]
hd = 3/16;
%volume of the diaphragm chamber [ft.^3]
V2 = ((dia^2)*length*pi)/(4*1728) +((hd^2)*hl*pi)/(4*1728);
%initial mass (atmospheric pressure)
m2(1) = (p0 * V2) / (R * T);
%initial measuring pressure p2
p2(1) = (R*T*m2(1))/V2;
p2gauge(1) = p2(1) - p0 ;
%initial cantilever beam deflection
xb(1) = ( ( 2*(p2gauge(1)/144)*Adiaph*(L1^2)*(2*L1+3*L2) ) / (E*b*h^3) )*25.4;
%maximum and minimum wheel gap values [mm.]
zmax = [ 1.3 ; 1.0 ; 0.7 ];
zmin = [ 0.1 ; 0.2 ; 0.3 ];
%algorithm for the RANGE-KUTTA-FEHLBERG method
phase = zeros(max(size(zmax)),max(size(tau)));
for kk = 1 : max(size(zmax));
  for ll = 1 : max(size(tau));
%maximum and minimum wheel gap values [ft.]
zmaxft=zmax(kk)/(12*25.4);
zminft=zmin(kk)/(12*25.4);
zbar=(zmaxft+zminft)/2;
zrange=(zmaxft-zminft)/2;
%time range
t = [0 : 0.005 : tau(ll)];
%other initial values
z = 0;
for i = 1 : max(size(t))-1;
```

```
z(i) = (zbar + zrange*sin(((2*pi)/tau(ll)) * t(i)) );   %[ft.]
k1 = h * functie1(t(i) , m2(i),p2(i),z(i));
k2 = h * functie1(t(i) + h/4 , m2(i) + k1/4,p2(i),z(i));
k3 = h * functie1(t(i) + (3*h)/8 , m2(i) + (3*k1)/32 + (9*k2)/32,p2(i),z(i));
k4 = h * functie1(t(i) + (12*h)/13 , m2(i) + (1932*k1)/2197 - (7200*k2)/2197 +
(7296*k3)/2197,p2(i),z(i));
k5 = h * functie1(t(i) + h ,m2(i) + (439*k1)/216 - 8*k2 + (3680*k3)/513 -
(845*k4)/4104,p2(i),z(i));
k6 = h * functie1(t(i) + h/2 , m2(i) - (8*k1)/27 + 2*k2 - (3544*k3)/2565 +
(1859*k4)/4104 - (11*k5)/40,p2(i),z(i));
m2(i+1) = m2(i) + ( (16*k1)/135 + (6656*k3)/12825 + (28561*k4)/56430 -
(9*k5)/50 + (2*k6)/55 );
error(i+1) = k1/360 - (128*k3)/4275 - (2197*k4)/75240 + k5/50 + (2*k6)/55;
p2(i+1) = (R*T*m2(i+1))/V2;
p2gauge(i+1) = p2(i+1) - p0;
xb(i+1) = ( ( 2*(p2gauge(i+1)/144)*Adiaph*(L1^2)*(2*L1+3*L2) ) / (E*b*thick^3)
)*25.4;
end
[minimum,index]=min(z);
www = size (t);
onestepangle = 360 / ( www(2) - 1 ) ;
[maximum,index1]=max(xb);
phase(kk,ll) = ( index1 - index ) * onestepangle;
%phase = ( index1 - index ) * onestepangle;
end
end
for jj = 1 : max(size(tau));
  freq(jj) = 1 / tau (jj)  ;
end
plot(freq,phase(1,:),'*-',freq,phase(2,:),'o-',freq,phase(3,:),'x-')
```

```
title('Plot of the theoretical results of phase angle')
xlabel('Wheel rotation frequency [Hz]')
ylabel('Phase angle [Deg.]')
legend('0.2 mm','0.4','0.6')
grid

%*****************************************************************************
%*                        SORIN HOMESCU                                      *
%*  MATLAB FUNCTION WHICH CONTAINS THE EQUATION OF MASS *
%*FLOW TO BE INTEGRATED WITH THE RUNGE-KUTTA-FEHLBERG  *
%*                           METHOD                                          *
%*                             UTK                                           *
%*****************************************************************************
function y = functie ( t , m2 ,p2 , gap);
%length of the diaphragm chamber [ft.]
length = 0.5;
%diameter of the diaphragm chamber [ft.]
dia = 1;
%hose length [in.]
hl = 8;
%hose inside diameter [in.]
hd = 3/16;
%volume of the diaphragm chamber [ft.^3]
V2 = ((dia^2)*length*pi)/(4*1728) +((hd^2)*hl*pi)/(4*1728);
%diameter of regulating nozzle [ft.]
d1 = 3/(12*25.4);
%diameter of measuring nozzle [ft.]
d2 = 4/(12*25.4);
%flow area of regulating nozzle [ft.^2]
A1 = (pi*(d1^2))/4;
%flow area of measuring nozzle [ft.^2]
```

```
A2 = pi*d2*gap;
%gas constant(air) [ft.*lb./lbm.*R]
R = 53.35;
%ambient temperature [R]
T = 530;
%adiabatic constant (for air)
alpha = 1.4;
%gravitational acceleration [ft./sec.^2]
g = 32.15;
%atmospheric pressure [psf]
p0 = 14.7*144;
%regulating pressure [psf] (absolute pressure)
p1 = (0.1*62.4)/(12) + p0;
%equation of the flow difference
C =  ( ( ( 2 * g * alpha ) / ( ( alpha - 1 ) * R * T ) )  )^(1/2);
y =  C * (A1*p1*sqrt( (p2/p1)^(2/alpha) - (p2/p1)^((alpha+1)/alpha) ) - ...
      A2*p2*sqrt( (p0/p2)^(2/alpha) - (p0/p2)^((alpha+1)/alpha) ) ) ;
```

APPENDIX G

SYSTEM PARAMETERS

Measuring nozzle diameter:	4 mm
Regulating nozzle diameter:	3 mm
Diaphragm cavity inside diameter:	1 inch
Diaphragm cavity length:	0.5 inch
Cantilever beam material:	brass
Cantilever beam thickness:	0.004 inches
Diaphragm hose length:	8 inches
Diaphragm hose inside diameter:	3/16 inches

Cantilever beam geometry:

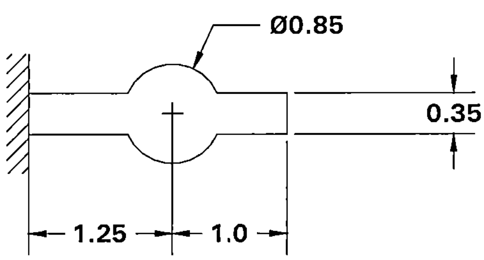

Stepping motor speed:	6π rad./sec.
Fan pressure (regulating chamber):	0.1 in.H_2O
Active distance between silver contacts	
(cantilever beam thickness subtracted):	0.13 mm

APPENDIX H

BASIC PROGRAM USED TO RUN THE STEPPING MOTOR

```
10 'PROGRAM TO RUN THE STEP MOTOR FROM THE LEXMARK PROJECT
20 'SORIN HOMESCU AUGUST 11, 2000
30 OUTPORT = &H378:              'SETS THE OUTPUT PORT
40 INPORT = &H379:               'SETS THE INPUT PORT
60 OUT OUTPORT, &H1              'HALF STEP/FOR STEP USE H1
70 IN% = INP(INPORT)
80 IF IN% > 150 THEN 100
90 IF IN% < 100 THEN 160
95 GOTO 60
100 OUT OUTPORT, &H1
120 FOR J = 1 TO 650: NEXT J
130 OUT OUTPORT, &H0
150 GOTO 60
160 OUT OUTPORT, &H3
180 FOR J = 1 TO 650: NEXT J
190 OUT OUTPORT, &H2
210 GOTO 60
```

APPENDIX I

COMPLETE RESULTS OF PROTOTYPE MODEL TESTING

The straight lines from the plots represent the limits of the wheel sinusoidal variation (see Figure I1).

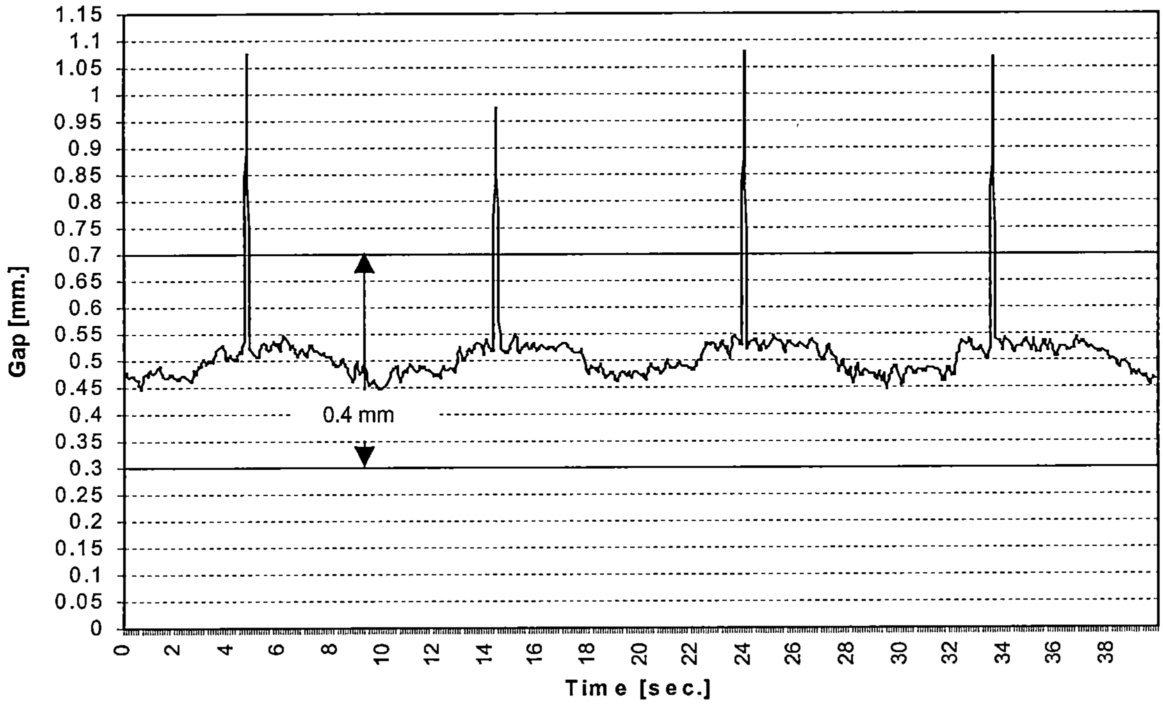

Figure I1 Results for single wheel amplitude 0.2 mm and frequency 0.1 Hz

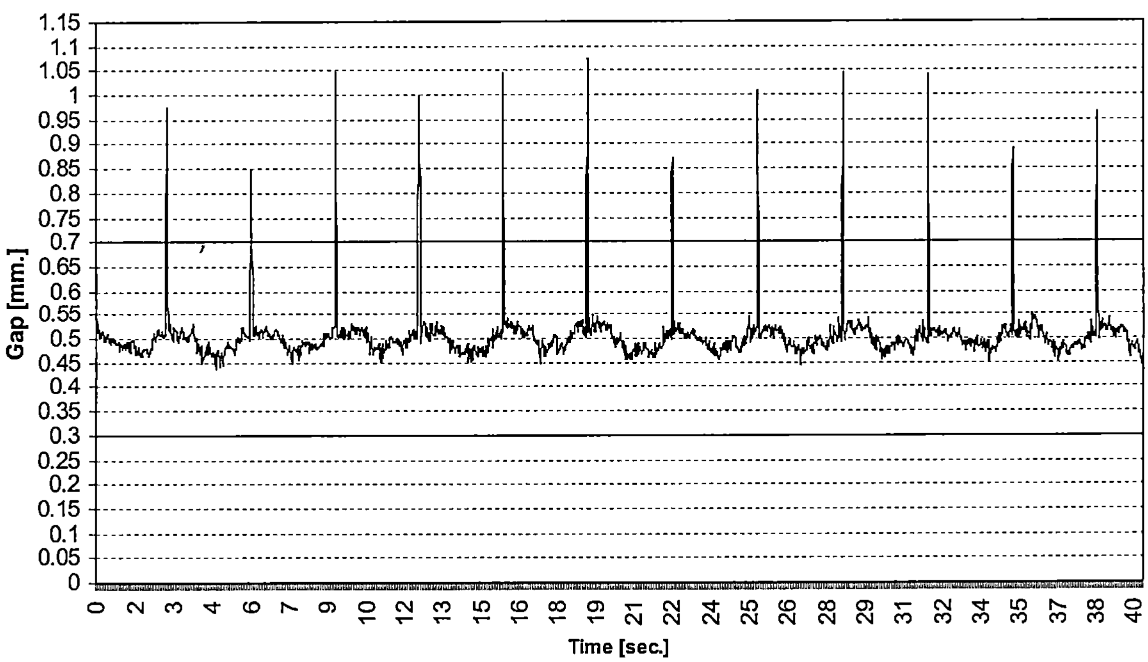

Figure I2 Results for single wheel amplitude 0.2 mm and frequency 0.3 Hz

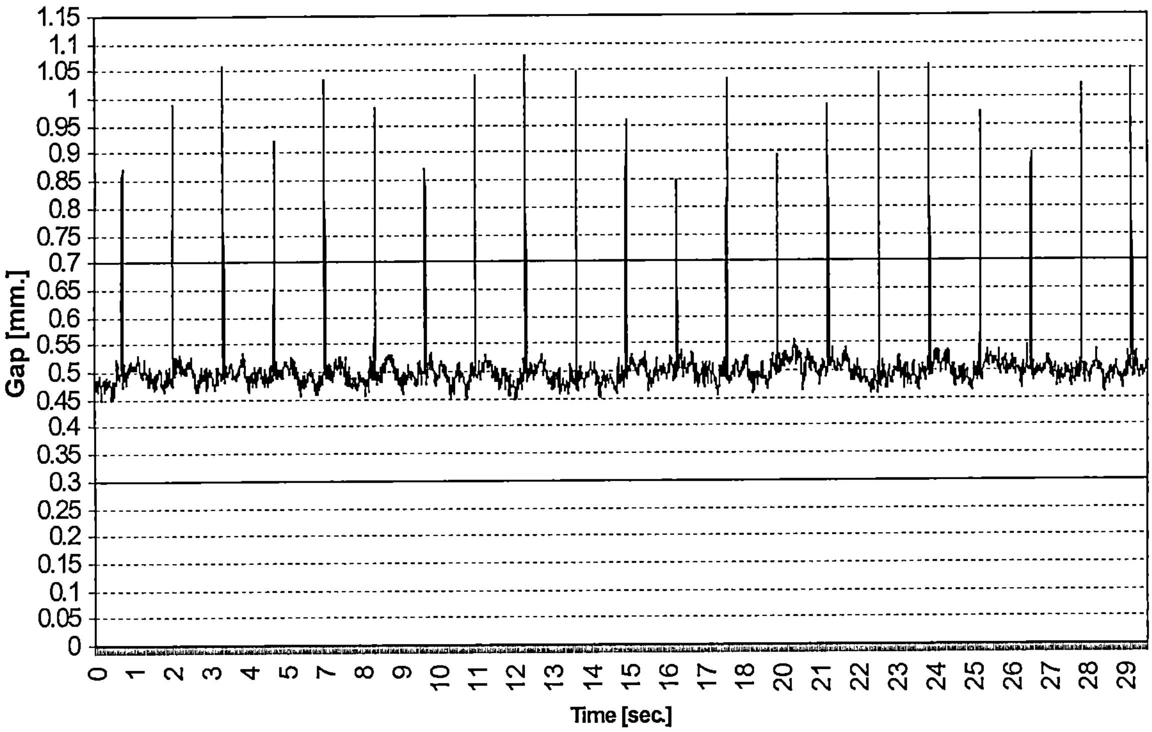

Figure I3 Results for single wheel amplitude 0.2 mm and frequency 0.7 Hz

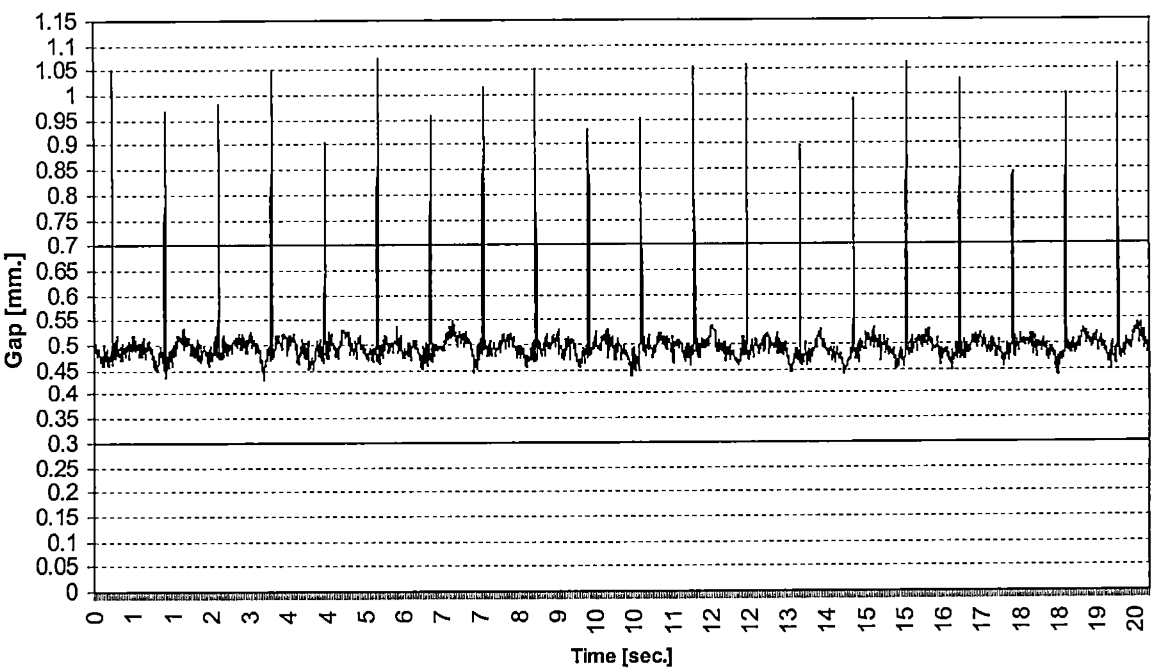

Figure I4 Results for single wheel amplitude 0.2 mm and frequency 1.0 Hz

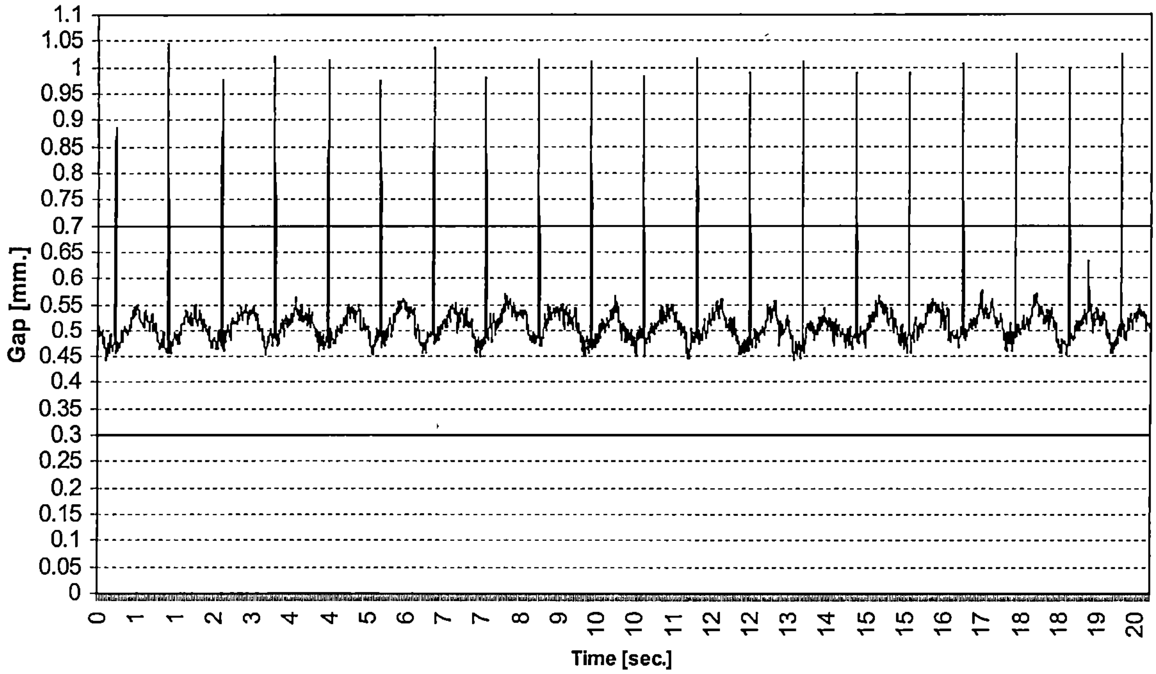

Figure I5 Results for single wheel amplitude 0.2 mm and frequency 1.5 Hz

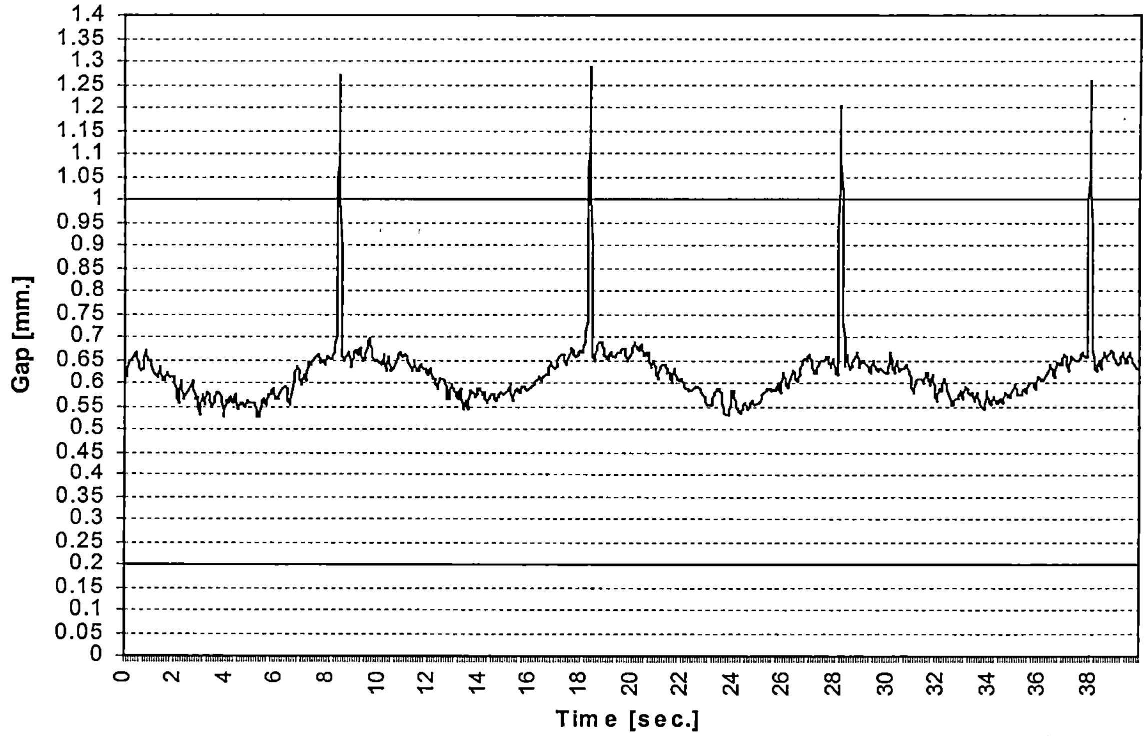

Figure I6 Results for single wheel amplitude 0.4 mm and frequency 0.1 Hz

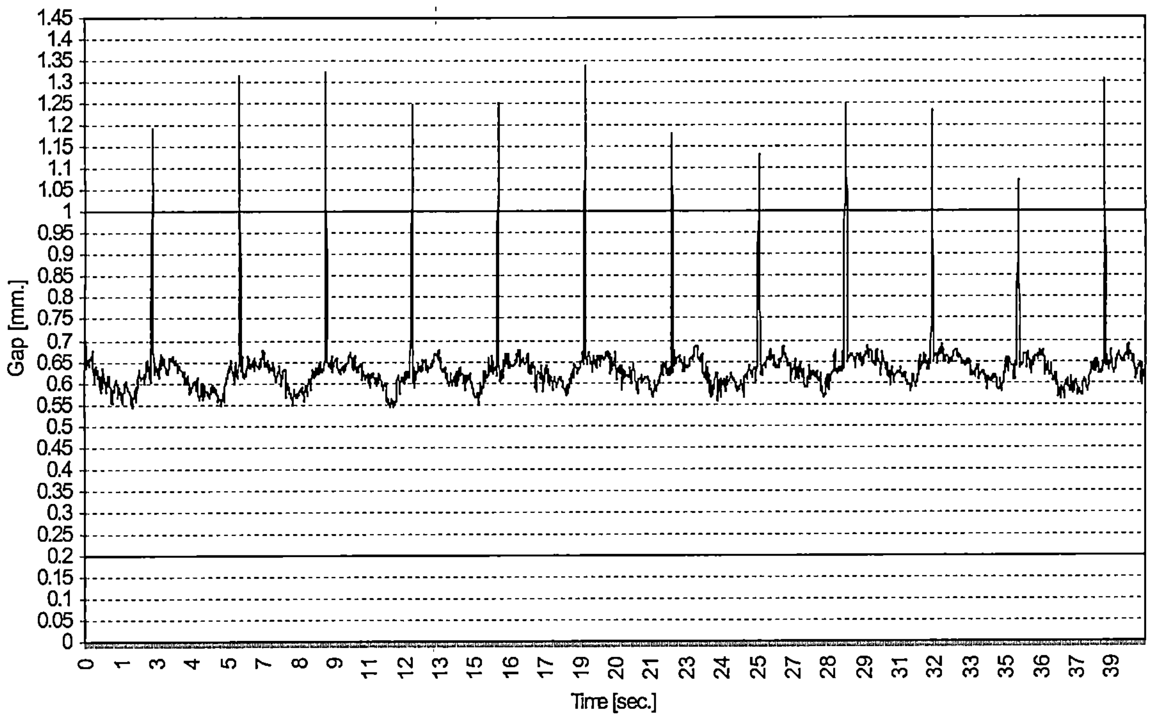

Figure I7 Results for single wheel amplitude 0.4 mm and frequency 0.3 Hz

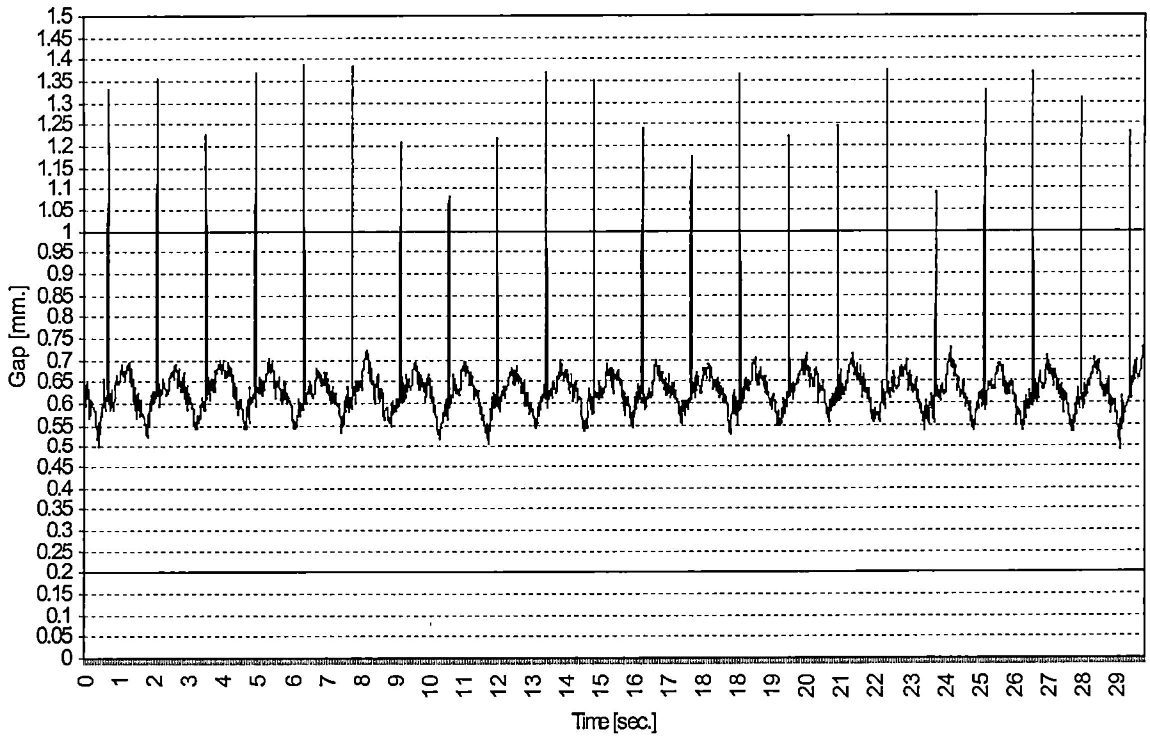

Figure I8 Results for single wheel amplitude 0.4 mm and frequency 0.7 Hz

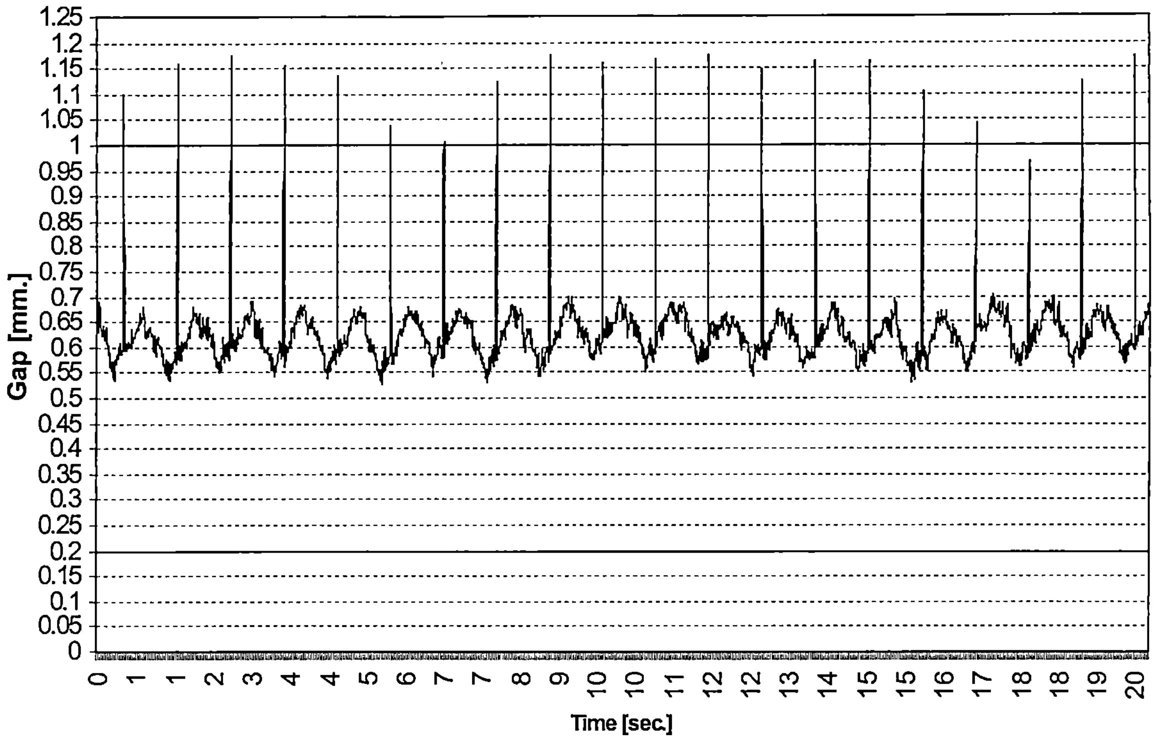

Figure I9 Results for single wheel amplitude 0.4 mm and frequency 1.0 Hz

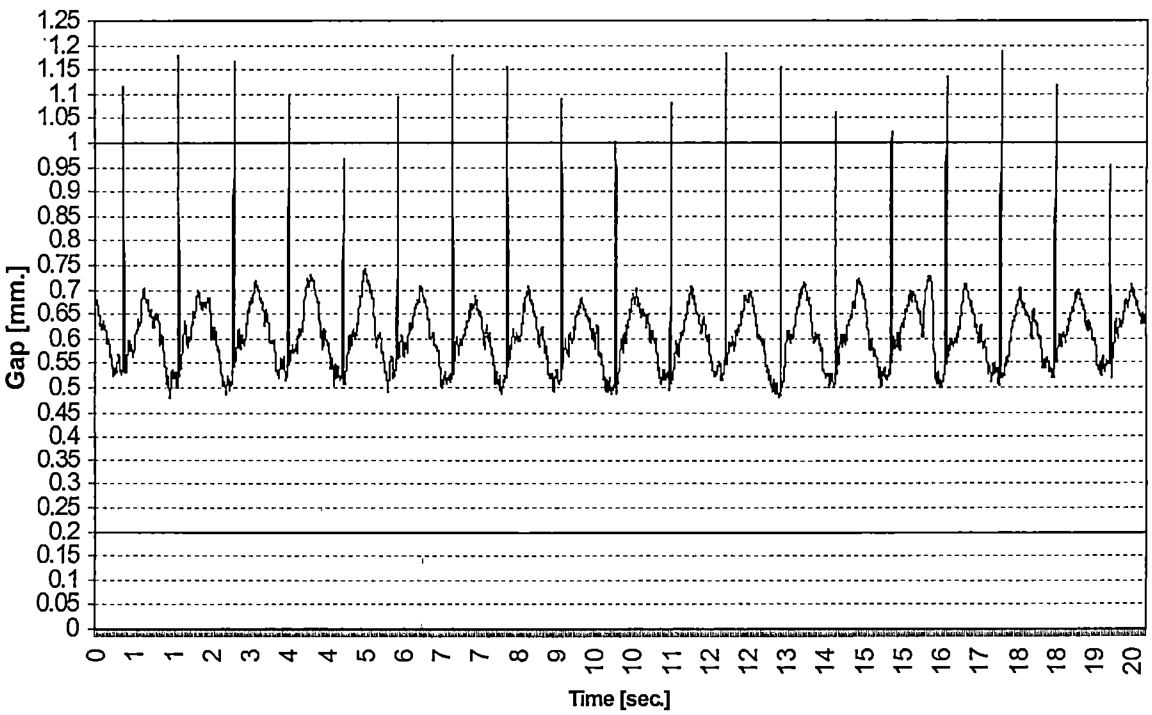

Figure I10 Results for single wheel amplitude 0.4 mm and frequency 1.5 Hz

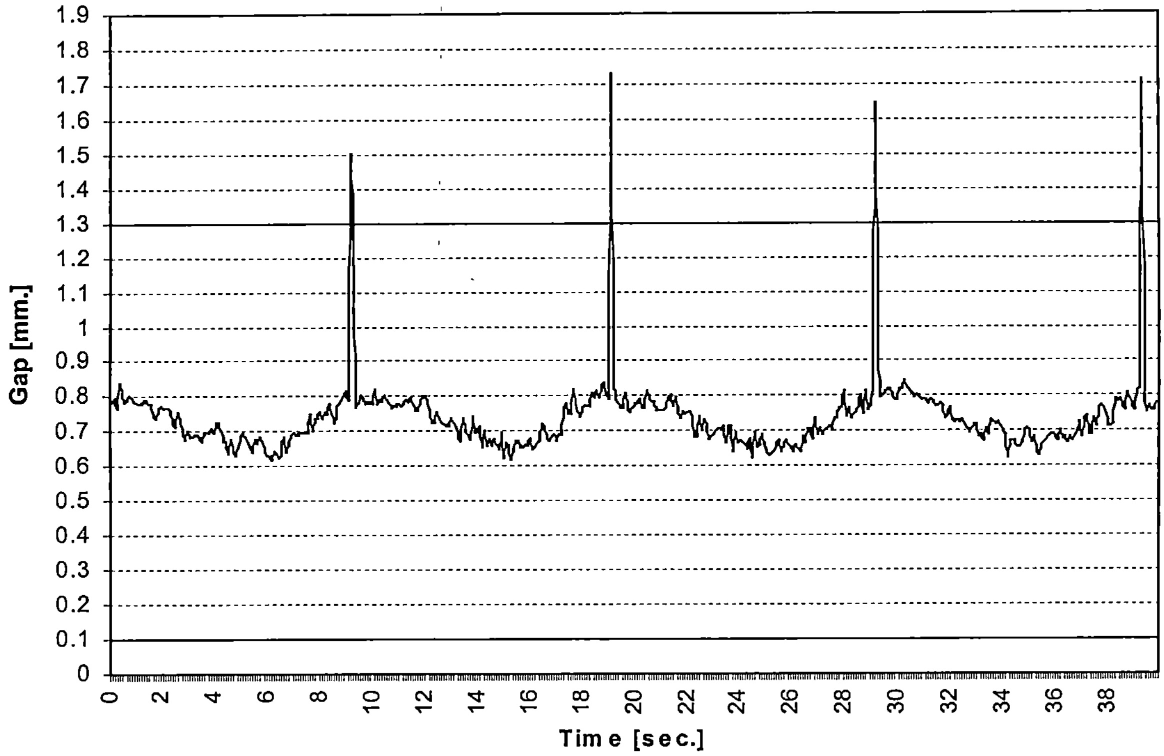

Figure I11 Results for single wheel amplitude 0.6 mm and frequency 0.1 Hz

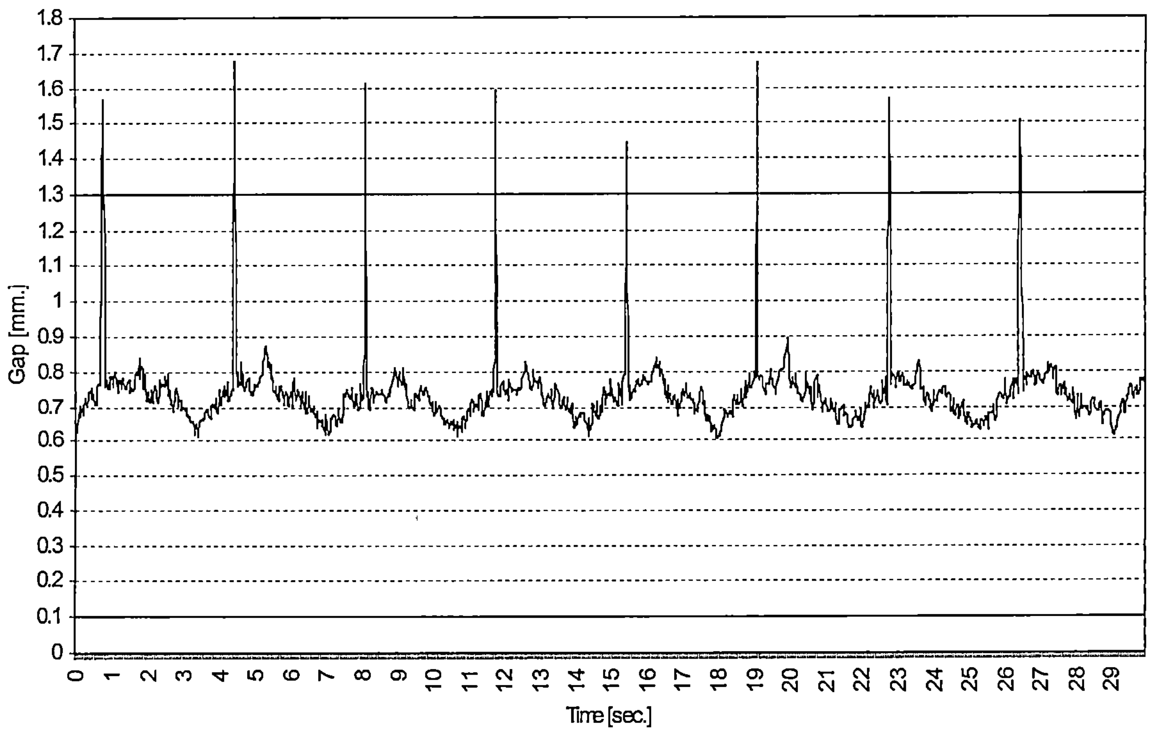

Figure I12 Results for single wheel amplitude 0.6 mm and frequency 0.3 Hz

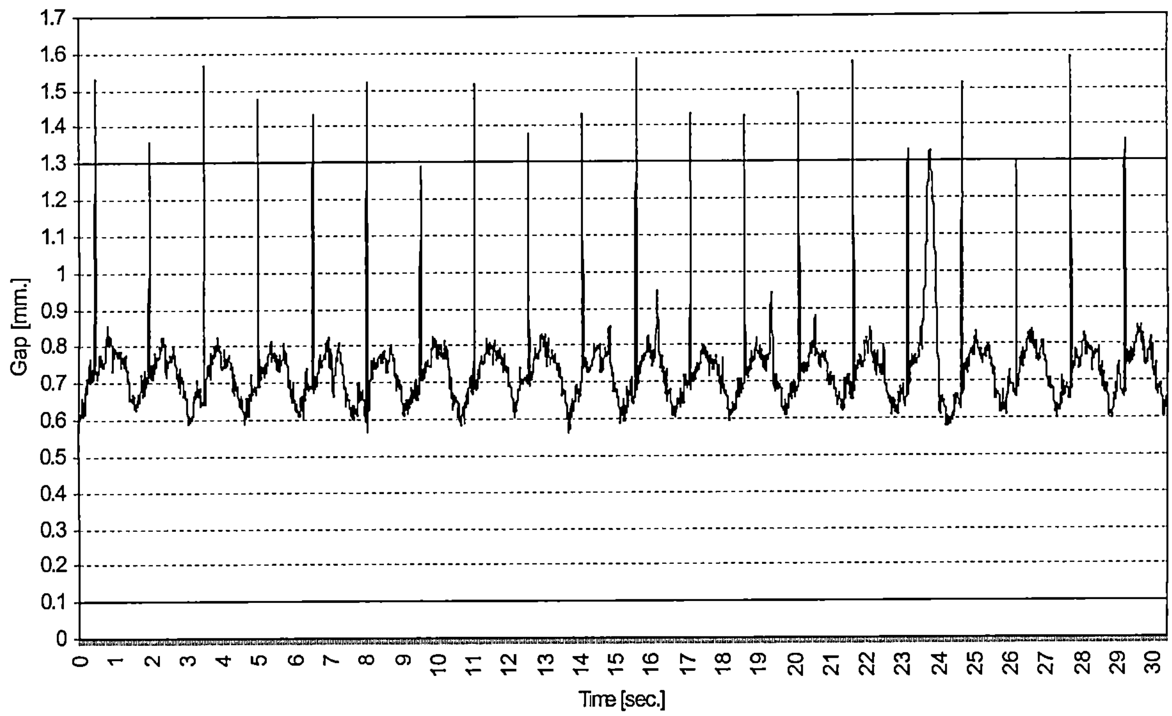

Figure I13 Results for single wheel amplitude 0.6mm and frequency 0.7 Hz

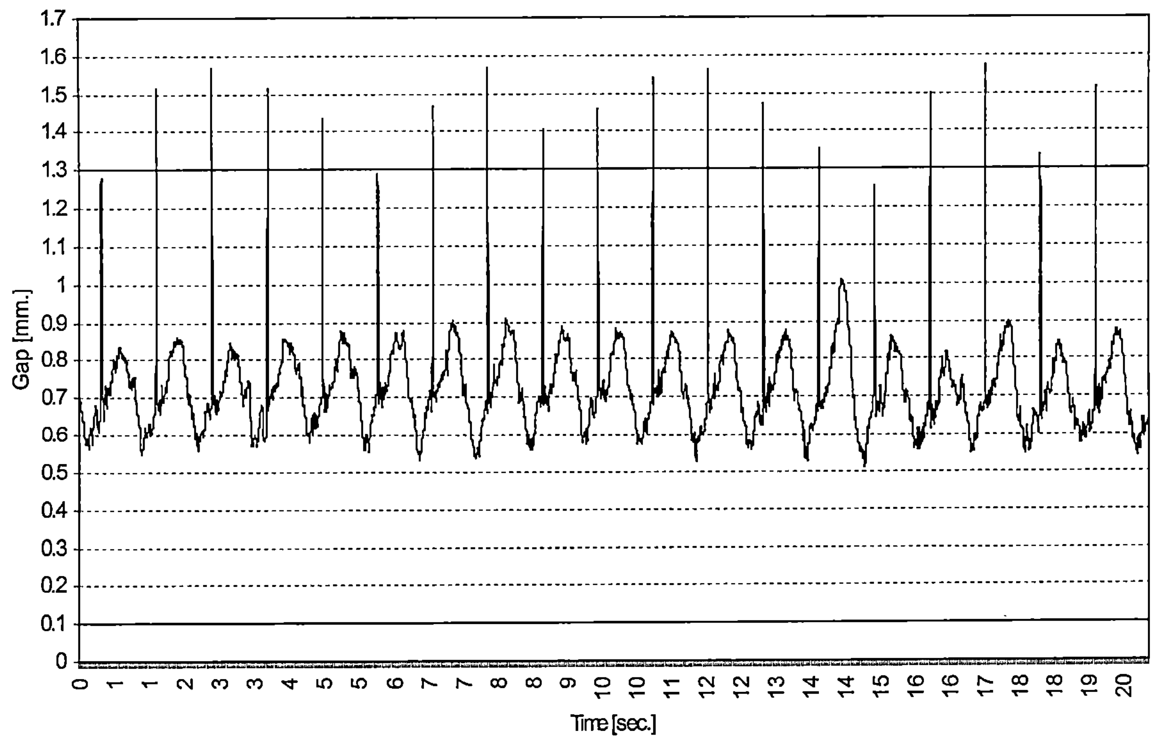

Figure I14 Results for single wheel amplitude 0.6 mm and frequency 1.0 Hz

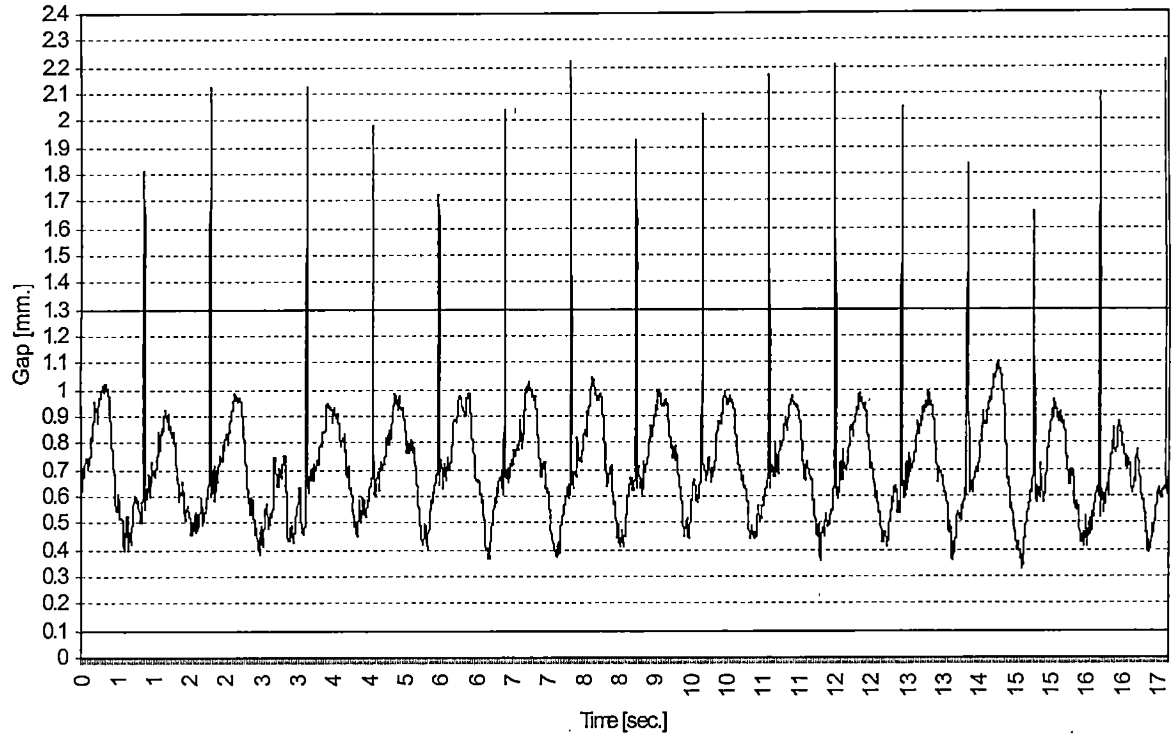

Figure I15 Results for single wheel amplitude 0.6 mm and frequency 1.5 Hz

VITA

Sorin Homescu was born in Bucharest, Romania on December 19, 1970. He attended the high school in the same city graduating in June, 1989 from Jean Monet High School.

He entered Technical University of Timisoara, Romania during September, 1990 where in June, 1995 he received the Bachelor of Science in Mechanical Engineering. He was immediately admitted in the Master's program at the same university, officially receiving the Master's degree in July, 1996.

After working four years Sorin Homescu entered University of Tennessee in August, 1999 to pursue his second Master of Science in Mechanical Engineering. The Master's degree was awarded in May 2001.